Appendix B.

Probabilistic Seismic Hazard Analyses

DRAFT
SUPPLEMENTAL
ENVIRONMENTAL
IMPACT STATEMENT

Brightwater
Regional Wastewater
Treatment System

Technical Appendices

Brightwater
King County TREATMENT SYSTEM

Appendix B

Revised Probabilistic Seismic Hazard Analyses

March 2005

Prepared for King County by
Shannon & Wilson, Inc. under subcontract to CH2M Hill

Alternative formats available upon request
by calling 206-684-1280 or 711 (TTY)

King County
Department of Natural Resources and Parks
Wastewater Treatment Division
King Street Center, KSC-NR-0505
201 South Jackson Street
Seattle, WA 98104

Revised Probabilistic Seismic Hazard Analyses
Brightwater Project SR-9 Site
King County Department of
Natural Resources, Washington

March 9, 2005

Prepared for King County by
Shannon & Wilson, Inc. under
Subcontract to CH2M Hill

21-1-20150-002

Executive Summary

This report presents the details and results of a revised probabilistic seismic hazard analyses (PSHA) performed for the Brightwater Treatment Plant SR-9 site. The purpose of the work was to develop an estimate of rock level ground motions with 2 percent probability of exceedance in 50 years (2,500 year return period) in the form of soft rock uniform hazard response spectra (UHS) for known and postulated mainland extension of the Southern Whidbey Island Fault (SWIF) from Puget Sound to south of the Plant site. The ground motion hazard was calculated for a case in which the extension was assumed, with 100 percent certainty, to be active. While this representation results in a conservative ground motion hazard estimate at the Plant site for the current state of knowledge, the ground motion hazard would still be suitable for design in the event that future research work by the U.S. Geological Survey (USGS) confirms that the location and activity of the postulated extensions are consistent with the assumptions used in this PSHA model.

The analysis was performed using a peer-reviewed PSHA model, developed by Shannon & Wilson, Inc., with modifications to consider recently postulated geometries and seismogenic models of the SWIF including possible mainland extensions. Our PSHA model was initially developed for the Second Tacoma Narrows Bridge, and subsequently, it has been modified for other major projects, including the Washington State Legislative Building, the Alaskan Way Viaduct, and the Seattle Monorail Project. For this project, we modified the model by developing a branch of the logic tree that used recent available airborne LIDAR mapping and published aeromagnetic anomaly data to estimate the location of the mainland extension of the SWIF. The results of this original PSHA study for the Plant and Portal sites were provided in "Final Report, Probabilistic Seismic Hazard Analyses, Brightwater Project, SR-9 and Portal 41 Sites, King County Department of Natural Resources, Washington," by Shannon & Wilson, Inc. to CH2M Hill, dated June 30, 2004. After submission of this report, fault trenching studies by the U.S. Geological Survey (USGS) and the King County design team were performed at Blakely et al's (2004) Lineament 4 at or near the Plant site. The original PSHA study was subsequently revised based on the results of the trenching studies, and the results of the revised PSHA study are presented in this report.

Following the introduction in Section 1.0, the methodology of PSHA is discussed in Section 2.0. The background and justification for the parameters used in our PSHA model are detailed in Section 3.0. Section 4.0 presents the results of our ground motion estimates with the soft rock uniform hazard spectra (UHS) calculated for the Plant site presented in Figure 4-1. The soft rock UHS presented in the figures include estimated spectra for our unmodified PSHA model (no mainland extension of the SWIF) and spectra at the Plant site assuming 100 percent certainty of mainland extensions of the SWIF. The difference between the UHS from the original PSHA study and the UHS from the revised PSHA study is relatively small with the UHS from the revised study only a maximum of 3 percent greater than the UHS from the original study. Finally, the modified PSHA results, including empirical estimated directivity effects are presented in Figure 4-15. If the potential mainland extension of the SWIF, as detailed in this report, is selected by the design team as a basis for design, the soft rock UHS presented in Figure 4-15 would be appropriate for design, with modification to account for soil effects as applicable.

TABLE OF CONTENTS

Page

Executive Summary i

1.0 Introduction 1
- 1.1 Purpose 1
- 1.2 Scope 2

2.0 Methodology 3

3.0 PSHA Model 4
- 3.1 Earthquake Sources 4
  - 3.1.1 Cascadia Subduction Zone 5
    - 3.1.1.1 Interplate Source 6
    - 3.1.1.2 Intraslab Source 10
  - 3.1.2 Regional Areal Crustal Source Zones 11
  - 3.1.3 Fault Specific Sources 12
    - 3.1.3.1 Seattle and Tacoma Faults 13
    - 3.1.3.2 Puget Sound Fault 16
    - 3.1.3.3 Southern Whidbey Island Fault (SWIF) Zone 17
    - 3.1.3.4 Utsalady Point Fault 20
    - 3.1.3.5 Strawberry Point Fault 21
    - 3.1.3.6 Devils Mountain Fault 21
    - 3.1.3.7 Olympia Fault 22
    - 3.1.3.8 Hood Canal Fault 22
- 3.2 Recurrence Models 23
- 3.3 Ground Motion Attenuation Relationships 24
  - 3.3.1 Cascadia Subduction Zone Earthquakes 24
  - 3.3.2 Shallow Crustal Earthquakes 24
- 3.4 Fault Activity Weighting Factors 25

4.0 Results of Probabilistic Seismic Hazard Analyses 25
- 4.1 Results Prior to PSHA Model Modification 25
- 4.2 Results With PSHA Model Modification 26
- 4.3 Results with Fault Directivity 27

5.0 Limitations 28

6.0 References 29

LIST OF TABLES

Table No.

3-1	Seismic Source Parameters for Interplate and Intraslab Source Zones
3-2	Seismic Source Parameters for Regional Areal Crustal Source Zones
3-3	Seismic Source Parameters for Specific Crustal Source Faults
3-4	Estimated CSZ Maximum Rupture Widths

LIST OF FIGURES

Figure No.

1-1	Vicinity Map and Major Crustal Structures in the Central Puget Sound and Adjacent Areas
2-1	Seismic Source Logic Tree
3-1	Seismogenic Plate Interface Alternatives
3-2	Cascadia Subduction Zone Typical Geologic Cross Section
3-3	Segmentation of the Cascadia Subduction Zone
3-4	Modeled Intraslab Source Zones
3-5	Modeled Crustal Source Zones
3-6	Modeled Crustal Faults
3-7	Puget Lowland Crustal Cross Section
3-8	Modeled Seattle, Puget Sound and Tacoma Faults
3-9	Southern Whidbey Island Fault Zone Model Y1 in the Plant Vicinity
3-10	Southern Whidbey Island Fault Zone Model Y2 in the Plant Vicinity
4-1	Soft Rock Acceleration Spectra
4-2	Seismic Source Contributions Peak Ground Acceleration
4-3	Seismic Source Contributions 0.1 Second Acceleration
4-4	Seismic Source Contributions 0.2 Second Acceleration
4-5	Seismic Source Contributions 0.5 Second Acceleration
4-6	Seismic Source Contributions 1.0 Second Acceleration
4-7	Seismic Source Contributions 2.0 Second Acceleration
4-8	Magnitude & Distance Contribution Peak Ground Acceleration 2500-year EQ
4-9	Magnitude & Distance Contribution 0.1 Second Acceleration 2500-year EQ
4-10	Magnitude & Distance Contribution 0.2 Second Acceleration 2500-year EQ
4-11	Magnitude & Distance Contribution 0.5 Second Acceleration 2500-year EQ
4-12	Magnitude & Distance Contribution 1.0 Second Acceleration 2500-year EQ
4-13	Magnitude & Distance Contribution 2.0 Second Acceleration 2500-year EQ
4-14	Spectral Acceleration Factors Average Directivity Effects
4-15	Soft Rock Acceleration Spectra With Directivity Effects

LIST OF APPENDICES

Appendix

A	Tectonics and Seismicity
B	Seismicity Catalog and Earthquake Recurrence
C	Important Information About Your Geotechnical Report

Revised
Probabilistic Seismic Hazard Analyses
Brightwater Project SR-9 Site
King County Department of Natural Resources, Washington

1.0 Introduction

1.1 Purpose

This report provides the results of revised probabilistic seismic hazard analyses (PSHA) performed for the SR-9 (Plant) site (47.7878°N, 122.1403°W, NAD83) of the proposed Brightwater Project. A Vicinity Map with the location of the Plant site is shown in Figure 1-1. The original PSHA was performed under contract to CH2M Hill, Contract No. E13035E, Change Notice No. 60, Purchase Order Number 63883, authorized on November 5, 2002, with Revision No. 4 dated February 23, 2004, and Revision No. 5 dated May 26, 2004. The results of the original PSHA were provided in a report by Shannon & Wilson, Inc. to CH2M Hill, dated June 30, 2004 (Shannon & Wilson, 2004a). The revised PSHA was performed under contract to CH2M Hill, Contract No. P93012P, Change Notice No. 44, Purchase Order Number 58871, Task Number 157689.EP.36.04, authorized on October 22, 2004, with Revision No. 8 dated January 7, 2005.

The purpose of the original PSHA work was to develop soft rock uniform hazard response spectra for the Plant and Portal 41 sites. Specifically, response spectra for ground motions with 2 percent probability of exceedance in 50 years (approximately 2,500-year return period) were developed using our existing PSHA model, with modifications to consider recently postulated geometries and seismogenic models of the Southern Whidbey Island Fault (SWIF), including possible mainland extensions. The results of regional geophysical studies suggest that the mainland extension of the SWIF may pass across or within a few kilometers (km) of the proposed Plant site; however, at the time the original PSHA was conducted (Shannon & Wilson, 2004a), detailed fault trenching for the mainland extension at or near the Plant site by the U.S. Geological Survey (USGS) and the King County design team to attempt to confirm the presence of a fault and its possible activity had not been done. Consequently, the ground motion hazard in the original PSHA was calculated for a case in which the extension was assumed, with 100 percent certainty, to be active to provide a suitable basis of design in the event that future

research work by the USGS and the King County design team confirmed the location and activity of the postulated extensions.

Since submission of the results of the original PSHA, the USGS and the King County design team have conducted fault trenching studies at and near the Plant site (see AMEC, 2005; personal communication with USGS investigators documented in Shannon & Wilson, 2004b) on the Bear Creek Lineament (lineament 4 of Blakely et al., 2004) and Cottage Lake Lineament of the Southern Whidbey Island Fault (SWIF) Zone. Therefore, the purpose of the revised PSHA is to re-calculate of the 2,500-year soft rock uniform hazard response spectrum at the plant site based on the available results of the fault trenching studies and peer review comments by USGS scientists.

1.2 Scope

Our scope of work for the revised PSHA, as outlined in our proposal of October 19, 2004 to CH2M Hill and our letter of November 17, 2004 to CH2M Hill regarding proposed revisions to the PSHA (Shannon & Wilson, 2004b), is summarized below.

We performed probabilistic seismic hazard analyses to develop soft rock uniform hazard response spectra (UHS) for 2,500-year return period ground motions at the Plant site. The PSHA involved characterization of the potential seismogenic sources (i.e., geometry, maximum magnitude, and recurrence rates) and source-dependent ground motion attenuation. A logic tree approach was used to account for the multiple seismogenic models and ground motion attenuation relationships.

For the revised PSHA study, characterization of the SWIF was modified from the original study based on the results of currently available fault trenching studies at or near the Plant site by the USGS and the King County design team (AMEC, 2005; personal communication with USGS investigators as documented in Shannon & Wilson, 2004b) and peer-review of the original PSHA by the USGS. Modifications to the SWIF in the PSHA model included (1) adjustments to the location of fault strands at or near the Plant site, (2) extending the SWIF farther on land to the southwest, (3) including a truncated Gutenberg-Richter magnitude earthquake recurrence relationship, and (4) including a possible thrust-type fault mechanism for the SWIF

We met with the King County design team and the USGS during the PSHA revision work to discuss the findings of the fault trenching studies, implications to ground motion hazards, and incorporation of these studies in the revised PSHA (see Shannon & Wilson, 2004b).

Based on the results from our revised PSHA, we developed hazard curves for spectral periods of 0, 0.1, 0.2, 0.5, 1, and 2 seconds. These hazard curves define the soft rock UHS for 2,500-year return period ground motions for each case. A deterministic estimate of fault near-source directivity effects and modified soft rock UHS were made for the postulated landward extension due to the proximity of the Plant site. A deaggregation of the revised PSHA results is also provided.

2.0 Methodology

Three fundamental parameters are required for calculation of the ground motion hazard. These fundamental parameters are:

- Physical size and location (geometry) of potential earthquake sources (e.g., fault length, orientation, dip, rupture width, depth, segmentation).
- How often these sources generate earthquakes (e.g., active versus inactive, slip rates, Gutenberg/Richter recurrence model versus characteristic model).
- Ground motion attenuation between a source and a given site.

Typically, not every aspect of these parameters is known precisely. Unlike many other loads on a structure, the uncertainties in the parameters that determine earthquake ground shaking can be enormous. Furthermore, even if all aspects of these parameters are known with no uncertainty, there is some amount of natural random variability associated with earthquakes (e.g., the same magnitude earthquakes on a given fault do not produce identical ground motions).

To develop design ground motions that account for uncertainties associated with these earthquake parameters and natural random variability of earthquake processes in a rational, consistent, quantifiable manner, a PSHA is used. Key to the PSHA is a logic tree, which is used to identify every significant aspect of the basic earthquake parameters. Where current knowledge of the various earthquake parameters is incomplete and allows for multiple models, the potential models are identified on the logic tree as a branch, and a degree of belief or weighting factor is assigned to each branch. Ground motions are calculated for every branch of the logic tree. The ground motion hazard is then the summation of the products of the calculated ground motions and the associated weighting factor of each branch.

Figure 2-1 shows a portion of the logic tree used in this study for the Cascadia Subduction Zone. Each node on the logic tree represents a source parameter; branches from the nodes indicate possible models for the parameter. The weighting factor for the particular branch or model parameter at the node is shown in parenthesis. The sum of the weighting factors for the branches at any given node must equal 1.0. We note that the logic tree shown in Figure 2-1 is not complete in that not every branch is shown in its entirety. Typically, only a few of the branches are shown completely to illustrate the various model parameters considered at each node; it is implicit that the model parameters at a given node shown on a given branch of logic tree are the same for those branches not shown.

The computer program HAZ35 (Abrahamson, 2003) was used to perform the PSHA for this project. HAZ35 calculates seismic hazard using the methodology for probabilistic hazard analysis originally developed by Cornell (1968), McGuire (1976, 1978), and Der Kiureghian and Ang (1975, 1977). The basic assumption of the model is that the spatial locations of earthquakes within a given source zone are completely random, and that they occur independently in time (i.e., as a Poisson process).

Because a PSHA is probabilistic, the ground motion hazard is typically expressed as the probability of a given ground motion level occurring during a given time or return period. For the Plant site, the ground motions were calculated for a 2 percent probability of exceedance in 50 years or about a 2,500-year return period. The 2,500-year return period is consistent with the International Building Code (IBC) 2003 requirements for seismic design, which is being used as a basis for design of the project.

3.0 PSHA Model

The geometries, recurrences, and ground motion attenuation relationships for the seismic sources modeled in the PSHA are provided in Tables 3-1 through 3-3. Also shown in Tables 3-1 through 3-3 are the weighting factors for the various models. In many cases, the parameters represented by the branches of the logic tree at a particular node are assigned equal weights. This uniform distribution of weighting factors was used when the available evidence did not indicate that one model was preferred over the others. Specific branches of the logic tree where data suggest alternative distributions of weighting factors are discussed in the following sub-sections of this report.

For the intraslab source zone in Table 3-1 and the areal crustal source zones listed in Table 3-2, a maximum earthquake magnitude is indicated. Earthquake magnitude is a function of the type and size of the fault or rupture area. For discrete sources where the geometry adequately describes the rupture area, the earthquake magnitude is implicit. For the areal source zones where discrete ruptures are not modeled, the maximum magnitude within the source zone must be specified.

The following sub-sections of the report describe the PSHA model, summarize the parameters in Tables 3-1 through 3-3 used in the PSHA, and detail the basis for parameter selection.

3.1 Earthquake Sources

Within the present understanding of the regional tectonics and historical seismicity presented in Appendix A, three broad seismogenic source zones have been identified, namely:

- The interplate portion of the Cascadia Subduction Zone (CSZ), which may produce large mega-thrust events.
- The deep intraslab portion of the CSZ, which has been the source of the largest historic earthquakes to affect the area.
- Shallow crustal sources.

In the PSHA, the CSZ interplate source is modeled as a discrete (albeit large) fault. The intraslab portion of the CSZ is modeled as an areal source zone at depth. The shallow crustal seismicity is modeled with nine areal source zones (Vancouver Island, Olympic Mountains, Willapa Hills, Coast Range, Willamette Lowland, North Puget Sound, Central Puget Sound, North Cascades, South Cascades) and nine discrete fault sources (Olympia Fault, Tacoma Fault, Puget Sound Fault, Seattle Fault, Hood Canal Fault, Southern Whidbey Island Fault, Utsalady Fault, Strawberry Point Fault, and the Devils Mountain Fault).

Areal source zones were used to model much of the crustal seismogenic potential because thick Quaternary deposits conceal the bedrock structure of most of the Puget Lowland, repeated geologically recent glaciation generally obliterates all but the most recent surface evidence of faulting, and historic shallow crustal seismicity does not appear associated with identified crustal faults. Large crustal faults or potential crustal faults identified within approximately 100 km of the Plant site, capable of producing earthquakes of at least magnitude 6.5, and with evidence of or postulated Late Pleistocene or Holocene movement or kinematically associated faults were modeled as discrete sources. These sources are summarized in Table 3-3.

A description of the specific earthquake sources and parameters are provided in the following subsections.

3.1.1 Cascadia Subduction Zone

The CSZ extends over a length of approximately 1,100 km from southern British Columbia in the north to northern California in the south (Figure 3-1). While there is a lack of historically observed interplate earthquakes on the CSZ, significant paleo-seismological evidence (Appendix A) suggests that large mega thrust events on the interface between the subducting and overriding plates occur on average about every 400 to 600 years.

Earthquakes also originate within the subducting plate. Such intraslab earthquakes are extensional events that occur within the subducting Juan de Fuca plate. As this plate subducts beneath the North American plate, stress and physical changes in the subducting plate produce high-angle normal faulting earthquakes such as the 1949 Olympia, 1965 Seattle-Tacoma, and 2001 Nisqually events.

Figure 3-2 shows a cross-section through the subduction zone and the central Puget Sound Basin that identifies these two earthquake sources based on Hyndman and Wang (1995) and Stanley et al. (1999). Shown on this figure are the locked and transitional portions of the interface between the North American Plate and the subducted Juan de Fuca Plate as well as the zone of free slippage. Movement along both the locked and transitional parts of the interface can generate large mega-thrust events. Also shown on this figure are the locations of the historical Juan de Fuca intraslab events within the Juan de Fuca slab. The interplate and intraslab sources are described in the following two sections.

3.1.1.1 Interplate Source

The seismogenic portion of the CSZ is bounded in both the updip and downdip directions. Because no direct measurements of the boundaries of the seismogenic portion are available, their positions must be estimated from indirect evidence.

Updip Extent. At depths shallower than the updip boundary, relative plate motion occurs aseismically. Hyndman and Wang (1993) used temperature considerations to conclude that brittle behavior would be associated with the dehydration of stable sliding clays above temperatures of 100°C to 150° C; thermal modeling suggested that the updip boundary of the CSZ is near the deformation front (Figure 3-1). Using geophysical data to map folds and faults along the CSZ in north-central Oregon, Goldfinger et al. (1992a, b) defined a slope break located approximately 30 km east of the deformation front, which was postulated as representing the updip boundary (Figure 3-1).

For the Plant site seismic hazard analysis, the following two updip boundaries were considered in the PSHA:

1. An updip boundary corresponding to the deformation front.

2. An updip boundary corresponding to the slope break identified by Goldfinger et al. (1992a, b).

As indicated in Table 3-1, equal weights (0.5) were assigned to both boundaries.

Downdip Extent. Crustal uplift and subsidence deformations measured preceding and following interface earthquakes in other parts of the world offer information on the downdip extent of rupture. The accumulation and eventual release of strain energy in a locked zone produces a pattern of surface uplift and subsidence that has been correlated to the spatial extent of rupture. The "zero isobase," or boundary between regions of surface uplift and subsidence (Plafker and Kachedoorian, 1969; Dragert et al., 1994) has been shown to approximate the downdip extent of rupture in past subduction earthquakes. The landward extent of the zero isobase boundary is shown in Figure 3-1 (a) and (d).

At depths greater than those corresponding to the downdip boundary, temperatures are high enough that the rock behaves in a ductile manner that accommodates plate motion aseismically. The transition between brittle and ductile behavior typically occurs at temperatures of 350° C to 450°C for metamorphosed sedimentary rocks (Hyndman and Wang, 1993). Tichelaar and Ruff (1993) used thermal characteristics and maximum rupture depths from worldwide subduction zones to infer that the brittle-ductile transition occurs at approximately 400°C for silicic upper plate rock and about 550°C when the upper plate contains mafic rock. Hyndman and Wang (1993, 1995) modeled the thermal regime along the CSZ and concluded that the subduction zone was locked at temperatures less than 350°C and uncoupled at temperatures above 450°C with a transition zone at intermediate temperatures (Figure 3-2). The

transition zone (at temperatures between 350°C and 450°C) was considered to be incapable of nucleating rupture but remained capable of propagating rupture. The landward extent of the assumed boundary for the midpoint of the transition is shown in Figure 3-1 (b) and (e).

Stanley et al. (1999) recently developed a three-dimensional velocity model of western Washington that indicated the presence of a high-velocity zone at the bottom of the North American plate beneath the Puget basin. The high velocity zone had a generally flat upper surface beginning at depths of about 14 to 16 km and a dipping lower surface from 18 km on the southwest to about 33 km on the northeast; the across-strike width is about 50 km. Stanley et al. (1999) interpret the high velocity zone as consisting of voluminous mafic and ultramafic rock, and conclude that the serpentinite minerals in the body could support brittle rupture at temperatures of 400°C to 600°C. This interpretation implies that the downdip boundary of the seismogenic portion of the CSZ could extend to depths of approximately 40 km rather than the maximum depth of about 25 km that corresponds to the midpoint of the transition zone. Stanley et al. (1999) provide detailed discussions of several factors that support and contradict this interpretation. The extent of the assumed boundary for the mafic zone is shown in Figure 3-1 (c) and (f).

For the Plant site, the following three downdip boundaries were considered:

1. A downdip boundary corresponding to the zero isobase.

2. A downdip boundary corresponding to the midpoint of the transition zone defined by Hyndman and Wang (1993, 1995).

3. A downdip boundary corresponding to the eastern edge of the mafic zone identified by Stanley et al. (1999) at locations where the mafic zone is in contact with the Juan de Fuca plate, and to points halfway between the zero isobase and midpoint of the transition zone elsewhere.

Unequal weights were assigned to the different downdip boundaries. The weighting factor for the zero isobase downdip extent was set higher (0.5) than those of the other two alternatives because of its basis in empirical observations from past subduction zone earthquakes. The weighting factor for the transition zone boundary (0.33) was higher than that of the mafic zone boundary (0.17) because of the additional uncertainty involved in the assumption of the mafic composition and thermo-mechanical behavior of the high-velocity region.

Maximum Magnitude. The maximum moment magnitude of a CSZ interplate event can be obtained from the estimated geometry of the rupture surface using correlations based on actual observations in past earthquakes. Correlations between magnitude and rupture area were used. All correlations are based on the assumption that rupture occurs over the entire seismogenic width of the CSZ.

Maximum Width. The maximum width of the CSZ depends on the locations of the updip and downdip boundaries of the seismogenic zone discussed previously. The estimated maximum widths corresponding to the 2 updip and 3 downdip CSZ boundaries give rise to the six estimated maximum widths shown in Table 3-4. The widths indicated for the zero isobase and transition zone downdip boundaries shown above were obtained by averaging the variable width of the CSZ over its entire length. The width for the mafic zone downdip boundary was obtained by adding 45 km to the widths associated with the midpoint of the transition zone. The additional 45 km represents the downdip length of the high-velocity mafic body in central Puget Sound. The six postulated updip and downdip boundaries are shown in Figure 3-1.

Maximum Length. The lack of interplate activity on the CSZ requires that maximum rupture length be estimated by indirect means such as paleoseismic data, fault segmentation, and empirical aspect ratio interpretation.

Paleoseismic investigations have identified geologic evidence of large earthquakes at numerous locations along the length of the CSZ. Dating of these features is imprecise, however, and a significant error band is associated with the times at which the event producing each feature is estimated to have occurred. The error bands are wide enough, and overlap so significantly, that evaluation of temporal/spatial patterns in paleoseismic evidence does not provide estimates of the rupture lengths of individual events.

Rupture lengths may be constrained by structural factors such as bends and discontinuities in fault geometry. Geomatrix (1995) reviewed previous fault segmentation studies and identified seven segmentation boundaries along the Juan de Fuca plate. The evidence for segmentation includes changes in strike and dip, variations in seismicity, topographic variations, and other factors. Changes in strike and dip of the subducting plate are more pronounced on the northern portion of the CSZ (i.e., adjacent to Washington) than the southern portion (adjacent to Oregon, which was the focus of the Geomatrix (1995) investigation). The identified segmentation boundaries define eight segments with an average length of approximately 135 km and are shown in Figure 3-3.

Observations of worldwide interplate ruptures indicate an empirical relationship between their lengths and widths. Because the width of the CSZ is known more accurately than segment lengths, an estimate of rupture length can be obtained using the anticipated width and historical length-to-width aspect ratios. Geomatrix (1993) compiled a database of 53 interplate events of $M > 7$ with well-defined source parameters and aftershock-based information on rupture lengths and widths; this database indicates that the average aspect ratio was 2.4 and that most interplate events had aspect ratios less than 4. The weighted average of the potential CSZ widths shown above is 75 km. Using this width, the average length would be on the order of 180 km, and most events would be expected to have lengths less than 300 km.

Comparing the segmentation-based average length of 135 km with the aspect ratio-based average length of 180 km suggests that an average segment length of 150 km is reasonable. To account for the fact that more than one segment could rupture at a given time, four possible rupture lengths were considered in the seismic hazard analysis:

1. A 150 km rupture length that corresponds to the rupture of a single segment. The aspect ratio of 2 for such an event would be consistent with the average aspect ratio observed in worldwide subduction earthquakes. As shown on Table 3-1, this rupture length was assigned a weight of 0.1.

2. A 250 km rupture length that represents the average length of the rupture of two adjacent segments. The aspect ratio of about 3 for such an event would be greater than most of the aspect ratios that have been observed in similar environments. This rupture length was assigned a weight of 0.2.

3. A 450 km rupture that represents the average length of the rupture of three adjacent segments. The aspect ratio of 6 for a 450 km rupture would be among the largest that have been observed worldwide. This rupture length was assigned a weight of 0.2.

4. A 1,100 km rupture that represents the entire length of the CSZ. The aspect ratio of such an event would be approximately 14, which would be larger than any that has previously been observed. However, based on tsunami records in Japan, Satake et al. (1996) estimate a magnitude 9 event occurred on the CSZ in 1700. A magnitude 9 event on this date is also consistent with observed coseismic subsidence (Leonard et al., 2003). Consequently, this rupture length was assigned a weight of 0.5.

Determination of M_{max}. Maximum moment magnitudes were determined in a manner that considered the various potential rupture lengths described above and maintained consistency with best estimates of the recurrence rates of CSZ earthquakes.

Empirical relations between rupture area and magnitude (Wells and Coppersmith, 1994) were used to estimate the maximum magnitude for each of the six updip/downdip boundary pairs, providing that the overall moment rate associated with rupture of the entire zone is conserved. Assuming that these earthquakes occur at an average recurrence interval of 600 years and making a reasonable estimate of the rigidity of the CSZ rock (Atwater and Hemphill-Haley, 1997), equivalent slip rates can be computed for each of these cases. Using these slip rates and conserving the overall moment rate, maximum magnitudes were computed for different recurrence intervals and rupture widths. For the assumed recurrence rates and various updip/downdip boundary pairs, area-based maximum magnitudes ranged from 8.0 (150 km rupture length) to 9.0 (1,100 km rupture length).

Earthquake Recurrence. The recurrence interval of characteristic CSZ earthquakes can be estimated from the results of recent paleoseismic investigations. Atwater and Hemphill-Haley (1997) summarized the results of several investigations conducted at different locations along the CSZ. At each site, time-datable evidence of a discrete number of different events was recorded and used to compute an average recurrence interval. Uncertainty in the assigned dates led Atwater and Hemphill-Haley (1997) to report ranges of recurrence intervals for each location. Assuming a symmetric, triangular probability distribution for each reported

interval and weighting each site equally, the average recurrence interval and standard deviation for large CSZ earthquakes based on geologic evidence along the entire CSZ is 657 and 204 years, respectively.

Adams (1990) reported age ranges for a series of Holocene turbidites assumed to have been derived from failures of canyon heads some 50 km west of Willapa Bay (Griggs and Kulm, 1970), an area directly above the probable area of shallow rupture on the CSZ (Hyndman and Wang, 1995). Adams interpreted the ages of the turbidites from the relatively uniform thicknesses of pelagic clay layers deposited between the turbidites. The estimated ages of five distinct events were 250-360 years, 570-830 years, 1,000-1,400 years, 1,730-2,640 years, and 2,270-3,300 years. By assuming that the ages of each of these events could be represented by symmetric, triangular probability distributions, a probability distribution for recurrence interval could be computed. This distribution indicated an average recurrence interval and standard deviation of 620 and 290, respectively years.

Atwater and Hemphill-Haley (1997) also reported ranges of age for seven distinct events based on buried soils in Willapa Bay. The estimated ages of these events were 290-310 years, 900-1,300 years, 1,110-1,350 years, 1,500-1,700 years, 2,390-2,780 years, 2,800-3,320 years, and 3,320-3,500 years. Again assuming triangularly distributed ages for each event, a probability distribution for recurrence interval based on buried soils at Willapa Bay was computed. This distribution indicated an average recurrence interval and standard deviation of 520 and 300 years, respectively.

The mean, coefficient of variation, and skew coefficients of each data set were averaged. The resulting average statistics were then utilized in a point-estimation procedure to obtain a discrete recurrence interval. The point estimation procedure produced a 600-year recurrence interval that was considered in the seismic hazard analysis.

3.1.1.2 Intraslab Source

The intraslab source represents extensional events that occur within the subducting Juan de Fuca plate. As the Juan de Fuca plate subducts beneath the North American plate, stress and physical changes in the subducting plate produce high-angle normal faulting earthquakes such as the 1949 Olympia, 1965 Seattle-Tacoma, and the 2001 Nisqually events.

Geometry. Because numerous intraslab earthquakes have been recorded, the geometry of the intraslab source is relatively well defined in Washington state. Most of these earthquakes are relatively small, but are useful for imaging the geometry of the intraslab source. Based on numerous such events, Crosson and Owens (1987) determined that the CSZ is arched, or curved, beneath Washington state. The axis of the arch, as determined by Crosson and Owens (1987) runs in a generally east-west direction. More recently, a three-dimensional velocity model developed on the basis of local earthquake tomography (Stanley et al., 1999) indicated a somewhat different arch shape with an axis that trends toward the northeast. An overlay of the

Crosson and Owens (1987) and Stanley et al. (1999) geometries is shown in Figure 3-4 and are the two source geometries used in the PSHA. A weighting factor of 0.75 was assigned to the Crosson and Owens (1987) geometry; a weighting factor of 0.25 was assigned to the Stanley et al. (1999) geometry. The Crosson and Owens (1987) geometry was weighted more heavily due to its basis in actual measured earthquake hypocentral locations.

Maximum Magnitude. Because intraslab events involve high-angle normal faulting, the area of the rupture surface is strongly dependent on the thickness of the subducting slab. Young subduction zones, such as the CSZ, generally have relatively thin subducting slabs. Thermal modeling of the CSZ (Hyndman and Wang, 1993) and the observed geometry of the Wadati-Benioff zone (Jarrard, 1986) confirm the likelihood that the subducting slab is relatively thin.

Worldwide observations indicate that the largest intraslab earthquakes are on the order of magnitude 7-1/2, with the largest of these occurring in older subducting slabs. The largest recorded intraslab earthquake beneath the Puget Lowland, 1949 Olympia earthquake, was a magnitude M_S 7.1 event. Based on these observations, the recorded intraslab seismicity of the CSZ, and the thin nature of the Juan de Fuca plate, maximum intraslab earthquake magnitudes used in the PSHA are 7.1, 7.25, and 7.5 with weighting factors of 0.2, 0.6, and 0.2, respectively.

3.1.2 Regional Areal Crustal Source Zones

The tectonic subprovinces described by McCrumb et al. (1989) within the fore-arc and volcanic arc (Figure A-1, Appendix A) were used as the basis for developing the regional aerial crustal zones. Based on historical seismicity rates, the Olympic Mountains, Willapa Hills, and Coast Range subprovinces were combined into a single areal source zone. The resulting areal source zones used in the seismic hazard analysis are shown in Figure 3-5.

Most of the historical shallow crustal seismicity in the region outside of the Puget Lowland is distributed between the depths of about 2 to 20 km. In regions outside the Puget Lowland (i.e., Vancouver Island, Olympic/Willapa/Coast Ranges, North Cascades, South Cascades, and Willamette) depths of 2 km (weighting factor = 0.2), 11 km (weighting factor = 0.6), and 20 km (weighting factor = 0.2) are used in the PSHA. A distribution about a depth of 11 km was assumed by using lower weighting factors at depths of 11-km-plus/minus-9-km. Within the Puget Lowland (i.e., the North Puget Sound and Central Puget Sound areal source zones), observed historical shallow crustal seismicity typically occurs at deeper depths with most instrumental seismicity occurring between depths of about 5 to 25 km. Consequently in the North Puget Sound and Central Puget Sound zones, depths of 5 km (weighting factor = 0.2), 15 km (weighting factor = 0.6), and 25 km (weighting factor = 0.2) are used in the PSHA.

With the exception of the Central Puget Sound, three different maximum magnitudes were considered: M7.0 (weighting factor = 0.2), M7.25 (weighting factor = 0.6), M7.5 (weighting factor = 0.2). These magnitudes and weighting factors were selected to be at least

equal to or larger than the largest crustal event historically observed in these zones (1872 North Cascades magnitude 6.8 +/- event), but not larger than the maximum magnitude assumed on the Seattle or Southern Whidbey Island Faults (M7.5). Within the Central Puget Sound, a maximum magnitude of 7.0 (weighting factor = 1.0) was used, because known or potential faults capable of generating magnitude 7.0 or greater earthquakes (e.g., Olympia, Tacoma Seattle, Hood Canal, Puget Sound, Southern Whidbey Island, Utsalady Point, Strawberry Point, Devils Mountain Fault) are explicitly modeled in the PSHA.

The lack of evidence of late Pleistocene or Holocene movement (e.g., ground surface rupture) would generally tend to indicate a smaller maximum earthquake magnitude. However, considering the thick mantle of Quaternary sediment, repeated glaciation of the Puget Lowland, and the generally thick vegetative cover in the region, it is plausible that such evidence of ground rupture has been obscured or has gone undetected.

Regions of higher shallow crustal seismicity around Mount St. Helens and Mount Rainier were incorporated into the larger South Cascades areal source zone and were not explicitly modeled. Given that the estimated maximum magnitude (M6.8 for the Mount St. Helens Zone [Weaver and Smith, 1983)], M5 ¾ for the Mount Rainier Zone), and the relatively large distance between the center of the zones and the Plant site (over 100 km to the center of either zone), and the location of larger crustal sources closer to the site, this simplification in the modeling is reasonable for the this study.

3.1.3 Fault Specific Sources

In addition to the areal crustal zones, fault specific sources were also considered. The Seattle, Puget Sound, Southern Whidbey Island, and Utsalady Point Faults were modeled in the PSHA explicitly as there is evidence of Holocene movement on these structures with estimates of slip rates and geologic evidence that, though preliminary, provide indications of possible recurrence rates. The Olympia, Tacoma, Strawberry Point, and Devils Mountain Faults were also included as there is postulated or evidence of Holocene or Pleistocene movement. Potential slip rates have been published for the Strawberry Point and Devils Mountain Faults, while likely bounding estimates on the slip rates on the Olympia and Tacoma Faults can be made from associated slip rates from the other faults in the Lowland and geodetic measurements. The Hood Canal Fault was also explicitly modeled due to its association with the other active faults within the Puget Lowland. The approximate locations of these faults modeled in the PSHA are shown on Figure 3-6.

3.1.3.1 Seattle and Tacoma Faults

There are three published models of the crustal structure of the central Puget Lowland. The postulated geometries of the Seattle and Tacoma Faults vary significantly among the published models. The published models consist of a "thin-skinned" model (Pratt et al., 1997), a "thick-skinned" model (Wells and Weaver, 1993; Brocher et al., 2001), and a "Passive Roof Duplex" model (Brocher et al., 2004). The cross-section through the Puget Lowland shown in Figure 3-7 illustrates the three models. Because of the significant variations in fault geometries among these models, all three models were considered in the PSHA. The "thin-skinned," "thick-skinned," and "Passive Roof Duplex" models are designated as Model A, B and C, respectively. The weighting factors for these models are shown on Table 3-3. Models A and B were given equal weights (0.25). A higher weight was given to Model C (0.5) as it is more consistent with the observed near surface fault scarps and folds.

The "thin-skinned" model is indicated as Model A in Table 3-3 and Figures 3-7 and 3-8. In Model A, the Seattle Fault is modeled with a 20 to 25 degree dip to the south and extending to a depth of 14 to 20 km. Calvert and Fisher (2001) indicate that within approximately one-half km of the ground, splays within the Seattle Fault Zone dip to the south at about 60 degrees and may vary between 80 and 40 degrees. Johnson et al. (1999) show the Seattle Fault dipping at about 60 to 85 degrees within 3 km of the surface. Splays that have been trenched to date show surface ruptures that are north dipping and must represent back-thrusts in this model; the south dipping master fault has not been observed in any of the fault trenching studies to date. The east segment of the Tacoma Fault is considered to be the down-dip extent of the Seattle Fault where it soles into a decollement at a depth of about 14 to 20 km and is not considered to be an independent crustal source in this model. The center segment of the Tacoma Fault is included in Model A as an independent source (based on observed scarp and trenching studies on this segment) with a north dip of 50 to 80 degrees and extending to a depth of 15 to 25 km. The north-south tear on the west end of the Tacoma Fault is also considered to be a seismogenic source in Model A.

The "thick-skinned" is indicated as Model B in Table 3-3 and Figures 3-7 and 3-8. In Model B, the Seattle Fault is modeled as three independent faults (north, center, and south) with 35 to 50 degree dips to the south and extending to a depth of 24 to 28 km to the base of the volcanic rock basement (Crescent Formation) beneath the Puget Lowland. Fault splays within the Seattle Fault Zone that have been trenched to date show surface ruptures that are north dipping and must represent back-thrusts in this model. The principal south dipping fault surfaces in this model have not yet been observed in any of the fault trenches to date. The east and center segments of the Tacoma Fault are modeled as independent of (i.e., not part of) the Seattle Fault. Both the center and east segments are modeled with a 50 to 80 degree dip to the north and extending to a depth of 15 to 25 km. One branch of this model assumes that the maximum earthquake magnitude from these segments is for a single event rupturing both segments; the alternate branch assumes that fault is segmented such that a single maximum event cannot rupture across both segments. The north-south tear on the west end of the Tacoma Fault is also considered to be a seismogenic source in Model B.

The "Passive Roof Duplex" model is indicated as Model C in Table 3-3 and Figures 3-7 and 3-8. In Model C, the Seattle uplift is underlain by two master floor thrusts; a south dipping Seattle Fault on the north, and a north dipping Tacoma Fault on the south. Both faults are interpreted as blind thrusts that flatten up-dip into bedding plane thrusts at a depth of about 4 km within the adjacent basins. The overlying shallow roof thrust is passive and only slips when the underlying master faults rupture. The up-dip extent of the seismogenic portions of the master floor thrusts is defined as the wedge tips (intersection) of the floor and roof thrusts in the basins. The approximate locations of the postulated Seattle and Tacoma Fault wedge tips are shown on Figures 3-7 and 3-8. The Passive Roof Duplex model is consistent with the lack of observed south-dipping fault surfaces in the fault trenches excavated to date within the Seattle Fault Zone; the observed north-dipping rupture surfaces sole into the passive roof thrusts while the south dipping master fault does not extend up to the ground surface. Similar to the thin-skinned model, the Seattle Fault in Model C of the PSHA has a shallow dip of 25 to 35 degrees to the south and extends to depths of 12 to 20 km where it soles into a decollement. The east and west segments of the Tacoma Fault are modeled as independent of (i.e., not part of) the Seattle Fault. Both the east and west segments of the Tacoma Fault are modeled with a 30 to 35 degree dip to the north and extending to a depth of 12 to 16 km where it soles into the Seattle Fault. One branch of this model assumes that the maximum earthquake magnitude from the Tacoma Fault segments is for a single event rupturing both segments; the alternate branch assumes that fault is segmented such that a single maximum event cannot rupture across both segments. The north-south tear on the west end of the Tacoma Fault is also considered to be a seismogenic source in Model C.

Seattle Fault Zone Segmentation. The location of the Seattle Fault used in the seismic hazard analysis is shown in Figure 3-8. The maximum fault rupture length is estimated to be approximately 60 km (Blakely et al., 2002; ten Brink et al., 2002). Two 1 km north-south offsets in the fault trend beneath the Puget Sound east of Bainbridge Island segment the Seattle Fault into an approximately 40 km-long east segment and 20 km-long west segment (Calvert et al., 2003; and Johnson et al., 1999). However, geologic evidence of rupture on this fault approximately 1,100 years before present suggests that this segmentation does not limit rupture length (i.e., rupture occurs across both segments). Therefore, a weighting factor of 0.0 was assigned to the possibility of fault segmentation constraining the rupture length on the Seattle fault.

Seattle Fault Zone Maximum Magnitude. In the "thin-skinned" model, the 30 to 40 km-long eastern portion of the Tacoma structure that defines the north edge of the Tacoma basin is interpreted as the south end of the Seattle Fault. This geometry results in a down dip width of approximately 32 to 43 km. Assuming dips of 20 to 25 degrees and maximum rupture depths between 14 and 20 km, the estimated mean maximum magnitude may be about 7.2 to 7.5. For the "thick-skinned" model (assuming a maximum rupture depth of 24 to 28 km and dips of about 40 to 50 degrees), estimated mean maximum magnitudes may be about 7.2 to 7.4, based on the relationship between rupture area and magnitude by Wells and Coppersmith (1994). For the "Passive Roof Duplex" model (assuming a maximum rupture depth of 12 to 20 km and dips of about 25 to 35 degrees), estimated mean maximum magnitudes may be about 7.0 to 7.4.

Seattle Fault Zone Slip Rate. From marine seismic reflection data Johnson et al. (1999) estimated a minimum slip rate of 0.6mm/yr on the northern most fault in the Seattle Fault and estimated a slip rate between 0.7 and 1.1 mm/yr across the entire zone. A slip rate of 0.7 mm/yr and characteristic earthquake magnitudes of 7.2 and 7.5 correspond to recurrence intervals of approximately 2,400 years to 3,000 years respectively; a slip rate of 1.1 mm/yr corresponds to an interval of approximately 1,600 to 2,300 years. Fault trenching studies by the USGS on the Toe Jam Hill Strand of the Seattle Fault on Bainbridge Island and Waterman Point Strand near Port Orchard begin to provide some indication of recurrence intervals on the fault. The trenching studies completed thus far seem to indicate that at least 4 to 5 events ruptured the ground surface on these strands of the fault over the last 16,000 years (Nelson et al., 2003a, 2003b) or roughly a recurrence rate of 3,000 to 4,000 years for an event large enough to result in ground surface rupture (about magnitude 6.5+), which would appear to be consistent with the recurrence rate estimated from the slip rates. However, the geologic data indicate that most of these events have been clustered over the last few thousand years. Event clustering observed on the Toe Jam Fault Strand in the Seattle Fault Zone results in a post-glacial (last 16,000 years) slip rate estimate of approximately 0.2 mm/year and a late Holocene slip rate (last few thousand years) of approximately 2 mm/year on this strand. The lack of observed uplifted terraces and similar geologic evidence used to infer the movement on the Seattle Fault 1,100 years ago suggests longer recurrence intervals on the order of 6,000 years (Bucknam, 2000).

For the PSHA, slip rates of 0.6, 1.0 and 1.4 mm/yr for the entire zone were used. A weighting factor of 0.6 was assigned to 1.0 mm/yr rate because it is the most consistent with the estimated slip rate across the zone. A weighting factor of 0.2 was assigned to minimum observed slip rate of 0.6 mm/year. A 1.4-mm/yr rate (approximately the best estimate slip rate plus the difference between the approximate best estimate slip rate and minimum slip rate) was also used in the PSHA and assigned a weighting factor of 0.2. In Model B (thick-skinned) these slip rates were partitioned among the three independent faults such that the slip rates on the northern two faults are equal and individually twice the slip rate on the southernmost fault. The slip rate was partitioned in this manner because the northern two fault traces appear to be more active (based on fault rupture locations observed to date) than the southern fault trace.

Tacoma Fault Maximum Magnitude. The location of the Tacoma structure is shown in Figure 3-8. Based on Brocher et al. (2001), the structure includes an approximately 20 km, northwest-southeast trending east section, an approximately 28-km long east-west trending center section, and an approximately 15 km long north-south trending west section. In the "Passive Roof Duplex" model (Model C), the east and west segments defined by the wedge tip are shown to be approximately 21 and 13 km long, respectively. In the "thin-skinned" model (Model A), the eastern portion of this structure is interpreted to be the back limb of a fault propagation fold formed by shallow, north-vergent thrusting on the Seattle Fault. In this model, the Tacoma structure represents the lower, downdip extent of the Seattle Fault where it joins the decollement at depth. In the "thick-skinned" (Model B) and "Passive Roof Duplex" (Model C) models, it is postulated that the Seattle Fault and the Tacoma structure are two separate faults (Brocher et al., 2001; Brocher et al., 2004). In these models, the Tacoma Fault is a north-

dipping reverse or thrust fault over its east and central sections with a north-south tear at the west end. The change in trend along this structure suggests the fault may be segmented.

Assuming a rupture length of 50 km (i.e., no segmentation between the east and center segments), a rupture depth of 25 km and a dip of approximately 67 degrees, the mean maximum magnitude is estimated to be about 7.1, based on the relationship between rupture area and magnitude by Wells and Coppersmith (1994). For independent ruptures on the east and central segments, mean maximum magnitudes are between 6.8 and 6.9, respectively. Based on a rupture length of 15 km for the north-south tear and using the relationship between rupture length and magnitude by Wells and Coppersmith (1994), the mean maximum magnitude for an earthquake on this segment is about 6.1.

Tacoma Fault Slip Rate. There are at present no estimates of slip rate or recurrence intervals reported for faulting on this structure. The upper bound slip rate on the east and center sections is likely bounded by estimated rates for the Seattle Fault (0.7 to 1.1 mm/yr). The absence of evidence of multiple Holocene rupture or movement would suggest a lower slip rate. For the PSHA it was assumed that slip rates on this fault would be between the slip rate on the Seattle Fault and the estimated rate of crustal shortening in southwest Washington south of the Puget Sound Basin (approximately 0.1 to 0.15 mm/yr from Wells and Johnson, 2001). Consequently, slip rates of 0.1 and 1 mm/yr were used with corresponding weighting factors of 0.4 and 0.6, respectively.

For the north-south tear structure on the west, Puget Sound Fault slip rates were assumed. This assumption is based on the relative proximity and similarities in orientation (north-south) and apparent fault type (strike slip fault) of the two faults.

3.1.3.2 Puget Sound Fault

This fault zone reported by Johnson et al. (1999) is a north-south trending zone of near vertical strike-slip fault strands. The location of the fault used in the seismic hazard analysis is shown in Figure 3-8. The total length of this zone mapped by Johnson et al. (1999) is about 55 km. While this fault may be segmented, it appears in offsets of the east-west trending Seattle fault such that segmentation may not limit rupture length. Johnson et al. (1999) do not indicate a maximum depth, but their seismic reflection data indicate a minimum depth of at least 6 km. It would be reasonable to assume that the fault extends to about the same depth of the Seattle Fault. Based on the relationship between rupture length and magnitude by Wells and Coppersmith (1994), and assuming a rupture length of 55 km (i.e., no segmentation) and a rupture depth of 15 to 25 km, the mean maximum magnitude is estimated to be about 6.9 to 7.1.

Slip rates on the Puget Sound Fault estimated from marine seismic reflection data are reported between 0.3 and 0.8 mm/yr. As indicated on Table 3-3, both slip rates were used in the PSHA with equal (0.5) weighting factors. Assuming a characteristic earthquake recurrence

model and a mean maximum magnitude of 6.9 to 7.1 (i.e., no segmentation), recurrence intervals range from about 1,800 to 5,100 years.

3.1.3.3 Southern Whidbey Island Fault (SWIF) Zone

Johnson et al. (1996) describe the SWIF Zone as a 6 to 11 km wide, northwest-trending, northeast steeply dipping zone extending at least 70 km from the eastern Strait of Juan de Fuca to as far south as Possession Sound, as shown by the solid lines on Figure 3-6. The zone is characterized by inferred reverse, thrust, and strike slip (dextral) displacement on different splays. Johnson et al. (1996) characterize dips on individual splays within the zone varying from vertical to 45 degrees, and the fault zone extending to a depth of at least 8 km and possibly as deep as 27 km. Based on land-level changes observed in coastal marshes on Whidbey Island, Kelsey et al. (2004) identify a magnitude 6.5 to 7.0 event on a northern splay approximately 2,800 to 3,200 years ago with approximately 1 to 2 meters ground surface uplift (north-side up). They postulate that the movement occurred on a steep, north-dipping, blind, reverse fault, and assuming a 60 degree dip, the net slip was at least 1.2 to 2.3 meters. Actual slip could be greater if there were a strike-slip component of movement.

On the mainland, approximately 4 to 5 instances of late Pleistocene to late Holocene vertical ground deformations ranging from 0.3 meters to 1 to 2 meters have been observed in recently completed and on-going trenching studies by the USGS and the King County design team (AMEC, 2005; personal communication with USGS investigators as documented in Shannon & Wilson, 2004b). Similar to the ground deformations reported by Kelsey et al. (2004), deformations observed to date on the mainland have been north-side up with an undetermined amount of movement parallel to the fault (i.e., strike-slip).

Based on similarities between the SWIF and the Seattle Fault Zone, an alternate to the SWIF model based on the description by Johnson et al. (1996) could be considered. Specifically, the north-side up ground surface deformations observed to date along with the location of a basin to northeast of the SWIF (i.e., the Everett Basin) is similar to the north-side up ground surface deformations and the Seattle Basin associated with the Seattle Fault Zone. The relationship between the north-side up ground surface deformations and basin on the northeast side of the fault can be explained by a south-southwest dipping master floor thrust with the tip of the thrust buried in the Everett Basin to the north-northeast, and an overlying passive roof thrust at or near the Plant Site, similar to the Passive Roof Duplex model for the Seattle Fault proposed by Brocher et al. (2004).

In the revised PHSA study, two models of the SWIF are considered: (1) a series of steeply dipping faults (Johnson et al., 1996 model and used in the original Shannon & Wilson (2004) PSHA) and (2) a single south-southwest dipping reverse fault (analogous to Brocher et al. 2004 Passive Roof Duplex model for the Seattle Fault). In the revised PSHA study, the SWIF

model base on Johnson et al., 1996 characterization is referred to as Model Y; the single south-southwest dipping reverse fault is referred to as Model Z. A weighting factors of two-thirds was assigned to Model Y and one-third to Model Z. A higher weighting factor was given to Model Y, the Johnson et al., 1996 model, as it has been published in a peer-reviewed journal; Model Z has only been suggested as a potential model (personal communication with USGS investigators documented in Shannon & Wilson, 2004b) and has not undergone the same level of peer-review.

The locations of the Southern Whidbey Island Fault zone used in the initial PSHA model and Model Y for the revised PSHA are shown in Figure 3-6. Based on Johnson et al. (1996) and Johnson et al. (2000), the zone north of the mainland was modeled with a northern, center, and a southern splay, with lengths of 68, 72, and 76 km, respectively, in the initial PSHA model. The splay locations northwest of the mainland are based on interpretation of industry and high resolution marine seismic-reflection data (offshore); on Whidbey Island, the splay locations are based on integrated investigations using onshore seismic-reflection data, onshore outcrops, borehole analysis, and geophysical anomalies by Johnson et al. (2000). This model is more detailed than the simplified model used in the USGS National Seismic Hazard Mapping Project (Frankel et al., 2002). In the USGS study, the SWIF Zone is model with a single, 62.5 km long fault (Haller et al., 2002), extending approximately 12 km onto the mainland (Frankel et al., 1996).

In the revised PSHA Model Y, the three splays were postulated to extend farther to the southeast onto the mainland, for a total length of approximately 140 km, as shown in Figure 3-1. These postulated mainland extensions between Puget Sound and approximately the King-Snohomish County line in the revised model are based on magnetic anomalies and topographic scarps and lineaments detected on LIDAR imaging (Blakely et al., 2003, 2004) and discussions with USGS investigators. South of the county line, the center splay was extended to include a northwest-trending fault through Rattlesnake Mountain south of North Bend mapped by the Washington Division of Geology and Earth Resources (WDGER, 2002). For modeling purposes, the northern and southern splays were extended south of the county line by paralleling the center splay at a distance of approximately 2 ½ km, resulting in a 5-km-wide zone (similar to observed for the SWIF farther to the northwest).

To consider the potential mainland extensions of the SWIF as identified by Blakely et al (2004) in the vicinity of the Plant site and subsequent fault trenching studies by the USGS and the King County design team, Model Y is further divided into two sub-models, namely Model Y1 and Y2. As shown on Table 3-3, these sub-models were given approximately equal weights in the revised PSHA study. The location of the magnetic anomalies, scarps, lineaments, and mainland extensions of the splays of the SWIF in Models Y1 and Y2 relative to the Plant site are shown in more detail in Figures 3-9 and 3-10, respectively.

In Model Y1, the mainland extension of the northern splay (Figure 3-9) follows a series of aeromagnetic lineaments that are roughly on strike with the portion of the fault identified northwest of the mainland. The LIDAR data examined by Blakely et al. (2003, 2004) are southwest of the mainland extension of the northern splay, so an assessment of LIDAR-based topographic scarps or lineaments has not been completed to date along this extension. The

mainland extension of the center splay also follows a series of aeromagnetic lineaments that are roughly on strike with the portion of the fault identified northwest of the mainland. The location of the mainland extension of the center splay is also based on the scarps and lineaments identified by LIDAR. Southeast of Turners Corner (the intersection of SR 9 and 212th St. S.E.), we have considered three potential locations of the center splay and are indicated as the Cottage Lake Extension, Bear Creek Extension, and Lineament X on Figure 3-9 and Table 3-3. The northern or Cottage Lake Extension of the center splay follows an aeromagnetic lineament and twelve LIDAR lineaments and scarps. Three of the scarps along this projection are identified as having high probabilities of being fault scarps (Blakely et al., 2004). The Model Y1 Cottage Lake Extension passes near Cottage Lake and within about 1 km of the Plant site. The center or Bear Creek extension of the center splay follows a series of magnetic anomalies and three LIDAR lineaments/scarps (including the lower Bear Creek drainage) and crosses the northern edge of the plant site. The single scarp identified along the Bear Creek extension of the center splay appears to be related to a landslide (Blakely et al., 2004) and may not be a fault scarp. Lineament X or the southern location of the center splay follows an aeromagnetic lineament that can be discerned from the Blakely et al (2004) data but is not specifically identified in their study. Lineament X crosses the southern tip of the Plant site. The probability of rupture assigned to the Cottage Lake, Bear Creek, and Lineament X extensions in Model Y1 are 0.4, 0.5, and 0.1, respectively. While single large (characteristic?) events with vertical displacements of 1 to 2 meters or more are observed in both the Crystal Lake trenches (Cottage Lake Extension) and the Lineament 4 trenches at or near the Plant site trench (Bear Creek Extension), we propose giving a greater weight to the Bear Creek Extension because multiple events were observed in the Lineament 4 trenches. The smallest weight is assigned to Lineament X because of the lack of observed ground surface scarps indicative of post-glacial movement on this lineament.

In Model Y2, the mainland extension of the northern splay (Figure 3-10), the Cottage Lake Extension is assumed to be the mainland extension of the northern splay. In Model Y2, the Bear Creek Extension and Lineament X are assumed to be on the center splay. The probability of rupture between the Bear Creek and Lineament X extensions in Model Y2 are 0.8 and 0.2, respectively. These weighting factors are based on the observation of multiple events in the Lineament 4 trenches (Bear Creek Extension) and a lack of observed ground surface scarps indicative of post-glacial movement along Lineament X.

For the single south-southwest dipping reverse fault (Model Z, analogous to Brocher et al. 2004 Passive Roof Duplex model for the Seattle Fault) the location of the fault tip is assumed to be no farther south than the location of the northern splay of the SWIF. Therefore, for Model Z of the revised PSHA study, the fault tip was modeled at the location of the northern Splay and northern edge of the aeromagnetic lineament zone in Blakely et al. (2004) (i.e., the same location as the northern splay in Model Y1). Because of the similar nature of the Seattle Fault Passive Roof Duplex Model (Model C) and the SWIF Model Z, the dips, depths, and corresponding weighting factors used in Model C are also used for the SWIF Model Z.

Assuming the entire length of the SWIF ruptures, the mean maximum magnitude is estimated to be about 7.5 based on the relationship between rupture length and magnitude for strike-slip faults by Wells and Coppersmith (1994). Based on Quaternary deformation observations, the slip rate is estimated to be at least 0.6 mm/yr (Johnson et al., 1996). Assuming a characteristic earthquake recurrence model for this fault and a characteristic earthquake magnitude of 7.5, this slip rate range corresponds to an earthquake recurrence interval of about 4,000 years.

As previously indicated, the minimum slip rate based on Quaternary deformation is estimated to be 0.6 mm/yr (Johnson et al., 1996), which is similar to the minimum slip rate estimated for the Seattle Fault Zone. Considering the evidence for large (magnitude 6.5 to 7.0) late Pleistocene and Holocene earthquakes (e.g., Kelsey et al., 2004; AMEC 2005) on the SWIF, the range of slip rates assumed in the PSHA, for this fault zone is the same as those used for the active Seattle Fault Zone. As shown in Table 3-3, these slip rates for the entire zone (0.6, 1.0 and 1.4 mm/yr with weighting factor of 0.2, 0.6, and 0.2, respectively) are used. For Model Y, these slip rates are partitioned equally among the three major (northern, center and southern) splays.

3.1.3.4 Utsalady Point Fault

The Utsalady Point Fault is described (Johnson et al., 2001) as a northwest-trending, subvertical, oblique-slip, transpressional fault with a length of approximately 28 km. Based on information provided in Johnson et al. (2000), a slightly longer fault length of 29 km was assumed in the PSHA. The location of the fault used in the PSHA is shown on Figure 3-6. Assuming a rupture length of 29 km, depth of rupture between 15 and 25 km and dips between 90 and 70 degrees, the mean maximum magnitude is estimated to be about 6.6 to 6.9 based on the relationship between rupture area and magnitude by Wells and Coppersmith (1994). Based on Quaternary deformation (Johnson et al., 2001), the slip rate is estimated to be between about 0.1 and 0.8 mm/yr with a best estimate of about 0.15 mm/yr. As shown in Table 3-3, these slip rates were used in the PSHA and were assigned weights of 0.2, 0.6 and 0.2, for 0.1, 0.15 and 0.8 mm/yr, respectively. Assuming a characteristic earthquake recurrence model for this fault and a characteristic earthquake magnitude of 6.6 to 6.9, the best estimate slip rate corresponds to an earthquake recurrence interval of about 5,800 to 9,200 years; slip rates between 0.1 and 0.8 mm/yr correspond to intervals of about 13,800 to 1,100 years with the shorter 1,100 year interval (based on 0.8 mm/yr slip rate and characteristic magnitude 6.6 earthquake) most consistent with the 600 to 2,100 year interval determined from the recent fault trenching studies (Johnson et al., 2003).

3.1.3.5 Strawberry Point Fault

The Strawberry Point Fault is described (Johnson et al., 2001) as a west-northwest-trending, subvertical, oblique-slip, transpressional fault with a length of approximately 25 km. Based on information provided in Johnson et al. (2000), a slightly longer fault length of 29 km was assumed in the PSHA. The location of the fault used in the PSHA is shown on Figure 3-6. Assuming a rupture length of 29 km, depth of rupture between 15 and 25 km and dips of 90 ±20 degrees, the mean maximum magnitude is estimated to be about 6.6 to 6.9 based on the relationship between rupture area and magnitude by Wells and Coppersmith (1994). Based on Quaternary deformation (Johnson et al., 2001), slip rate is estimated to be between about 0.1 and 0.9 mm/yr with a best estimate of about 0.25 mm/yr. As show in Table 3-3, these slip rates were used in the PSHA and were assigned weights of 0.2, 0.6 and 0.2, for 0.1, 0.25 and 0.9 mm/yr, respectively. Assuming a characteristic earthquake recurrence model for this fault and a characteristic earthquake magnitude of 6.6 to 6.9, the best estimate slip rate corresponds to an earthquake recurrence interval of about 3,600 to 5,500 years; slip rates between 0.1 and 0.9 mm/yr correspond to intervals of about 13,800 to 1,000 years.

3.1.3.6 Devils Mountain Fault

The Devils Mountain Fault as described by Johnson et al. (2001) is a master, transpressional, oblique slip reverse fault, characterized by both north-south shortening on a north-dipping fault plane and left lateral slip. The fault extends from the western foothills of the Cascade Mountains, west approximately 125 km to Vancouver Island. Its location is identified by geologic mapping in the Cascades (e.g., Tabor, 1994) and marine seismic reflection profiles in Skagit Bay and the Strait of Juan de Fuca (Johnson et al., 2001). The location of the Devils Mountain Fault is shown on Figure 3-6. Johnson et al. (2001) indicate that the maximum fault rupture length is estimated to be approximately 125 km. They also recognize two possible segment boundaries (one east of Whidbey Island in Skagit Bay and one in the Strait of Juan de Fuca south of southeastern San Juan Island) that might limit the rupture length; however, they have been unable to find data to test this hypothesis.

Based on marine seismic reflection profiles, Johnson et al. (2001) indicate that the fault dips between 45 to 75 degrees within the upper 1 to 2 km of the ground surface. Assuming a rupture length of 125 km (i.e., no segmentation), depth of rupture between 15 and 25 km and dips between 75 and 45 degrees, the mean maximum magnitude is estimated to be about 7.2 to 7.6 based on the relationship between rupture area and magnitude by Wells and Coppersmith (1994).

Late Quaternary and Pleistocene vertical slip rates on the Devils Mountain Fault have been estimated from stratigraphy based on well logs on Whidbey Island and on marine seismic reflection data (Johnson et al., 2001). Vertical slip rates are estimated at between 0.05 and 0.30 mm/yr with a mean between 0.15 to 0.18 mm/year. No data exist at present to

determine horizontal slip rates. As shown in Table 3-3, slip rates of 0.10, 0.16 and 0.3 mm/yr were used in the PSHA and were assigned weights of 0.2, 0.6 and 0.2, respectively. Assuming a characteristic earthquake recurrence model for this fault and a characteristic earthquake magnitude of 7.2 to 7.6, the mean slip rate corresponds to an earthquake recurrence interval of about 11,000 to 16,000 years; slip rates between 0.05 and 0.30 mm/yr correspond to intervals of about 52,000 to 5,600 years.

3.1.3.7 Olympia Fault

The location of the Olympia structure is shown on Figure 3-6. Gower et al. (1985) locate this structure at the northeast side of a positive gravity anomalies that may represent a northeast dipping homocline of Eocene basalt, with a length of 78 km. This structure was indicated to be 88 km long and considered capable in the seismic hazard assessment for the WNP-3 site at Satsop, Washington. Rogers et al. (1996) identify this structure as an 82 km long fault with potential Quaternary movement. Stanley et al. (1999) postulate that this fault dips steeply down to the southwest and forms the southern boundary of the Seattle-Tacoma Basins. Sherrod (1999) provides evidence of approximately 1 meter of rapid subsidence and liquefaction in the south Puget Sound in the vicinity of Olympia occurring approximately 1,100 years ago. He postulates that movement on the Olympia Fault could be an explanation for the observed subsidence and liquefaction.

Assuming a rupture length of 78 km (i.e., no segmentation), depth of rupture between 15 and 25 km and dips between 80 and 50 degrees, the mean maximum magnitude is estimated to be about 7.0 to 7.4 based on the relationship between rupture area and magnitude by Wells and Coppersmith (1994). This fault may or may not be segmented.

There is currently no estimate of slip rate or recurrence intervals reported for faulting on this structure. Slip rates are likely bounded by estimated rate on the active Seattle Fault within the Puget Sound Basin and the lower crustal shortening rates across southwest Washington south of the basin. The absence of evidence of multiple Holocene rupture or movement would suggest a slip rate lower than the Seattle Fault. Consequently, slip rates of 0.1 and 1 mm/yr were used with corresponding weighting factors of 0.7 and 0.3, respectively.

3.1.3.8 Hood Canal Fault

The location of the Hood Canal Fault is shown in Figure 3-6. While no evidence of Holocene or late Pleistocene movement has been observed, nor does historical seismicity seem to occur along this structure, it is associated with the much smaller East and West Saddle Mountain Faults on which Holocene movement has occurred (Wilson et al., 1979). These two small faults that are approximately 4 km combined length are roughly parallel to the Hood Canal Fault and are located approximately 3 to 5 km west of the south end of the Hood Canal Fault.

This structure was also considered capable in the seismic hazard assessment for the WNP-3 site at Satsop, Washington.

As shown in Figure 3-6, the fault is approximately 87 km long, with its location based on topography, gravity anomalies, and 3-dimensional seismic imaging (Gower et al., 1985; Johnson et al., 1994; Brocher et al., 2001). While there are no published estimates of the fault dip, the sense of movement is the west side up relative to the east and may include some strike-slip movement accommodating relative movement between the Olympic Mountains and the Puget Sound Basin.

Assuming a rupture length of 87 km (i.e., no segmentation), depth of rupture between 15 and 25 km and dips between 80 and 50 degrees, the mean maximum magnitude is estimated to be about 7.0 to 7.4. This fault may or may not be segmented. If segmented, changes in fault orientation (i.e., changes from north-south to northeast-southwest in the central portion of the fault) suggest that segments could be on the order of 40 km.

There is currently no estimate of slip rate or recurrence intervals reported for faulting on this structure. Slip rates are likely bounded by estimated rate on the active Seattle Fault within the Puget Sound Basin and the lower crustal shortening rates across southwest Washington south of the basin. The absence of evidence of multiple Holocene rupture or movement would suggest a slip rate lower than the Seattle Fault. Consequently, slip rates of 0.1 and 1 mm/yr were used with corresponding weighting factors of 0.7 and 0.3, respectively.

3.2 Recurrence Models

The magnitude-frequency recurrence relationship describes the expected distribution of earthquakes magnitudes produced by a seismogenic source. Two recurrence relationships were used in the PSHA: the truncated exponential (Gutenberg-Richter) distribution and the characteristic earthquake distribution. The Gutenberg-Richter model is typically applied to zones where the observed seismicity includes contributions from multiple sources. This relationship was used for all areal source zones. Individual faults tend to produce repeated earthquakes of similar magnitude, which is described by the characteristic earthquake model. The characteristic earthquake distribution was used to describe earthquake recurrence for the Interplate CSZ and the nine discrete shallow crustal fault sources. Appendix B provides a more detailed description of both relationships and development of the recurrence parameters for the individual seismic sources considered in the PSHA.

For the revised PSHA, both characteristic and the truncated exponential distributions were used for the SWIF. The truncated exponential distribution was included in the revised PSHA as this distribution allows for smaller magnitude earthquakes to occur on this source. The need to consider earthquakes on the SWIF significantly smaller than a characteristic earthquake is based on the fault trenching studies at Lineament 4 by the USGS and the King County design team. Specifically, there are significant differences in the amount of ground deformations observed

among the various paleoseismic events interpreted from these studies. The difference in deformations could be related to earthquakes on the SWIF with correspondingly different magnitudes. Consequently, a truncated exponential distribution was included in the revised PSHA. As indicated on Table 3-3, the characteristic distribution was given a weight of two-thirds in the revised PSHA, and the truncated exponential distribution was given a weight of one-third. A higher weighting is given to the characteristic model as this model is more typical of seismicity on an individual fault.

3.3 Ground Motion Attenuation Relationships

Ground motion attenuation relationships describe the amplitude of various ground motion parameters. Multiple relationships were used to predict ground motions from each seismic source, and equal weighting factors were used for all relationships used to predict ground motions from a particular source. The following subsections describe the ground motion attenuation relationships used in the PSHA.

3.3.1 Cascadia Subduction Zone Earthquakes

There are a limited number of attenuation relations appropriate for modeling interplate and intraslab subduction zone earthquakes. Two empirical attenuation relationships were used in the PSHA to characterize ground motion attenuation for interplate and intraslab subduction earthquakes. The first is by Atkinson and Boore (2003), which merges the subduction databases compiled by Crouse (1991) and Youngs et al. (1997) and adds data from recent Cascadia, Japan, Mexico, and Central America events. The second is by Youngs et al. (1997).

3.3.2 Shallow Crustal Earthquakes

Many more empirical attenuation relationships are available for shallow than deep earthquakes. Selection of appropriate relationships for the PSHA involved careful consideration of the consistency between the attenuation database and shallow crustal sources in the Pacific Northwest, and the range of periods over which spectral acceleration predictions can be made.

To characterize the attenuation of ground motion on soft rock from shallow crustal earthquakes, four empirical attenuation relationships were used: the relationships developed by Abrahamson and Silva (1997), Boore et al. (1997), Sadigh et al. (1997), and Campbell and Bozorgnia (2003a,b,c). These attenuation relationships are widely used to characterize the ground motions produced by shallow earthquakes and are based primarily on California strong motion data with additional selected records from Mexico, Iran, USSR, and other countries.

3.4 Fault Activity Weighting Factors

Fault activity weighting factors are used to incorporate the uncertainty associated with the activity of a fault (i.e., whether or not a fault is active). The weighting factors used in these analyses are shown in Tables 3-1 through 3-3. A weighting factor of 1.0 indicates the fault is active; 0.0 indicates the fault is inactive. For faults or seismic sources with recorded historical earthquakes, strong evidence of Holocene paleoseismicity, or close physical and likely kinematic association with a fault with these characteristics, a weighting factor of 1.0 is generally assigned. Accordingly, a weighting factor of 1.0 was assigned to both CSZ sources, all areal source zones, and the Seattle, Southern Whidbey Island, Utsalady Point, Strawberry Point, Devils Mountain, and the east-central portion of the Tacoma Fault. Faults without strong evidence of Holocene movement but with either some indication of possible Holocene movement or possible kinematic association with a fault with known Holocene movement were assigned a weighting factor of 0.5. Faults that were assigned a weighting factor of 0.5 include the Olympia, Hood Canal, Puget Sound, and the north-south tear segment of the Tacoma Fault.

4.0 Results of Probabilistic Seismic Hazard Analyses

The probabilistic seismic hazard for the Plant site was estimated for horizontal spectral accelerations for oscillator periods 0 to 2 seconds (soft rock UHS), using the existing initial PSHA model (i.e., without landward extension) and with the postulated extension past the Plant site. The soft rock UHS were extended to a period of 5 seconds using the results of the PSHA that incorporated the available attenuation relationships that extend to 5 seconds. The soft rock UHS were further modified to include the potential for near-fault rupture directivity effects resulting from movement along the postulated extension. The resulting UHS and a discussion of these results follow.

4.1 Results Prior to PSHA Model Modification

The soft rock UHS for 2,500-year return period ground motions calculated with our existing initial PSHA model without modification (no extension of the SWIF) is presented in Figure 4-1. For comparison, corresponding results of the USGS PSHA (Frankel et al., 2002) are also presented in the same figure. We note that in the USGS model, the SWIF does not extend as far inland as in our revised PSHA model. In our revised PSHA model, the splays extend approximately 60 km farther to the southeast beyond the Plant site than the USGS model. Compared to our PSHA model, the USGS model predicts higher ground motions at periods below 1 second and slightly lower ground motions at periods above 1 second. The differences in calculated ground motions may be due in large part to newer, updated ground motion attenuation relationships and areal crustal zone parameters used in our PSHA.

4.2 Results With PSHA Model Modification

Our PSHA model was modified by extending the SWIF onto the mainland as discussed in the previous sections of this report. In the revised PSHA model, the postulated extensions of the SWIF onto the mainland past the plant site to Rattle Snake Mountain were effectively given a weight of 1.0 (i.e., assumes 100 percent certainty that the fault splays extend onland as shown in Figure 3-9). While this assumption results in a higher (more conservative) estimate of the ground motion hazard, it was made so that in the event future studies by the USGS confirm that the postulated extensions indeed exist and are active, the ground motion hazard from the PSHA using the revised model would still provide an appropriate basis for seismic design for the Plant site or if design is complete, minimize the need for seismic retrofit to higher design motions. This approach was considered more cost effective by the design team than having to design or retrofit to higher ground motions at a later date.

The soft rock UHS for 2,500-year return period ground motions, including the mainland representation of the SWIF, are presented in Figure 4-1 for the Plant site. For comparison, the soft rock UHS from the June 30, 2004 PSHA report (Shannon & Wilson, 2004a) are also plotted on Figure 4-1. As can be seen on Figure 4-1, the difference in the spectra between the original June 30, 2004 PSHA study and the revised study described in this report are relatively small, with the UHS from the revised study a maximum of approximately 3 percent greater than the UHS from the original June 30, 2004 PSHA study. The calculated UHS with the model for the revised PSHA study are larger than the results from the initial existing, more general model of Western Washington without the landward extension because of the proximity of the postulated extensions to the Plant site.

The hazard curves from our revised PSHA model are presented in Figures 4-2 through 4-7 for periods of 0 (PGA), 0.1, 0.2, 0.5, 1, and 2 seconds. The hazard curves show (for a particular spectral acceleration) the contribution to total hazard of each of the modeled seismic sources for a specified return period (return period = 1/ Mean Annual Rate of Exceedance). These figures show that for periods of primary interest to the designers (i.e., less than 1 second) the SWIF Zone source dominates the ground motion hazard, contributing over 80 percent to the hazard.

The deaggregation results from our PSHA model are shown in Figures 4-8 through 4-13 for periods of 0 (PGA), 0.1, 0.2, 0.5, 1, and 2 seconds. The deaggregation plots show the magnitude and distance of earthquake events that contribute most significantly to hazard at the project site. As shown in these figures, the most significant hazard to the site, as modeled by the PSHA, is due to the various splays of the SWIF.

The ground motion hazard calculated from the initial and revised PSHA studies are consistent with paleoseismic studies in the region. For instance, paleoseismic studies in the nearby Snohomish River delta, located about 20 km north of the plant site and about 10 km northeast of the northern splay of the SWIF, have found evidence of at least 3 events that caused liquefaction features (Bourgeois and Johnson, 2001) and possibly two other events that caused rapid subsidence and/or tsunami deposits. The corresponding recurrence interval for earthquakes

strong enough to cause these features preserved in the recent geologic record is about 240 to 400 years. Peak ground accelerations calculated from the PSHA with return periods of 240 and 400 years are about 0.22g and 0.27g, respectively (Figure 4-2) and could occur as a result of earthquakes from seismogenic sources (e.g., intraslab source zone, random crustal seismicity) other than the SWIF. Based on geotechnical engineering studies for state highway bridges in the delta (Shannon & Wilson, 1997), these peak ground accelerations are strong enough to cause the liquefaction and settlement of the sandy soils in the Snohomish River delta.

4.3 Results with Fault Directivity

The proximity of the Plant site to the extensions would require modification of the calculated soft rock UHS to account for directivity effects. Directivity refers to the spatial variation of ground motion amplitude around a fault; the change or "amplification" of the ground motion due to directivity at a given site over what may typically be expected without directivity effects is a function of the fault type, orientation of the site relative to the fault, and direction of rupture.

As an example, the effect of directivity was clearly seen in ground motion recordings of the 1992 Landers Earthquake. The earthquake occurred on a strike-slip fault and ruptured northward. Nearby strong motion recording stations toward which the fault ruptured recorded motions with large velocity pulses and relatively shorter duration due to the rupture propagation and waves traveling toward the recording site. Strong motion recording stations toward the south (away from the direction of fault rupture) did not record a strong velocity pulse. The magnitude of the motions was also smaller and the duration was longer relative to the motions recorded to the north. A corresponding effect (though smaller) can also be seen for dip-slip faults.

For the SWIF, some strike-slip and dip-slip components of motion are expected; however, what are not known is what part of the fault would rupture and whether the propagation of rupture would be toward or away from the site. Somerville et al. (1997) provide an empirical procedure for estimating fault directivity effects for either strike-slip or dip-slip events. Figure 4-14 presents the factors to be applied to the rock UHS for strike-slip movement toward the site, strike-slip movement away from the site, and for dip-slip movement. The average of the factors for strike-slip movement is very similar to the amplifications factors for dip-slip movement. Thus, we applied the average strike-slip amplification factors to our soft rock UHS.

The soft rock UHS for 2,500-year ground motions from our revised PSHA study, including empirical directivity effects, is presented in Figure 4-15. This spectrum should be modified to account for soil effects as applicable. Where a design spectrum based on the UHS in Figure 4-15 is less than the minimum values presented by the appropriate building code (e.g., IBC, 2003), the minimum values prescribed by the code should be used.

5.0 Limitations

Within the limitations of scope, schedule, and budget, the analyses, conclusions, and recommendations presented in this report were prepared in accordance with generally accepted professional geologic and geotechnical engineering principles and practices in this area at the time this report was prepared. We make no other warranty, either express or implied. The conclusions are based on our understanding of the project as described in this report. Additional information regarding the limitations and use of this report are provided in Appendix C.

This report was prepared for the exclusive use of CH2M Hill and King County for evaluation of ground motions and design of facilities at the proposed Brightwater Treatment Plant SR-9 site.

SHANNON & WILSON, INC.

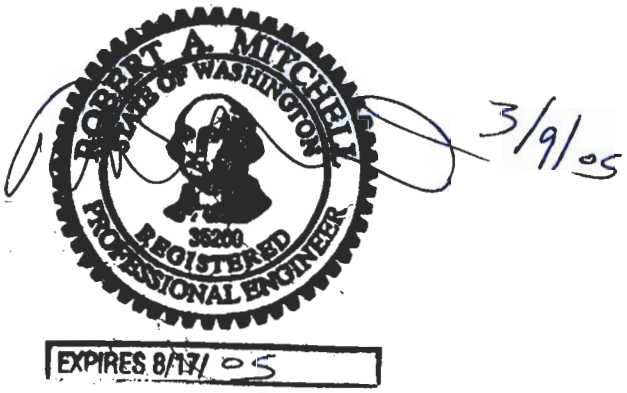

Robert Mitchell, P.E.
Senior Principal Engineer

Susan W. Chang, Ph.D., P.E.
Senior Principal Engineer

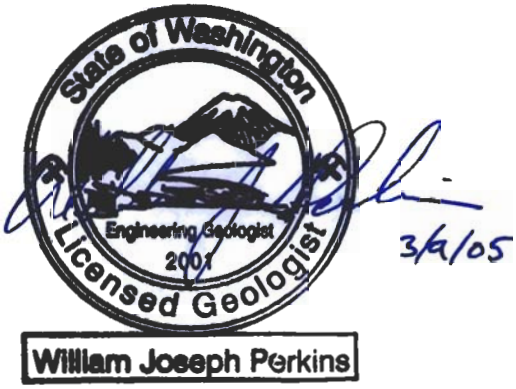

William J. Perkins, L.E.G.
Associate

CLR:RAM:SWC:WJP:WTL/wjp

6.0 References

Abrahamson, N.A., 2003, HAZ35, Probabilistic seismic hazard analysis program.

Abrahamson, N.A., and Silva, W.J., 1997, Empirical response spectral attenuation relations for shallow crustal earthquakes: Seismological Research Letters, v. 68, no. 1, January/February, p. 94-127.

Adams, J., 1990, Paleoseismicity of the Cascadia Subduction Zone: evidence from turbidities off the Oregon-Washington margin: Tectonics, v. 9, no. 4, p. 569-583.

AMEC Earth & Environmental, Inc., 2005, Draft report: surface-fault-rupture hazard evaluation, Brightwater Wastewater Treatment Plant site, Snohomish County, Washington: Report by AMEC Earth & Environmental, Anaheim, Calif., 4-212-102100, for Bob Peterson, King County – Wastewater Treatment Division, Seattle, Wash., January.

Atkinson, G.M., and Boore, D.M., 2003, Empirical ground-motion relations for subduction-zone earthquakes and their application to Cascadia and other regions: Bulletin of the Seismological Society of America 92(4), p. 1703-1729.

Atwater, B.F., and Hemphill-Haley, E., 1997, Recurrence intervals for great earthquakes of the past 3500 years at Northeastern Willapa Bay, Washington: U.S. Geological Survey Professional Paper 1576.

Blakely, R.J., Sherrod, B.L., Wells, R.E., Weaver, C.S., McCormack, D.H., Troost, K.G., and Haugerud, R.A., 2004, The Cottage Lake aeromagnetic lineament-A possible onshore extension of the southern Whidbey Island fault, Washington: U.S. Geological Survey Open-File Report 2004-1204, 60 p.

Blakely, R.J., Weaver, C.S., Sherrod, B.L., Troost, K.G., Haugerud, R.A., Wells, R.E., and McCormack, D.E., 2003, The Cottage Lake lineament, Washington: Onshore extension of the southern Whidbey Island fault?: EOS, American Geophysical Union Transactions, 8-12 December 2003, San Francisco, Calif, v. 84, no. 46, p. F1092.

Blakely, R.J., Wells, R.E., Weaver, C.S., and Johnson, S.Y., 2002, Location, structure, and seismicity of the Seattle fault, Washington: Evidence from aeromagnetic anomalies, geologic mapping, and seismic-reflection data: Geological Society of America Bulletin, v. 114, p. 169-177.

Boore, D.M., Joyner, W.B., and Fumal, T.E., 1997, Equations for estimating horizontal response spectra and peak acceleration from Western North American earthquakes: A summary of recent work, Seismological Research Letters, v. 68, 128-153.

Bourgeois, J., and Johnson, S.Y., 2001, Geologic evidence of earthquakes at the Snohomish delta, Washington, in the past 1200 yr: Geological Society of America Bulletin, v. 113, no. 4, p. 482-494.

Brocher, T.M., Parsons, T., Blakely, R.J., Christensen, N.I., Fisher M.A., Wells, R.E., and the SHIPS Working Group, 2001, Upper crustal structure in Puget Lowland, Washington, results from the 1998 Seismic Hazards Investigation in Puget Sound: Journal of Geophysical Research, v. 106, no. B7, July 10, p. 13,541-13,564.

Brocher, T. M., Blakely, R. J., and Wells, R. E., 2004, Interpretation of the Seattle uplift, Washington, as a passive-roof duplex: Bulletin of the Seismological Society of America, v. 94, no. 4, p. 1379-1401.

Bucknam, R.C., 2000, Personal communication.

Byrne, D., Davies, D., and Sykes, L., 1988, Loci and maximum size of thrust earthquakes and the mechanics of the shallow region of subduction zones: Tectonics, v. 7, p. 833-857.

Calvert, A.J., Fisher, M.A., and Johnson, S.Y., 2003, Along-strike variations in the shallow seismic velocity structure of the Seattle Fault Zone: Evidence for fault segmentation beneath Puget Sound: Journal of Geophysical Research, v. 108, no. B1.

Calvert, A.J., and Fisher, M.A., 2001, Imaging of the Seattle Fault Zone with high resolution seismic tomography: Geophysical Research Letters, 28(12), p. 2337-2340.

Campbell, K.W., and Bozorgnia, Y., 2003a, Updated near-source ground-motion (attenuation) relations for the horizontal and vertical components of peak ground acceleration and acceleration response spectra: Bulletin of the Seismological Society of America, 93(1), p. 314-331.

Campbell, K.W., and Bozorgnia, Y., 2003b, Updated near-source ground-motion (attenuation) relations for the horizontal and vertical components of peak ground acceleration and acceleration response spectra (errata): Bulletin of the Seismological Society of America, 93(3), p. 1413.

Campbell, K.W., and Bozorgnia, Y., 2003c, Updated near-source ground-motion (attenuation) relations for the horizontal and vertical components of peak ground acceleration and acceleration response spectra (errata): Bulletin of the Seismological Society of America, 93(4), p. 1872.

Cornell, C.A., 1968, Engineering Seismic Risk Analysis: Bulletin of the Seismological Society of America, v. 58, p. 1583-1606.

Crosson, R.S., and Owens, T.J., 1987, Slab geometry of the Cascadia Subduction Zone beneath Washington from earthquake hypocenters and teleseismic converted waves: Geophysical Research Letters, v. 14, p. 824-827.

Crouse, C., 1991, Ground motion attenuation equations for Cascadia subduction zone earthquakes: Earthquake Spectra, 7, p. 201-236.

Der Kiureghian, A., and Ang, A.H.S., 1975, A line source model for seismic risk analysis," University of Illinois Technical Report, UILU-ENG-75-2023, Urbana, October, 134 p.

Der Kiureghian, A., and Ang, A.H.S., 1977, A fault-rupture model for seismic risk analysis: Bulletin of the Seismological Society of America, v. 67, no. 4, p. 1173-1194.

Dragert, H., Hyndman, R.D., Rogert, G.C., and Wang, K., 1994, Current deformations and the width of the seismogenic zone of the northern Cascadia subduction thrust: Journal of Geophysical Research, v. 99, p. 653-668.

Frankel, A., Mueller, C., Barnhard, T., Perkins, D., Leyendecker, E.V., Dickman, N., Hanson, S., and Hopper, M., 1996, National seismic hazard maps, June 1996 Documentation: U.S. Geological Survey Open-File Report 96-532.

Frankel, A., Petersen, M., Mueller, C., Haller, K., Wheeler, R., Leyendecker, E., Wesson, R., Harmsen, S., Cramer, C., Perkins, D., and Rukstales, K., 2002, Documentation for the 2002 update of the national seismic hazard maps: U.S. Geological Survey Open-File Report 02-420, 39 p.

Geomatrix Consultants, 1993, Seismic margin earthquake for the Trojan site: Final unpublished report prepared for Portland General Electric Trojan Nuclear Plant, Rainier, Oregon.

Geomatrix Consultants, 1995, Seismic design mapping, State of Oregon final report, prepared for Oregon Department of Transportation, Personal Services Contract 11688, Project No. 2442, January.

Goldfinger, C., Kulm, L.D., Yeats, R.S., Mitchell, C., Weldon, R.E., Peterson, C., Darienzo, M., Grant, W., and Priest, G., 1992a, Neotectonic map of the Oregon continental margin and adjacent abyssal plain, Oregon Department of Geology and Mineral Industries, Open File report O-92-4, 17 p.

Goldfinger, C., Kulm, L.D., Yeats, R.S., Applegate, B., MacKay, M.E., and Moore, G.F., 1992b, Transverse structural trends along the Oregon convergent margin: Geology, v. 20, p.141-144.

Gower, H.D., Yount, J.D., and Crosson, R.S., 1985, Seismotectonic map of the Puget Sound region, Washington: U.S. Geological Survey Miscellaneous Investigations Series Map I-1613, scale 1:250,000.

Griggs, G.B., and Kulm, L.D., 1970, Sedimentation in Cascadia deep-sea channel: Geological Society of America Bulletin, v. 81, p. 1361-1384.

Haller, K., Wheeler, R., and Rukstales, K., 2002, Documentation of changes in fault parameters for the 2002 National Seismic Hazards Maps – conterminous United States except California: U.S. Geological Survey Open-File Report 02-467.

Hyndman, R.D., and Wang, K., 1993, Thermal constraints on the zone of major thrust earthquake failure: the Cascadia Subduction Zone: Journal of Geophysical Research, v. 98, p.2039-2060.

Hyndman, R.D., and Wang, K., 1995, The rupture zone of Cascadia great earthquakes from current deformation and the thermal regime: Journal of Geophysical Research, v. 100, no. 22, p. 133-154.

International Code Council, Inc., 2003, International Building Code, Building Officials and Code Administrators International, Inc.: Country Club Hills, IL; International Conference of Building Officials, Whittier, CA; and Southern Building Code Congress International, Inc., Birmingham, AL.

Jarrard, R.D., 1986, Relations among Subduction parameters: Review of Geophysics, v. 24, no. 2, p. 217-284.

Johnson, S.Y., and others, 2003, Evidence for one or two late Holocene earthquakes on the Utsalady Point fault, Northern Puget Lowland, Washington: Abstracts with Program, Annual National Meeting, Geological Society of America.

Johnson, S.Y., Dadisman, S.V., Childs, J.R., and Stanley, W.D., 1999, Active tectonics of the Seattle Fault and Central Puget Sound, Washington--implications for earthquake hazards: Geological Society of America Bulletin, v. 111, No. 7, July, p. 1042-1053.

Johnson, S.Y., Dadisman, S.V., Mosher, D.C., Blakely, R.J., and Childs, J.R., 2001, Active tectonics of the Devils Mountain Fault and related structures, northern Puget Lowland and eastern Strait of Juan de Fuca Region, Pacific Northwest: U.S. Geological Society Professional Paper 1643.

Johnson, S.Y. , Mosher, D.C., Dadisman, S.V., Childs, J.R., and Rhea, S.B., 2000, Tertiary and Quaternary structures of the eastern Juan De Fuca Strait: interpreted map, in: Mosher, D.C., and Johnson, S.Y. (eds.), Rathwell, G.J., Kung, R.B., and Rhea, S.B. (compilers), Neotectonics of the eastern Juan de Fuca Strait; a digital geological and geophysical atlas: Geological Survey of Canada Open File Report 3931.

Johnson, S.Y., Potter, C.J., and Armentrout, J.M., 1994, Origin and evolution of the Seattle Basin and Seattle Fault: Geology, v. 22, p. 71-74.

Johnson, S.Y., Potter, C.J., Armentrout, J.M., and others, 1996, The Southern Whidbey Island Fault, an active structure in the Puget Lowland, Washington: Geological Society of America Bulletin, v. 108, p. 334-354.

Kelsey, H. M., Sherrod, Brian, Johnson, S. Y., and others, 2004, Land-level changes form a late Holocene earthquake in the northern Puget Lowland, Washington: Geology, v. 32, no. 6, p. 469-472.

Leonard, L., Hyndman, R.D., and Mazzotti, S., 2003, Coseismic subsidence in the 1700 great Cascadia earthquake: Coastal estimates versus elastic dislocation models, Geological Society of America Bulletin, in press.

McCrumb, D.R., Galster, R.W., West, D.O., Crosson, R.S., Ludwin, R.S., Hancock, W.E., and Mann, L.V., 1989, Tectonics, seismicity, and engineering seismology, in Washington, *in* Galster, Richard W., Engineering geology in Washington, v.1: Washington Division of Geology and Earth Resources Bulletin 78, p.97-120.

McGuire, R.K., 1978, FRISK: Computer program for seismic risk analysis using faults as earthquake sources: U.S. Geological Survey Open-File Report 78-1007, 70 p.

McGuire, R.K., 1976, FORTRAN computer program for seismic risk analysis: U.S. Geological Survey Open-File Report 76-67, 90 p.

Nelson, A.R, Johnson, S.Y., Kelsey, H.M., Sherrod, B.L., Wells, R.E., Bradley, L.-A., Okumura, K., and Bogar, R., 2003a, Late Holocene earthquakes on the Waterman Point reverse fault, another ALSM-discovered fault scarp in the Seattle fault zone, Puget Lowland, Washington: Geological Society of America Abstracts with Program (Abstract for talk in topical session on "Earthquake geology in reverse faulting terrains" at the Nov 03 Annual Meeting of The Geological Society of America in Seattle Washington).

Nelson, A.R., Johnson, S.Y., Kelsey, H.M., Wells, R.E., Sherrod, B.L., Pezzopane, S.K., Bradley, L.-A., and Koehler, R.D., III, 2003b, Late Holocene earthquakes on the Toe Jam Hill fault, Seattle fault zone, Bainbridge Island, Washington: Geological Society of America Bulletin, v. 115, 1388-1403.

Peterson, C.D., Darienzo, M.E., Burns, S.F., and Burris, K., 1993, Field trip guide to Cascadia paleoseismic evidence along the northern Oregon coast – Evidence of subduction zone seismicity in the central Cascadia margin: Oregon Geology, v. 55, p. 99-114.

Plafker, G., and Kachadoorian, R., 1969, Geologic effects of the March 1964 earthquake and associated seismic sea waves on Kodiak and Nearby Islands of Alaska: U.S. Geological Survey Professional Paper 543-D, 46 p.

Pratt, T.L., Johnson, S.Y., Potter, C.J., and others, 1997, Seismic-reflection images beneath Puget Sound, Western Washington State: Journal of Geophysical Research, v. 102, p. 469-490.

Rogers, A.M., Walsh, T.J., Kockelman, W.J., and Priest, G.R., 1996, Earthquake hazards in the Pacific Northwest--an overview *in* A.M. Rogers, T.J. Walsh, W.J. Kockelman, and G.R. Priest (eds.), Assessing Earthquake Hazards and Reducing Risk in the Pacific Northwest, U.S. Geological Survey Professional Paper 1560, v. 1, p. 1-54.

Sadigh, K., Chang, C.-Y., Egan, J.A., Makdisi, F., and Youngs, R.R., 1997, Attenuation relationships for shallow crustal earthquakes based on California strong motion data: Seismological Research Letters, v. 68, no. 1, January/February, p. 180-189.

Satake, K.; Shimazaki, K.; Tsuji, Y.; and Ueda, K., 1996, Time and size of a giant earthquake in Cascadia inferred from Japanese tsunami records of January 1700: Nature, v. 378, no. 18, January, p. 246-249.

Shannon & Wilson, Inc.,1997, WSDOT special bridges seismic evaluation Everett - Marysville, Washington: Report by Shannon & Wilson, Inc., Seattle, WA, W-7479-01, for Andersen Bjornstad Kane Jacobs, Inc., Seattle, WA, June.

Shannon & Wilson, Inc., 2004a, Final report: probabilistic seismic hazard analyses, Brightwater Project, SR-9 and Portal 41 sites, King County Department of Natural Resources, Washington: Report by Shannon & Wilson, Inc., Seattle, Wash., 21-1-09869-010, for CH2M Hill, Bellevue, Wash., June 30.

Shannon & Wilson, Inc., 2004b, Proposed revisions to the SWIF model for the revised Brightwater PSHA based on recent USGS/project team fault studies and reviews: Report by Shannon & Wilson, Inc., Seattle, Wash., 21-1-20150-002, for CH2M Hill, Bellevue, Wash., November 17.

Sherrod, B.L., 1999, Earthquake-induced subsidence about 1,100 years ago around southern Puget Sound, Washington: Seismological Research Letters, v. 70, no. 2, March/April.

Somerville, P.G., Smith, N.F., Gaves, R.W., and Abrahamson, N.A., 1997, Modification of empirical strong ground motion attenuation relations to include the amplitude and duration effects of rupture directivity: Seismological Research Letters, v. 68, no. 1, January/February, p. 199-222.

Stanley, D., Villasenor, A., and Benz, H., 1999, Subduction zone and crustal dynamics of Western Washington: a tectonic model for earthquake hazards evaluation: U.S. Geological Survey Open-File Report 99-311 on-line edition, 66 p.

Tabor, R.W., 1994, Late Mesozoic and possible early Tertiary accretion in western Washington State: the Helena-Haystack mélange and the Darrington-Devils Mountain Fault Zone: Geological Society of America Bulletin, v. 106, no. 2, p. 217-232.

ten Brink U.S., Molzer, P.C., Fisher, M.A., Blakely, R.J., Bucknam, R.C., Parsons, T., Crosson, R.S., and Creager, K.C., 2002, Subsurface geometry and evolution of the Seattle fault zone and the Seattle basin, Washington: Bulletin of the Seismological Society of America, v. 92, p. 1737-1753.

Tichelaar, B.W., and Ruff, L.J., 1993, Depth of seismic coupling along subduction zones: Journal of Geophysical Research, v. 98, p. 2017-2037.

Washington Division of Geology and Earth Resources staff, 2002, Digital geologic maps of the 1:100,000 quadrangles of Washington: Olympia, Wash., Washington Division of Geology and Earth Resources Digital Report 2, October edition, 1 CD-ROM disk.

Weaver, C.S., and Smith, S.W., 1983, Regional tectonic and earthquake hazard implications of a crustal fault zone in southwestern Washington: Journal of Geophysical Research, v. 88, no. B12, p. 10371-10383.

Wells, D.L., and Coppersmith, K.J., 1994, New empirical relationships among magnitude, rupture length, rupture width, rupture area, and surface displacement: Bulletin of the Seismological Society of America, v. 84, no. 4, p. 974-1002.

Wells, R.E., and Johnson, S.Y., 2001, Deformations of Western Washington resulting from northward migration of the Cascadia Forearc: Seismological Research Letters, v. 72, no. 2, March/April.

Wells, R.E., and Weaver, C.S., 1993, Block deformation in Puget Lowland *in* Proceedings of the National Earthquake Prediction Evaluation Council, Frizzel, V.E., ed., U.S. Geological Survey Open File Report 93-333, p. 14-16.

Wilson, J. R., Bartholomew, M. J., and Carson, R. J., 1979, Late Quaternary faults and their relationship to tectonism in the Olympic Peninsula, Washington: Geology, v. 7, p. 235-239.

Youngs, R.R., Chiou, S.-J., Silva, W.J., and Humphrey, J.R., 1997, Strong ground motion attenuation relationships for subduction zone earthquakes: Seismological Research Letters, v. 68, No. 1, January/February, p. 58-73.

Table 3-1. Seismic Source Parameters for Interplate and Intraslab Source Zones

Seismic Source [Probability of Activity]	Maximum Updip Extent [Weight]	Maximum Downdip Extent [Weight]	Recurrence Interval (years)	Rupture Length (km) [Weight]	Maximum Magnitude Approach
Interplate [1.0]	Slope Break [0.5] Deformation Front [0.5]	Zero Isobase [0.50] Midpt. Transition Zone [0.33] Mafic Zone [0.17]	600 [1.0]	150 [0.1] 250 [0.2] 450 [0.2] 1100 [0.5]	Rupture Area [1.0]

Seismic Source [Probability of Activity]	Intraslab Geometry [Weight]	Maximum Magnitude [Weight]
Intraslab [1.0]	Crosson & Owens [0.75] Stanley et al. [0.25]	7.1 [0.2] 7.25 [0.6] 7.5 [0.2]

Note:
The following attenuation relationships were used with equal weight given to each:
Youngs et al. (1997)
Atkinson and Boore (2003)

Table 3-2. Seismic Source Parameters for Regional Areal Crustal Source Zones

Seismic Source [Probability of Activity]	Source Depth (km) [Weight]	Maximum Magnitude [Weight]	Earthquake Recurrence Model
Vancouver Island [1.0]	2 [0.2] 11 [0.6] 20 [0.2]	7.0 [0.2] 7.25 [0.6] 7.5 [0.2]	Exponential
North Cascades [1.0]	2 [0.2] 11 [0.6] 20 [0.2]	7.0 [0.2] 7.25 [0.6] 7.5 [0.2]	Exponential
Olympic/Willapa/ Coast Ranges [1.0]	2 [0.2] 11 [0.6] 20 [0.2]	7.0 [0.2] 7.25 [0.6] 7.5 [0.2]	Exponential
South Cascades [1.0]	2 [0.2] 11 [0.6] 20 [0.2]	7.0 [0.2] 7.25 [0.6] 7.5 [0.2]	Exponential
Willamette [1.0]	2 [0.2] 11 [0.6] 20 [0.2]	7.0 [0.2] 7.25 [0.6] 7.5 [0.2]	Exponential
North Puget Sound [1.0]	5 [0.2] 15 [0.6] 25 [0.2]	7.0 [0.2] 7.25 [0.6] 7.5 [0.2]	Exponential
Central Puget Sound [1.0]	5 [0.2] 15 [0.6] 25 [0.2]	7.0 [1.0]	Exponential

Note:
The following attenuation relationships were used with equal weight given to each:
Boore et al. (1997)
Abrahamson and Silva (1997)
Sadigh et al. (1997)
Campbell and Bozorgnia (2003)

Table 3-3. Seismic Source Parameters for Specific Crustal Source Faults

Seismic Source (Slip Type) [Probability of Activity]	SWIF Model [Weight]	Seattle Fault Model [Weight]	Dip (Degrees) [Weight]	Source Depth (km) [Weight]	Slip Rate (mm/year) [Weight]	Rupture Length (km) [Splay and Weight]	Segmentation [Weight]	Earthquake Recurrence Model [Weight]
Seattle Fault (Reverse) [1.0]	Y and Z [0.67 and 0.33]	A (Low Angle) [0.25]	20 [0.5] 25 [0.5]	14 [0.5] 20 [0.5]	0.6 [0.2] 1.0 [0.6] 1.4 [0.2]	60 [1.0]	Unsegmented [1.0] Segmented [0.0]	Characteristic [1.0]
		B (High Angle) [0.25]	50 [0.5] 35 [0.5]	24 [0.5] 28 [0.5]	0.24 [0.2] 0.40 [0.6] 0.56 [0.2]	57 [Center, 1.0] 60 [Northern, 1.0]	Unsegmented [1.0] Segmented [0.0]	
					0.12 [0.2] 0.20 [0.6] 0.28 [0.2]	51 [Sourthern, 1.0]	Unsegmented [1.0] Segmented [0.0]	
		C [0.5]	20 [0.5] 25 [0.5]	12 [0.5] 16 [0.5]	0.6 [0.2] 1.0 [0.6] 1.4 [0.2]	60 [1.0]	Unsegmented [1.0] Segmented [0.0]	
Tacoma Fault (Reverse) [1.0]	Y and Z [0.67 and 0.33]	A (Center Segment) [0.25]	50 [0.5] 80 [0.5]	15 [0.5] 25 [0.5]	0.1 [0.4] 1.0 [0.6]	28 [Center, 1.0]	Unsegmented [1.0] Segmented [0.0]	Characteristic [1.0]
		B (Center and East Segments) [0.25]	50 [0.5] 80 [0.5]	15 [0.5] 25 [0.5]	0.1 [0.4] 1.0 [0.6]	48 [Center and East, 1.0]	Unsegmented [0.5]	
						28 [Center, 1.0] 20 [East, 1.0]	Segmented [0.5]	
		C [0.5]	30 [0.5] 35 [0.5]	12 [0.5] 16 [0.5]	0.1 [0.4] 1.0 [0.6]	34 [1.0]	Unsegmented [0.5]	
						21 [West, 1.0] 13 [East, 1.0]	Segmented [0.5]	
Tacoma Fault (Reverse) [0.5]	Y and Z [0.67 and 0.33]	A (North-South Tear) [0.25]	80 [0.33] 90 [0.34] 100 [0.33]	15 [0.5] 25 [0.5]	0.3 [0.5] 0.8 [0.5]	15 [1.0]	Unsegmented [1.0] Segmented [0.0]	Characteristic [1.0]
		B (North-South Tear) [0.25]	80 [0.5] 100 [0.5]	15 [0.5] 25 [0.5]	0.3 [0.5] 0.8 [0.5]	15 [1.0]	Unsegmented [1.0] Segmented [0.0]	
		C (North-South Tear) [0.5]	80 [0.5] 100 [0.5]	15 [0.5] 25 [0.5]	0.3 [0.5] 0.8 [0.5]	15 [1.0]	Unsegmented [1.0] Segmented [0.0]	
Olympia Fault (Reverse) [0.5]	Y and Z [0.67 and 0.33]	A [0.25]	50 [0.33] 65 [0.34] 80 [0.33]	15 [0.5] 25 [0.5]	0.1 [0.7] 1.0 [0.3]	78 [1.0]	Unsegmented [0.5]	Characteristic [1.0]
						47 [1.0]	Segmented [0.5]	
		B [0.25]	50 [0.5] 80 [0.5]	15 [0.5] 25 [0.5]	0.1 [0.6] 1.0 [0.4]	78 [1.0]	Unsegmented [0.5]	
						47 [1.0]	Segmented [0.5]	
		C [0.5]	50 [0.5] 80 [0.5]	15 [0.5] 25 [0.5]	0.1 [0.6] 1.0 [0.4]	78 [1.0]	Unsegmented [0.5]	
						47 [1.0]	Segmented [0.5]	
Hood Canal Fault (Strike-Slip) [0.5]	Y and Z [0.67 and 0.33]	A [0.25]	50 [0.33] 65 [0.34] 80 [0.33]	15 [0.5] 25 [0.5]	0.1 [0.7] 1.0 [0.3]	87 [1.0]	Unsegmented [0.5]	Characteristic [1.0]
						38 [1.0]	Segmented [0.5]	
		B [0.25]	50 [0.5] 80 [0.5]	15 [0.5] 25 [0.5]	0.1 [0.6] 1.0 [0.4]	87 [1.0]	Unsegmented [0.5]	
						38 [1.0]	Segmented [0.5]	
		C [0.5]	50 [0.5] 80 [0.5]	15 [0.5] 25 [0.5]	0.1 [0.6] 1.0 [0.4]	87 [1.0]	Unsegmented [0.5]	
						38 [1.0]	Segmented [0.5]	
Puget Sound Fault (Strike-Slip) [0.5]	Y and Z [0.67 and 0.33]	A [0.25]	85 [0.33] 90 [0.34] 95 [0.33]	15 [0.5] 25 [0.5]	0.3 [0.5] 0.8 [0.5]	55 [1.0]	Unsegmented [0.5]	Characteristic [1.0]
						25 [1.0]	Segmented [0.5]	
		B [0.25]	85 [0.5] 95 [0.5]	15 [0.5] 25 [0.5]	0.3 [0.5] 0.8 [0.5]	55 [1.0]	Unsegmented [0.5]	
						25 [1.0]	Segmented [0.5]	
		C [0.5]	85 [0.5] 95 [0.5]	15 [0.5] 25 [0.5]	0.3 [0.5] 0.8 [0.5]	55 [1.0]	Unsegmented [0.5]	
						25 [1.0]	Segmented [0.5]	
Southern Whidbey Island Fault (Reverse/Strike-Slip) [1.0]	Y1 (Strike-Slip & Reverse) [0.34]	A, B, and C [0.25, 0.25, and 0.5]	45 [0.5] 90 [0.5]	15 [0.5] 27 [0.5]	0.2 [0.2] 0.33[0.6] 0.47 [0.2]	137 [Northern, 1.0]	Unsegmented [1.0] Segmented [0.0]	Characteristic [0.67] Exponential [0.33]
			80 [0.5] 100 [0.5]	15 [0.5] 27 [0.5]	0.2 [0.2] 0.33[0.6] 0.47 [0.2]	140 [Center-Cottage Lake, 0.4] 140 [Center-Bear Creek, 0.5] 140 [Center-Lineament X, [0.1]	Unsegmented [1.0] Segmented [0.0]	
			45 [0.5] 80 [0.5]	15 [0.5] 27 [0.5]	0.2 [0.2] 0.33 [0.6] 0.47 [0.2]	136 [Southern, 1.0]	Unsegmented [1.0] Segmented [0.0]	
	Y2 (Strike-Slip & Reverse) [0.33]	A, B, and C [0.25, 0.25, and 0.5]	45 [0.5] 90 [0.5]	15 [0.5] 27 [0.5]	0.2 [0.2] 0.33[0.6] 0.47 [0.2]	135 [Northern-Cottage Lake, 1.0]	Unsegmented [1.0] Segmented [0.0]	
			80 [0.5] 100 [0.5]	15 [0.5] 27 [0.5]	0.2 [0.2] 0.33[0.6] 0.47 [0.2]	140 [Center-Bear Creek, 0.8] 140 [Center-Lineament X, 0.2]	Unsegmented [1.0] Segmented [0.0]	
			45 [0.5] 80 [0.5]	15 [0.5] 27 [0.5]	0.2 [0.2] 0.33 [0.6] 0.47 [0.2]	136 [Southern, 1.0]	Unsegmented [1.0] Segmented [0.0]	
	Z (thrust) [0.33]	A, B, and C [0.25, 0.25, and 0.5]	20 [0.3] 30 [0.4] 35 [0.3]	12 [0.3] 16 [0.4] 20 [0.3]	0.6 [0.2] 1.0 [0.6] 1.4 [0.2]	137 [1.0]	Unsegmented [1.0] Segmented [0.0]	
Utsalady Fault (Oblique-Slip) [1.0]	Y and Z [0.67 and 0.33]	A, B, and C [0.25, 0.25, and 0.5]	45 [0.5] 75 [0.5]	15 [0.5] 25 [0.5]	0.1 [0.2] 0.15 [0.6] 0.8 [0.2]	29 [1.0]	Unsegmented [1.0] Segmented [0.0]	Characteristic [1.0]

Table 3-3. Seismic Source Parameters for Specific Crustal Source Faults

Seismic Source (Slip Type) [Probability of Activity]	SWIF Model [Weight]	Seattle Fault Model [Weight]	Dip (Degrees) [Weight]	Source Depth (km) [Weight]	Slip Rate (mm/year) [Weight]	Rupture Length (km) [Splay and Weight]	Segmentation [Weight]	Earthquake Recurrence Model [Weight]
Strawberry Point Fault (Oblique-Slip) [1.0]	Y and Z [0.67 and 0.33]	A, B, and C [0.25, 0.25, and 0.5]	70 [0.5] 110 [0.5]	15 [0.5] 25 [0.5]	0.1 [0.2] 0.25 [0.6] 0.9 [0.2]	29 [1.0]	Unsegmented [1.0] Segmented [0.0]	Characteristic [1.0]
Devils Mountain Fault (Oblique-Slip Reverse) [1.0]	Y and Z [0.67 and 0.33]	A, B, and C [0.25, 0.25, and 0.5]	45 [0.5] 75 [0.5]	15 [0.5] 25 [0.5]	0.1 [0.2] 0.16 [0.6] 0.3 [0.2]	125 [1.0]	Unsegmented [1.0] Segmented [0.0]	Characteristic [1.0]

Note:
The following attenuation relationships were used with equal weight given to each:
Boore et al. (1997), Abrahamson and Silva (1997), Sadigh et al. (1997), and Campbell and Bozorgnia (2003).

Table 3-4. Estimated CSZ Maximum Rupture Widths

Boundary Locations	Updip Boundary at Deformation Front	Updip Boundary at Slope Break
Downdip boundary at zero isobase	90 km	65 km
Downdip boundary at midpoint of transition zone	75 km	50 km
Downdip boundary at edge of mafic zone	120 km	95 km

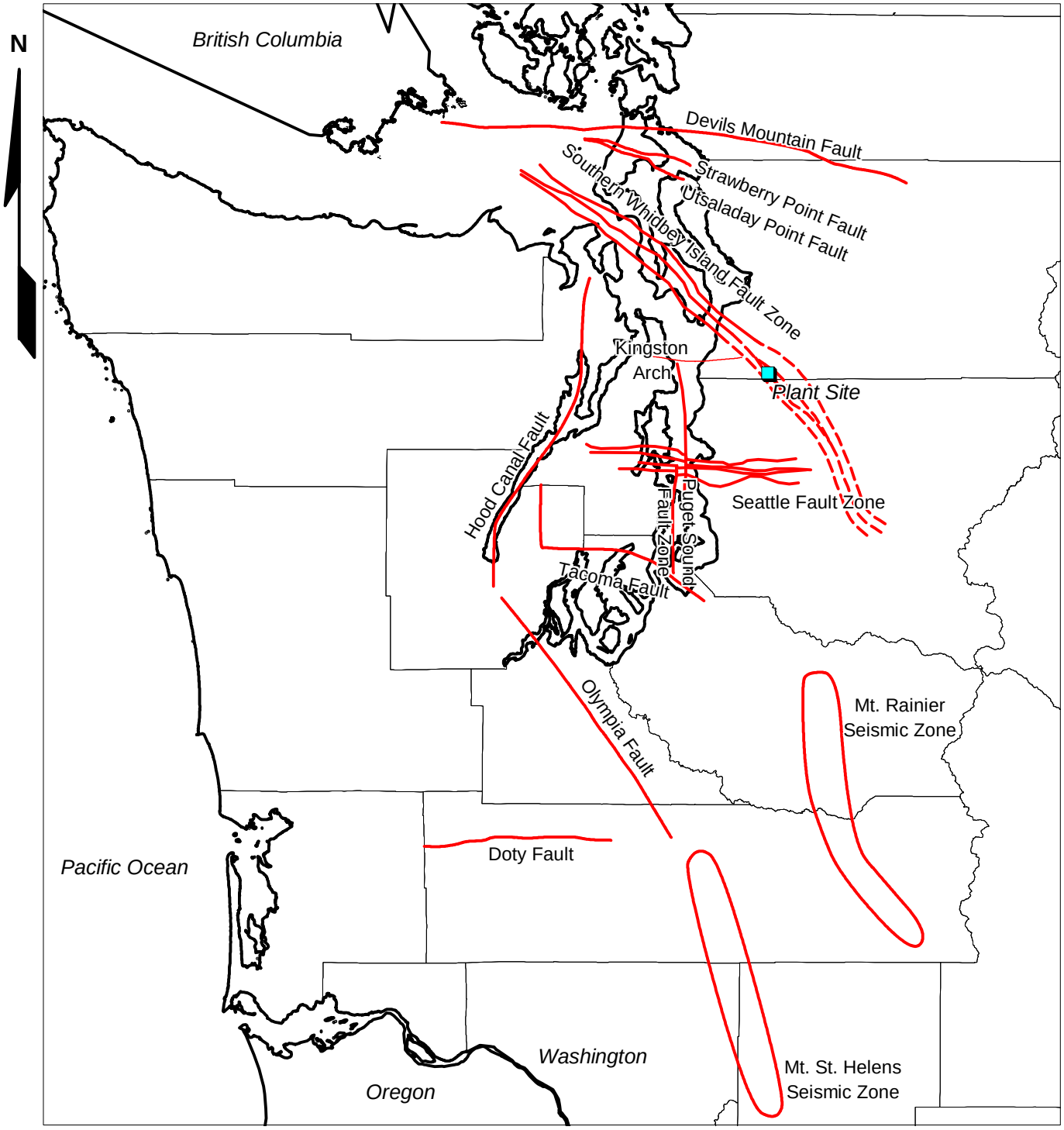

NOTES

1. Figure shows major crustal structures in and adjacent to the Central Puget Sound that are or may be associated with current tectonic stresses with known or possible Quaternary movement.
2. Structural features after Gower et al. (1985), Johnson et al. (1999), Johnson et al. (2000), Johnson et al. (2001), Brocher et al. (2001), Dragovich et al. (2002), Blakely et al. (2004).
3. Mainland extensions of the Southern Whidbey Island Fault Zone modeled in the revised PSHA and described in this report are indicated with dashed lines.

Brightwater Project
Seismic Hazard Analysis
King County Department of Natural Resources

VICINITY MAP & MAJOR CRUSTAL STRUCTURES IN THE CENTRAL PUGET SOUND & ADJACENT AREAS

Janaury 2005

FIG. 1-1

File: 21-1-20150-002, Fig 1-1 Vicinity Map.WOR Date: 01/04/05 Author: Shannon & Wilson (WJP)

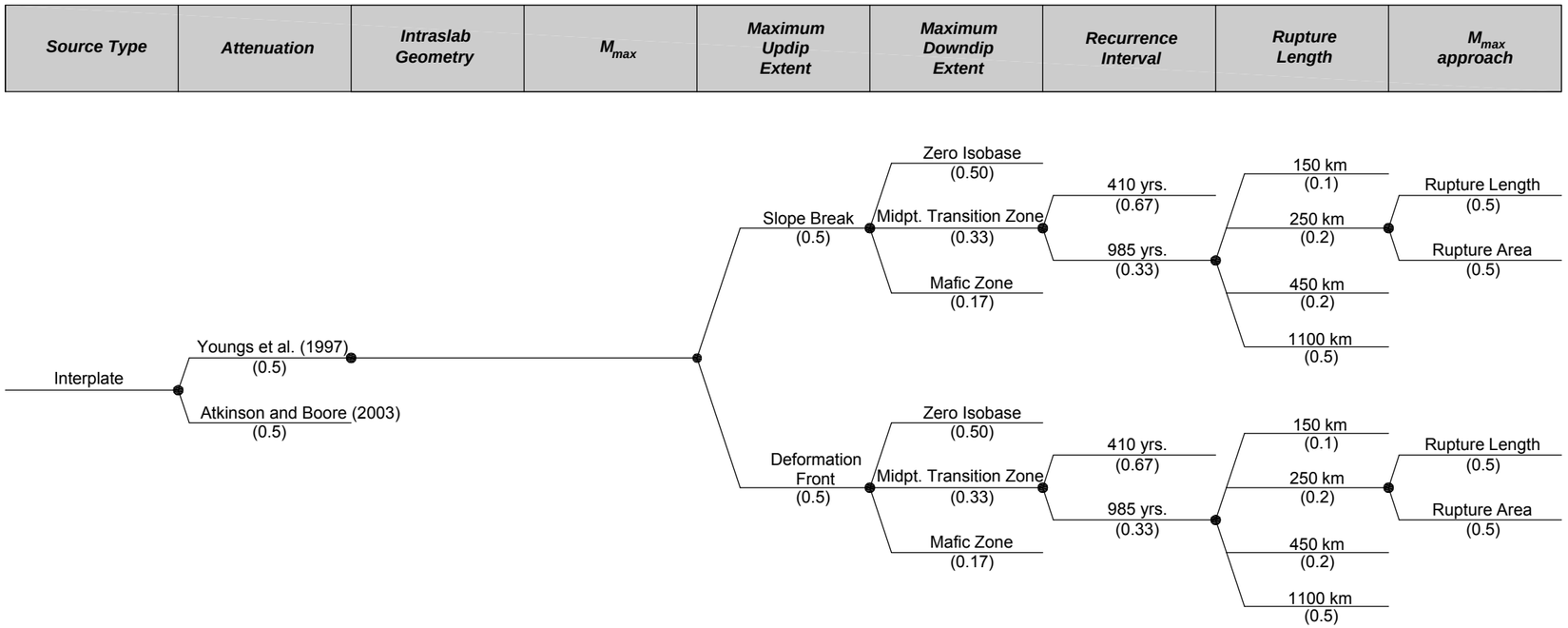

NOTE

Assumed weights for the various logic tree branches are indicated in parenthesis.

Brightwater Project
Seismic Hazard Analysis
King County Department of Natural Resources

SEISMIC SOURCE LOGIC TREE

January 2005 | **FIG. 2-1**

File: I:\Drafting\211\20150-002\21-1-20150-002 Fig 2-1.dwg Date: 12-28-2004 Author: SAC Shannon & Wilson, Inc.

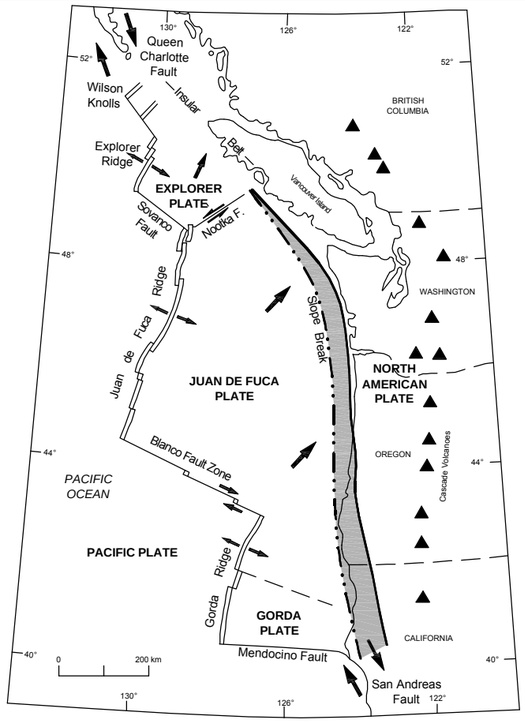

(a) Updip Extent: Slope break
Downdip Extent: Zero isobase

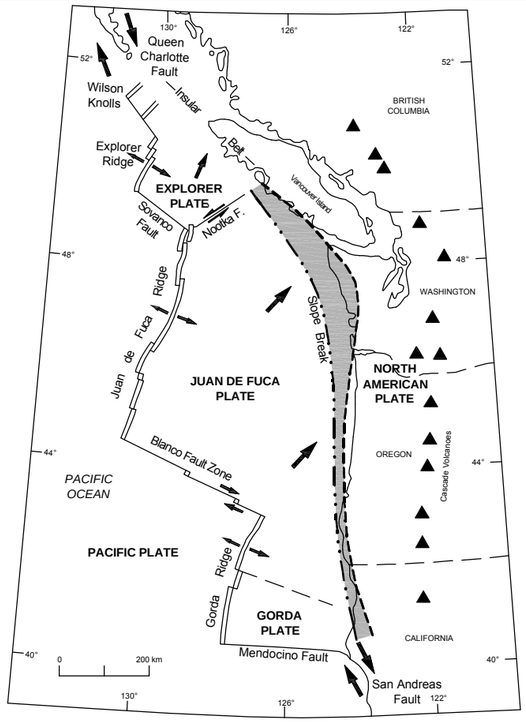

(b) Updip Extent: Slope break
Downdip Extent: Midpoint of Transition Zone

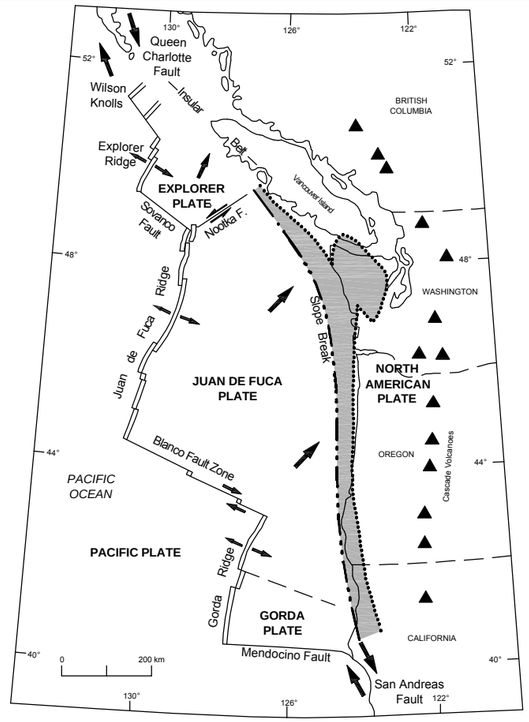

(c) Updip Extent: Slope break
Downdip Extent: Mafic Zone

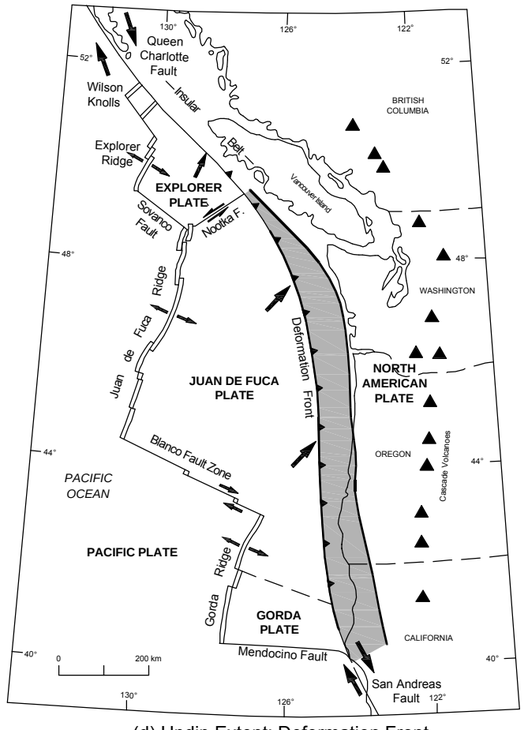

(d) Updip Extent: Deformation Front
Downdip Extent: Zero isobase

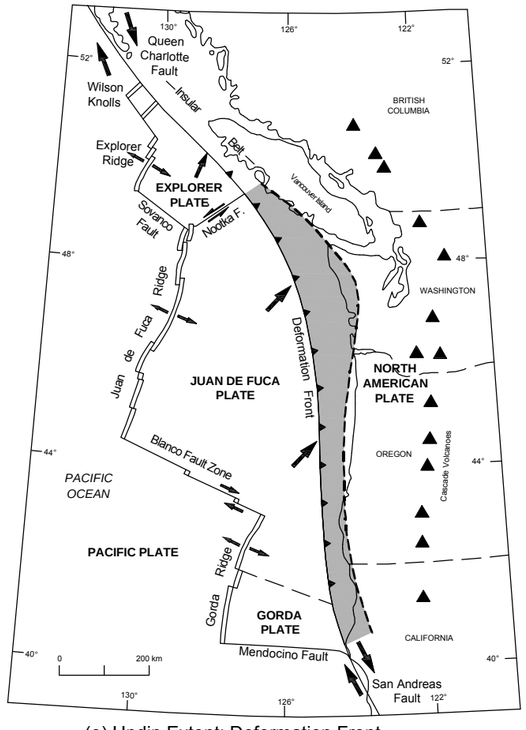

(e) Updip Extent: Deformation Front
Downdip Extent: Midpoint of Transition Zone

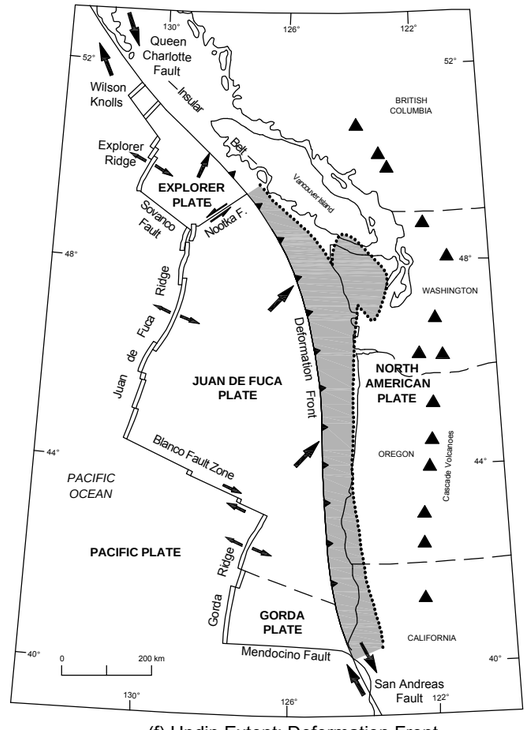

(f) Updip Extent: Deformation Front
Downdip Extent: Mafic Zone

NOTES

1. Shaded zones indicate the surface projection of the CSZ interface alternatives.
2. ▲ Symbols indicate location of Cascade volcanoes.

Brightwater Project
Seismic Hazard Analysis
King County Department of Natural Resources

SEISMOGENIC PLATE INTERFACE ALTERNATIVES

January 2005 | **FIG. 3-1**

File: I:\Drafting\211\20150-002\21-1-20150-002 Fig 3-1.dwg Date: 01-04-2005 Author: SAC Shannon & Wilson, Inc.

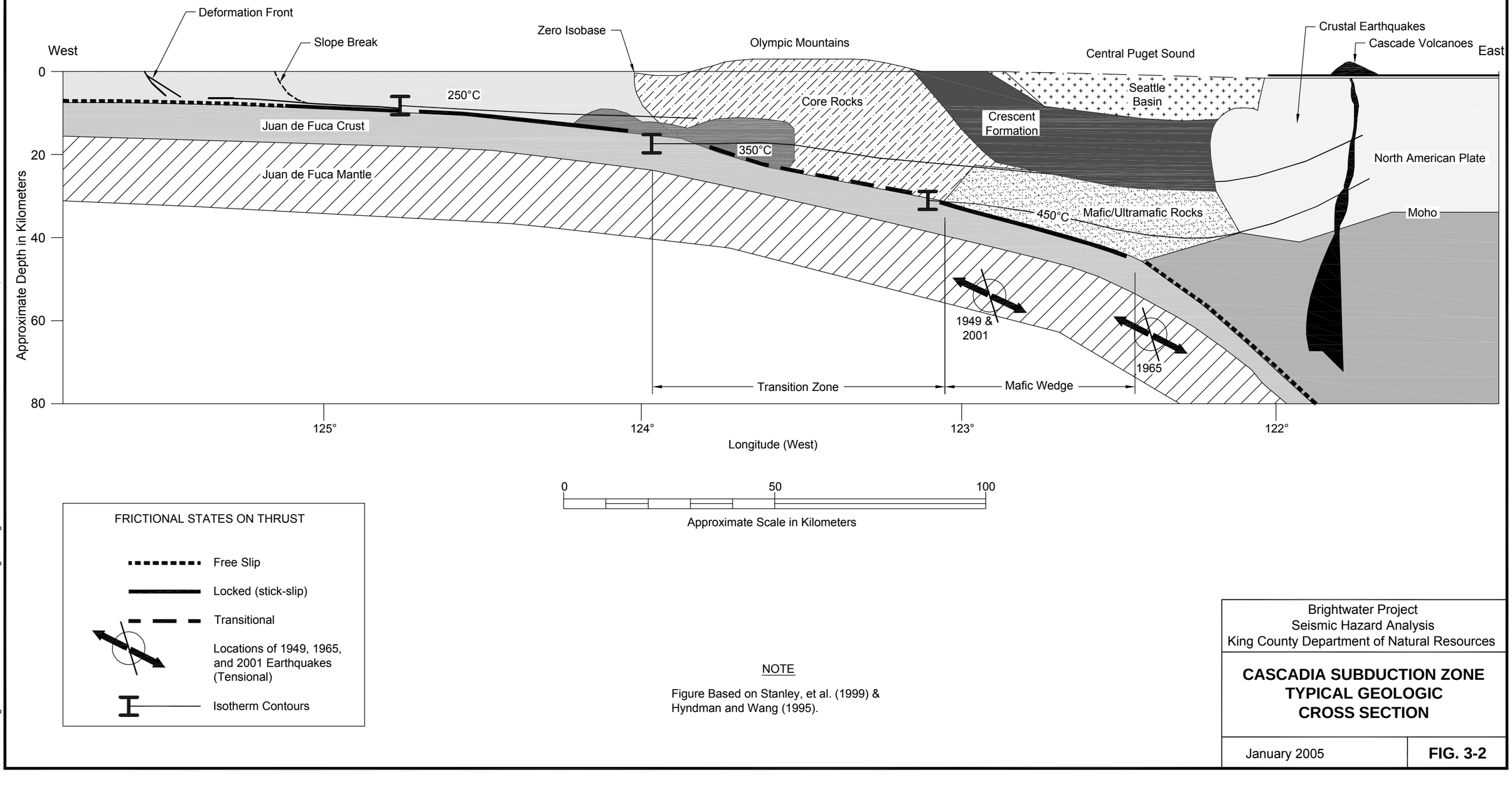

NOTE

Figure Based on Stanley, et al. (1999) & Hyndman and Wang (1995).

Brightwater Project
Seismic Hazard Analysis
King County Department of Natural Resources

CASCADIA SUBDUCTION ZONE TYPICAL GEOLOGIC CROSS SECTION

January 2005 | **FIG. 3-2**

File: i:\Drafting\211\20150-002\21-1-20150-002 Fig 3-2.dwg Date: 12-28-2004 Author: SAC Shannon & Wilson, Inc.

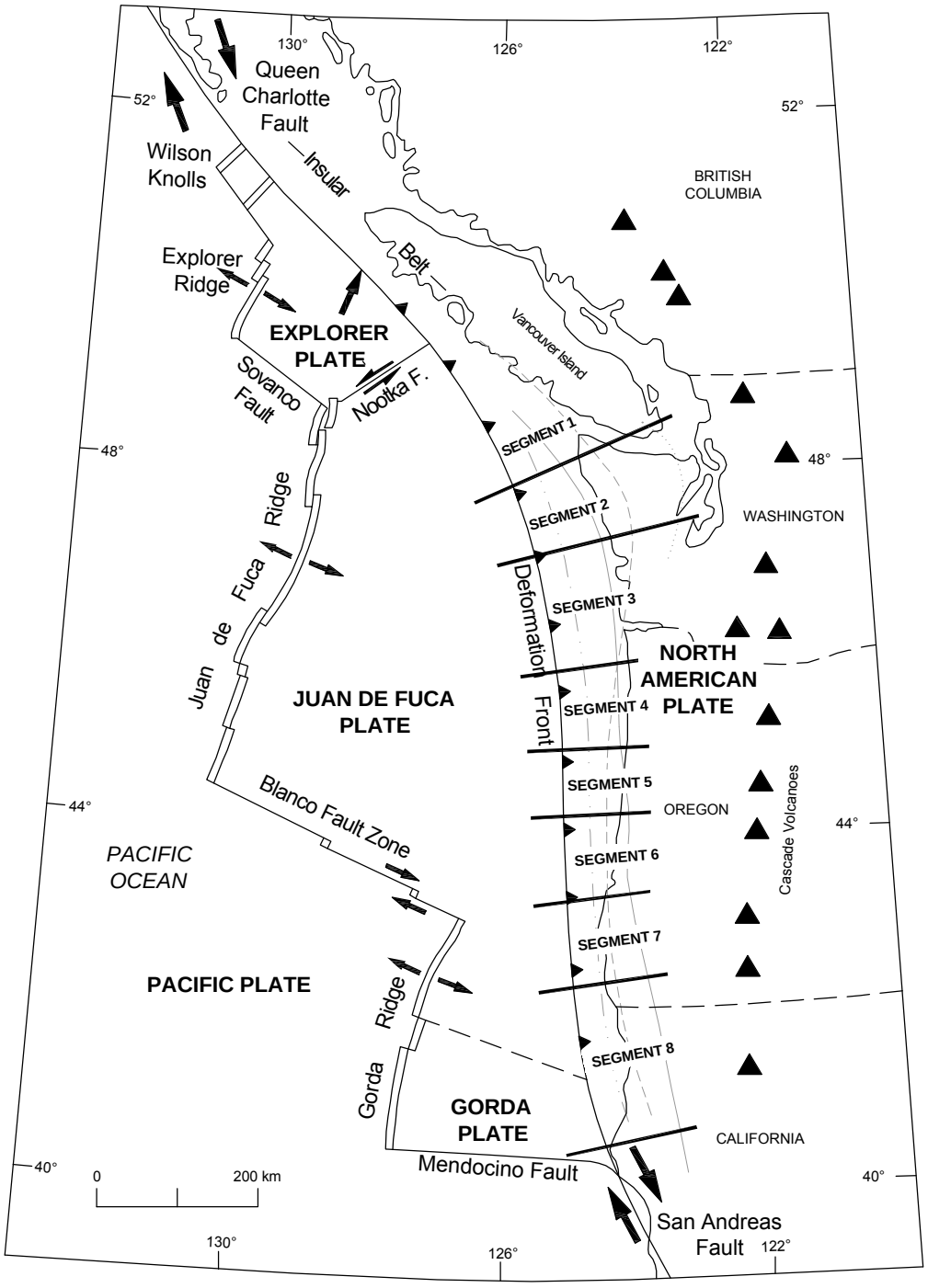

Map based on Hyndman and Wang (1993), Peterson et al. (1993), and Geomatrix (1995)

Brightwater Project
Seismic Hazard Analysis
King County Department of Natural Resources

SEGMENTATION OF THE CASCADIA SUBDUCTION ZONE

January 2005 | **FIG. 3-3**

File: I:\Drafting\211\20150-002\21-1-20150-002 Fig 3-3.dwg Date: 12-28-2004 Author: SAC Shannon & Wilson, Inc.

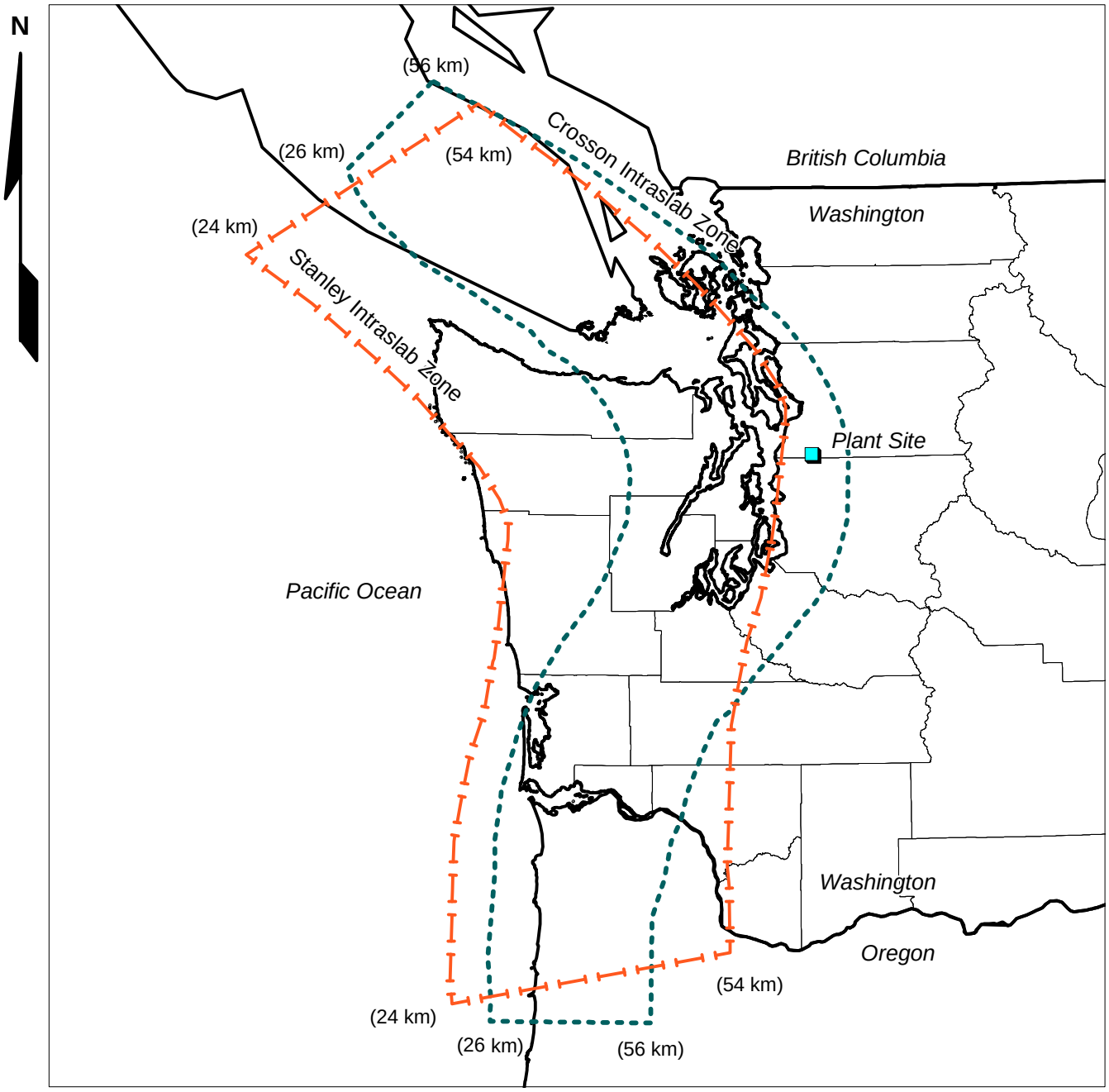

0 80 160

Scale in Kilometers

LEGEND

Stanely et al. (1999) Source Zone

Crosson and Owens (1987) Source Zone

NOTE

Depth of corner modeled zone is indicated in parenthesis.

Brightwater Project
Seismic Hazard Analysis
King County Department of Natural Resources

MODELED INTRASLAB SOURCE ZONES

Janaury 2005

FIG. 3-4

File: 21-1-20150-002, Fig 3-4 Modeled Intraslab Source Zones.WOR Date: 01/04/05 Author: Shannon & Wilson (WJP)

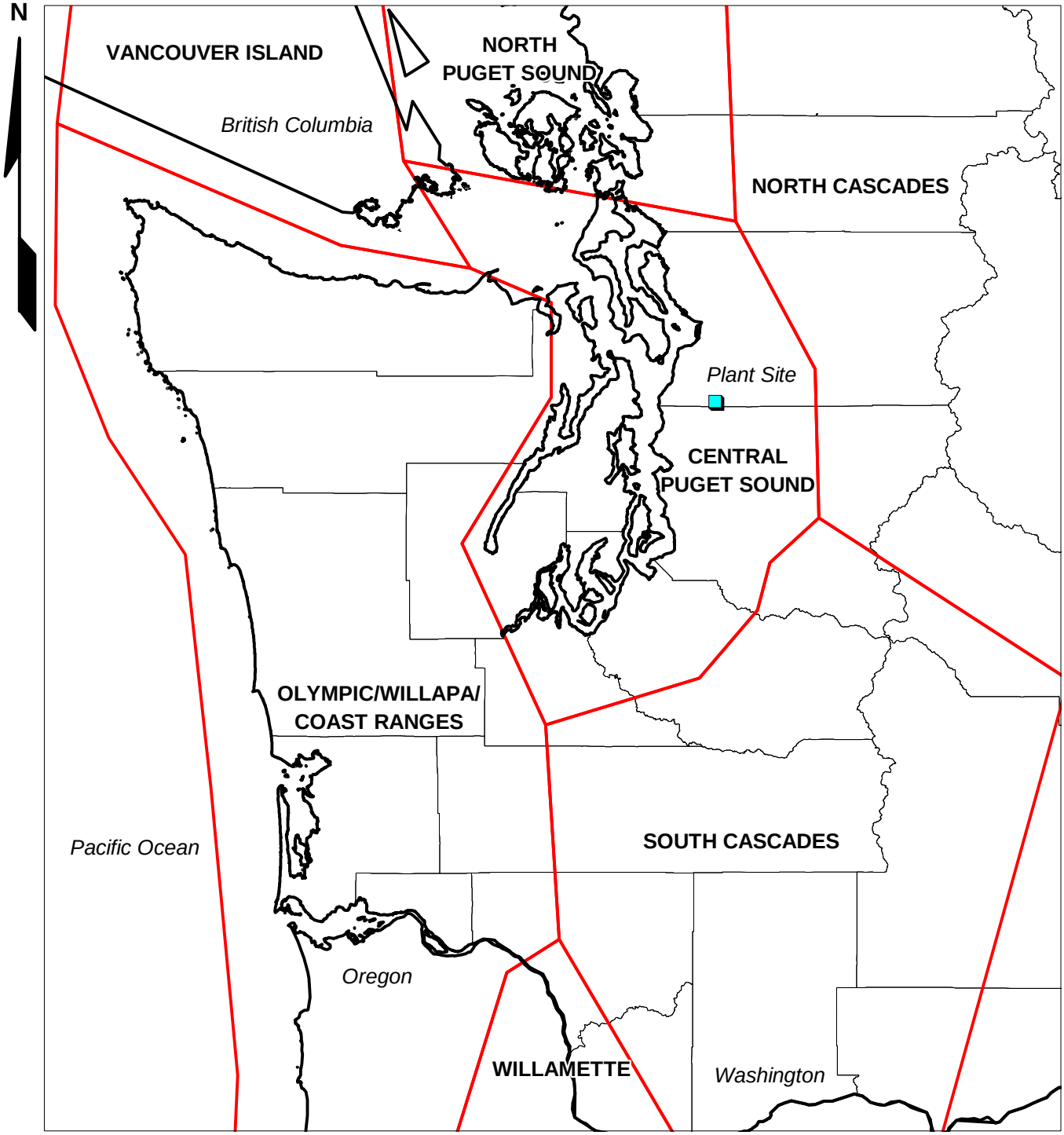

0 50 100

Scale in Kilometers

Brightwater Project
Seismic Hazard Analysis
King County Department of Natural Resources

MODELED CRUSTAL SOURCE ZONES

Janaury 2005

FIG. 3-5

File: 21-1-20150-002, Fig 3-5 Modeled Crustal Source Zones.WOR Date: 01/04/05 Author: Shannon & Wilson (WJP)

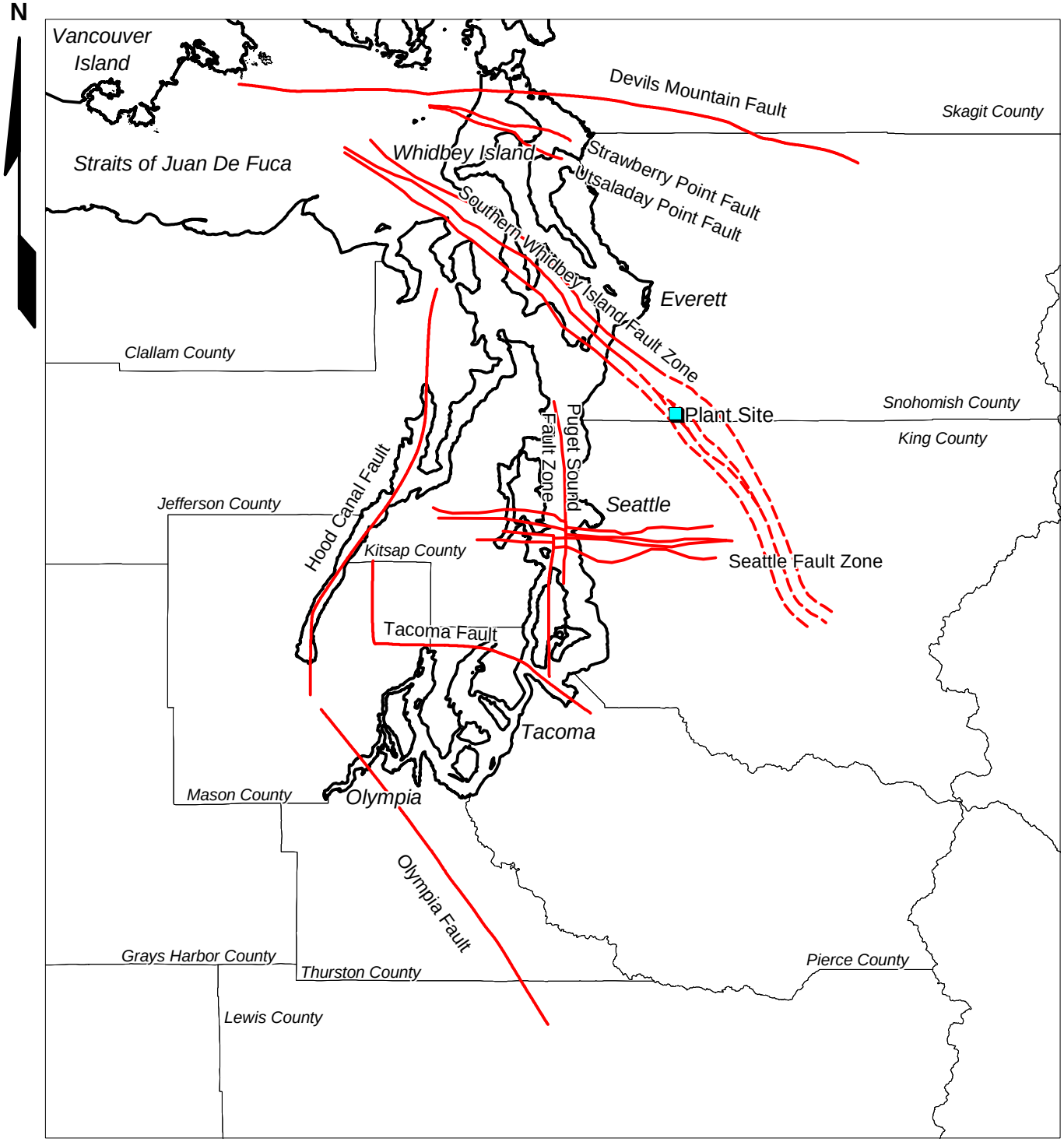

0 30 60

Scale in Kilometers

Mainland extensions of the Southern Whidbey Island Fault Zone modeled in the revised PSHA and described in this report are indicated with dashed lines.

Brightwater Project
Seismic Hazard Analysis
King County Department of Natural Resources

MODELED CRUSTAL FAULTS

Janaury 2005

FIG. 3-6

File: 21-1-20150-002, Fig 3-6 Modeled Crustal Faults.WOR Date: 01/04/05 Author: Shannon & Wilson (WJP)

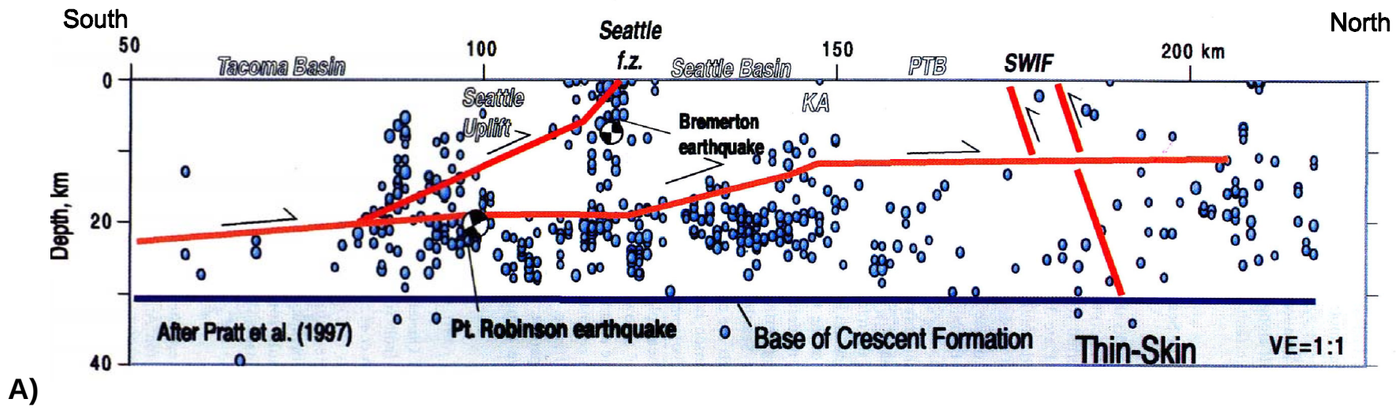

A)

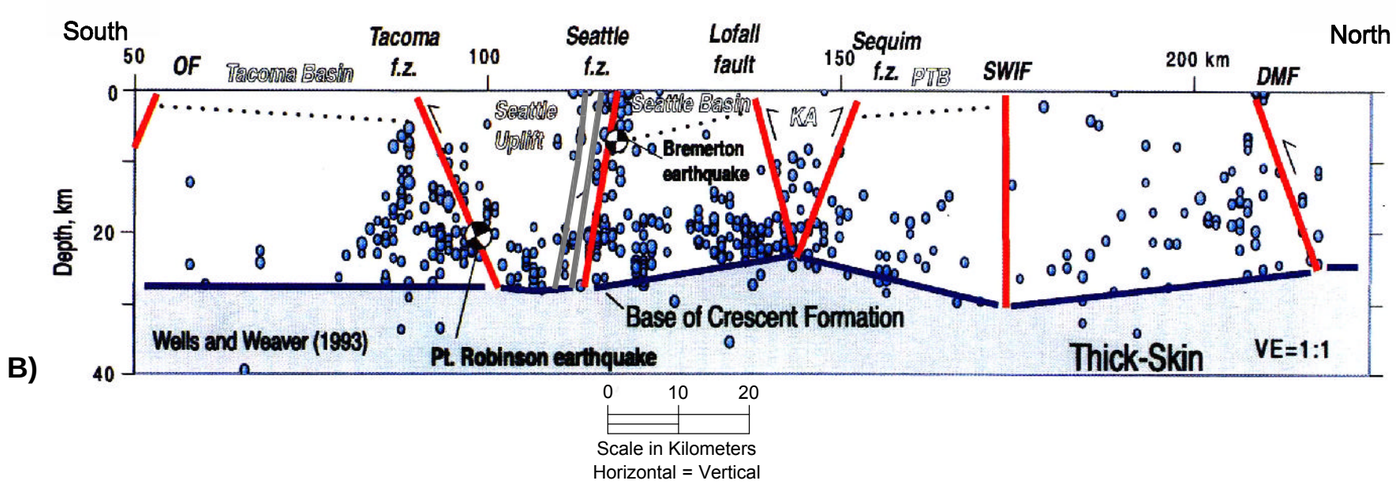

B)

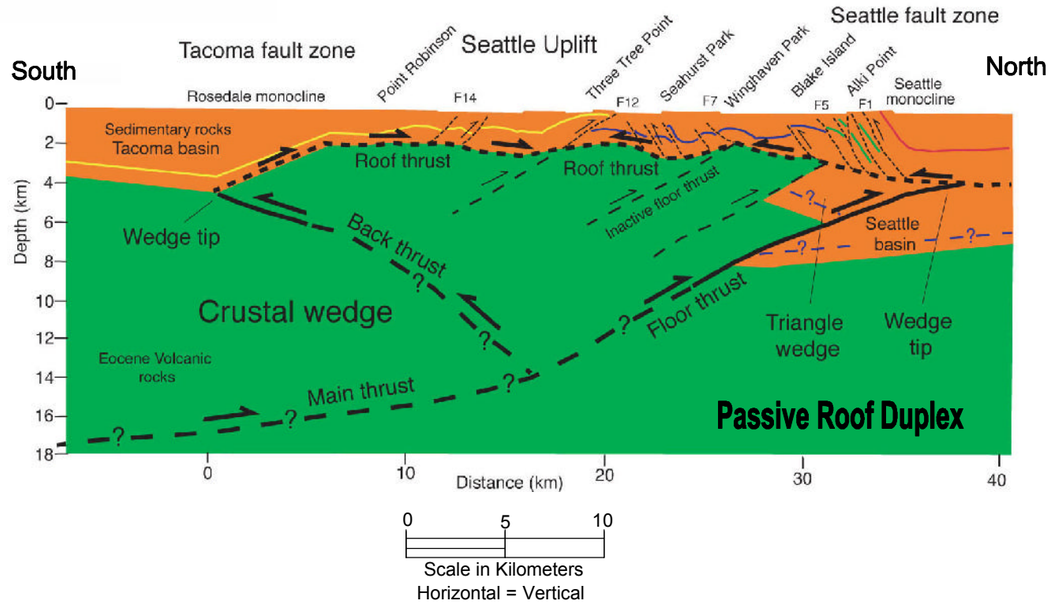

C)

NOTES

1. Figures A and B from *Brocher et al.*, 2001. Cross sections show Thick- and Thin-Skinned models of fault geometry in the Puget Lowland and relation of microseismicity to inferred crustal faults. The 660 hypocenters are for magnitude ≥2 earthquakes between 1970 and 1999. The hypocenters were projected E-W along a 40 km wide swath.

2. Figure C from *Brocher et al.*, 2004.

Brightwater Project
Seismic Hazard Analysis
King County Department of Natural Resources

PUGET LOWLAND CRUSTAL CROSS SECTION

January 2005 | **FIG. 3-7**

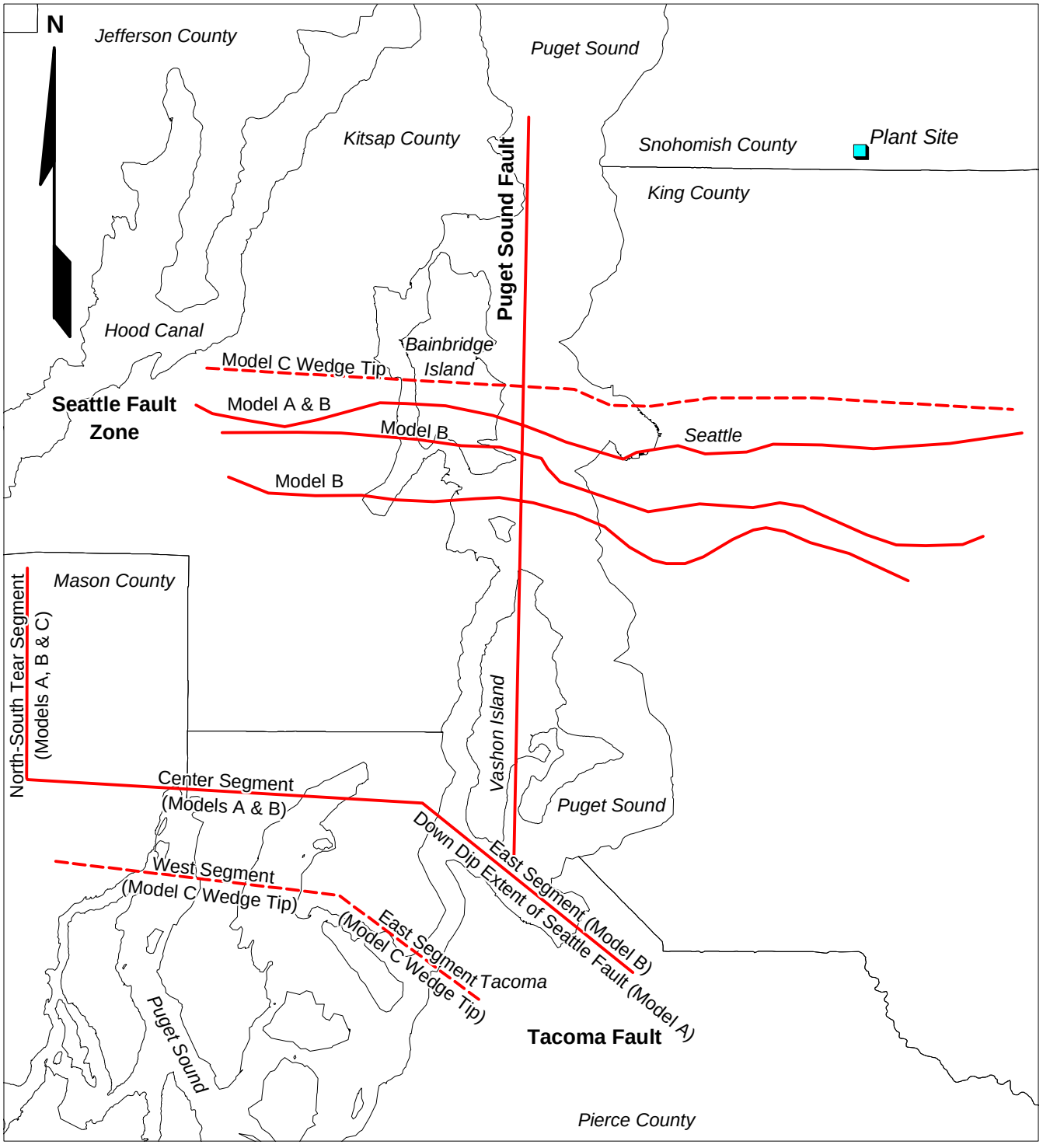

Brightwater Project
Seismic Hazard Analysis
King County Department of Natural Resources

MODELED SEATTLE PUGET SOUND AND TACOMA FAULTS

Janaury 2005

FIG. 3-8

File: 21-1-20150-002, Fig 3-8 Modeled Seattle Tacoma PS faults.WOR Date: 01/04/05 Author: Shannon & Wilson (WJP)

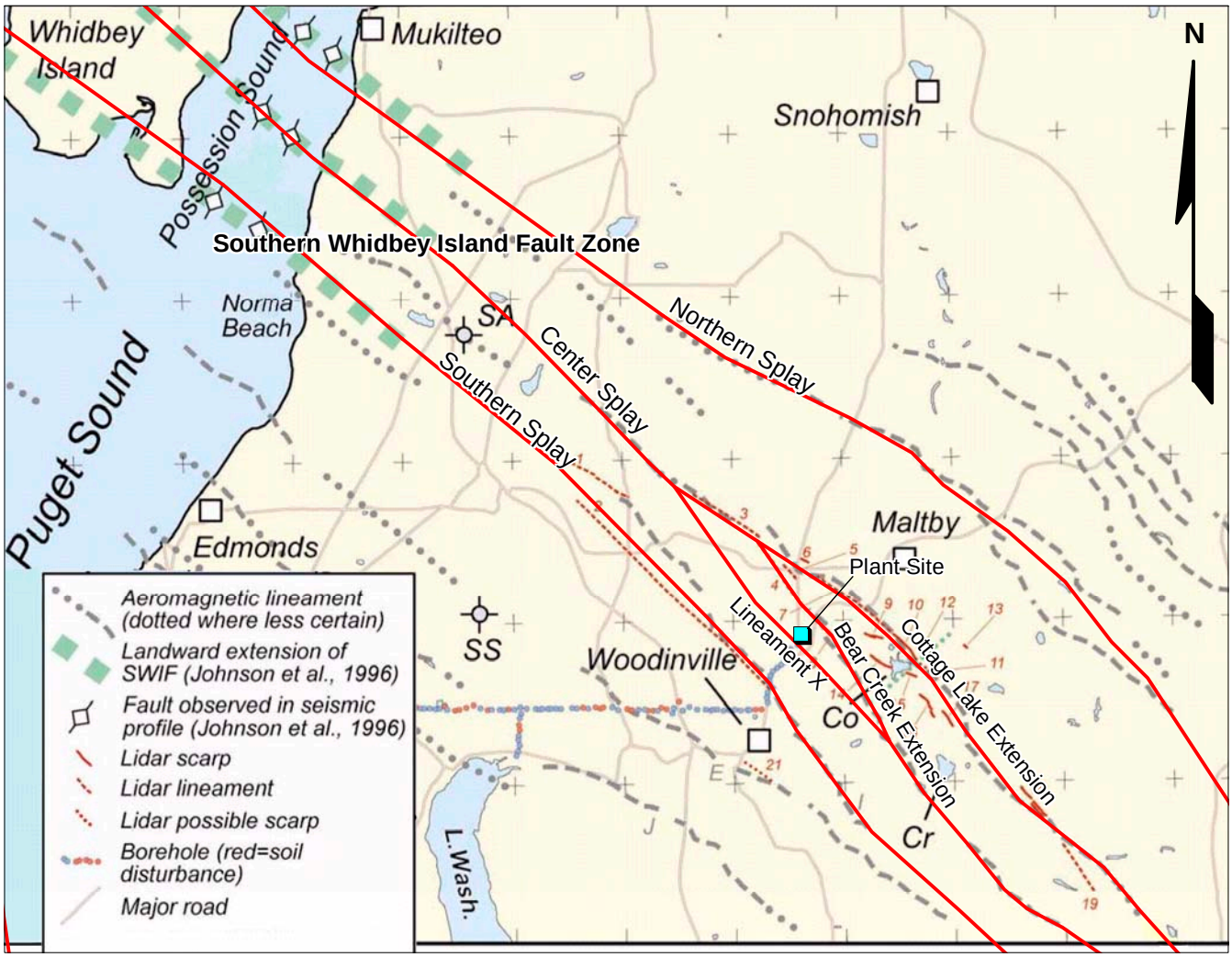

0 5 10

Scale in Kilometers

NOTES

1. Base map is from Blakely et al. (2004).

2. Solid red lines show Southern Whidbey Island Fault Zone splays assumed in the revised PSHA model Y1. The fault splay locations are based on the location of magnetic anomolies and topographic scarps and lineaments in Blakely et al. (2004).

Brightwater Project
Seismic Hazard Analysis
King County Department of Natural Resources

SOUTHERN WHIDBEY ISLAND FAULT ZONE MODEL Y1 IN THE PLANT VICINITY

Janaury 2005

FIG. 3-9

File: 21-1-20150-002, Fig 3-9 SWIF Model Y1.WOR Date: 01/04/05 Author: Shannon & Wilson (WJP)

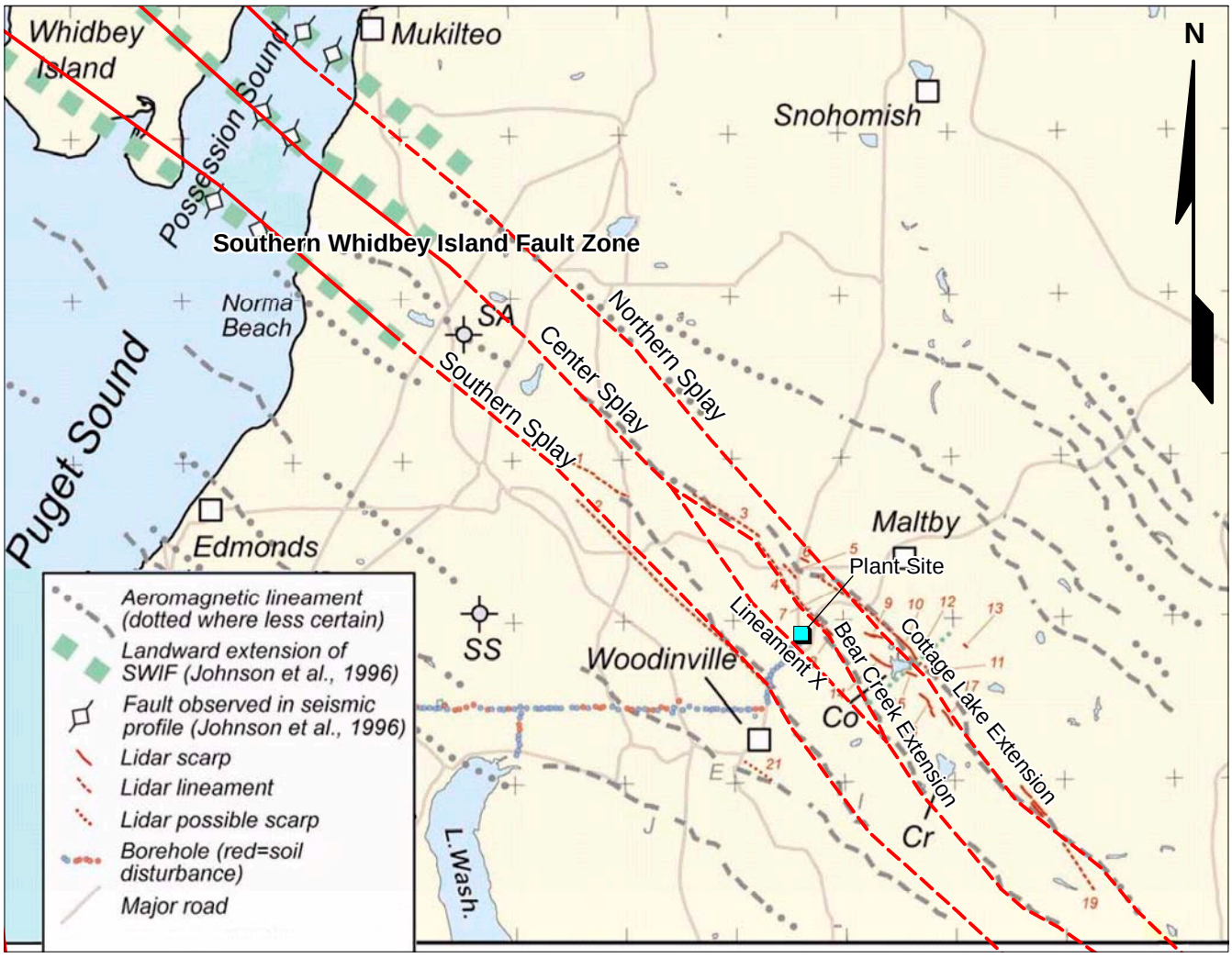

0 5 10

Scale in Kilometers

NOTES

1. Base map is from Blakely et al. (2004).

2. Solid red lines show Southern Whidbey Island Fault Zone splays assumed in the revised PSHA model Y2. The fault splay locations are based on the location of magnetic anomolies and topographic scarps and lineaments in Blakely et al. (2004).

Brightwater Project
Seismic Hazard Analysis
King County Department of Natural Resources

SOUTHERN WHIDBEY ISLAND FAULT ZONE MODEL Y2 IN THE PLANT VICINITY

Janaury 2005

FIG. 3-10

File: 21-1-20150-002, Fig 3-10 SWIF Model Y2.WOR Date: 01/04/05 Author: Shannon & Wilson (WJP)

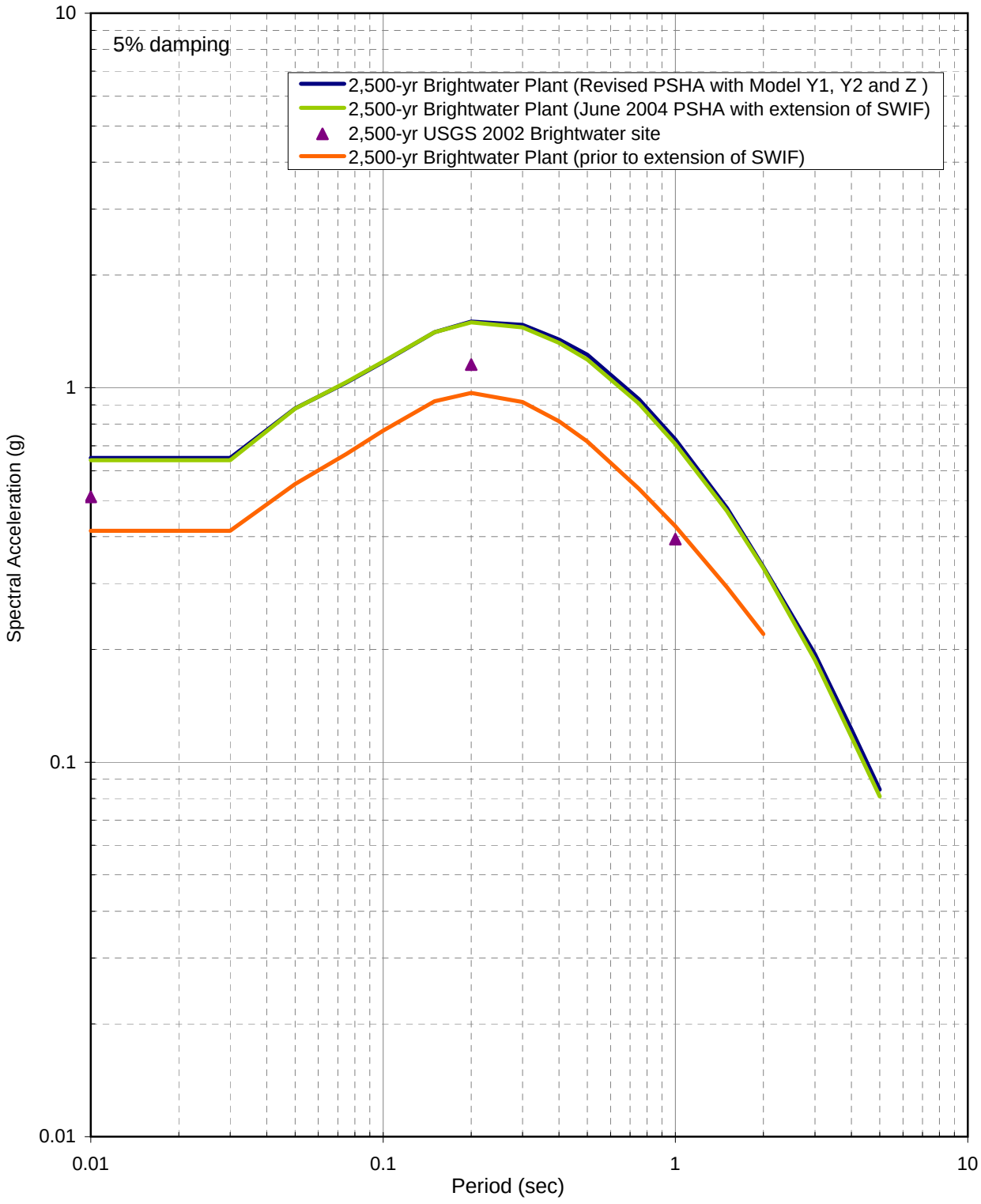

Brightwater Project
Seismic Hazard Analysis
King County Department of Natural Resources

SOFT ROCK
ACCELERATION SPECTRA

January 2005

FIG. 4-1

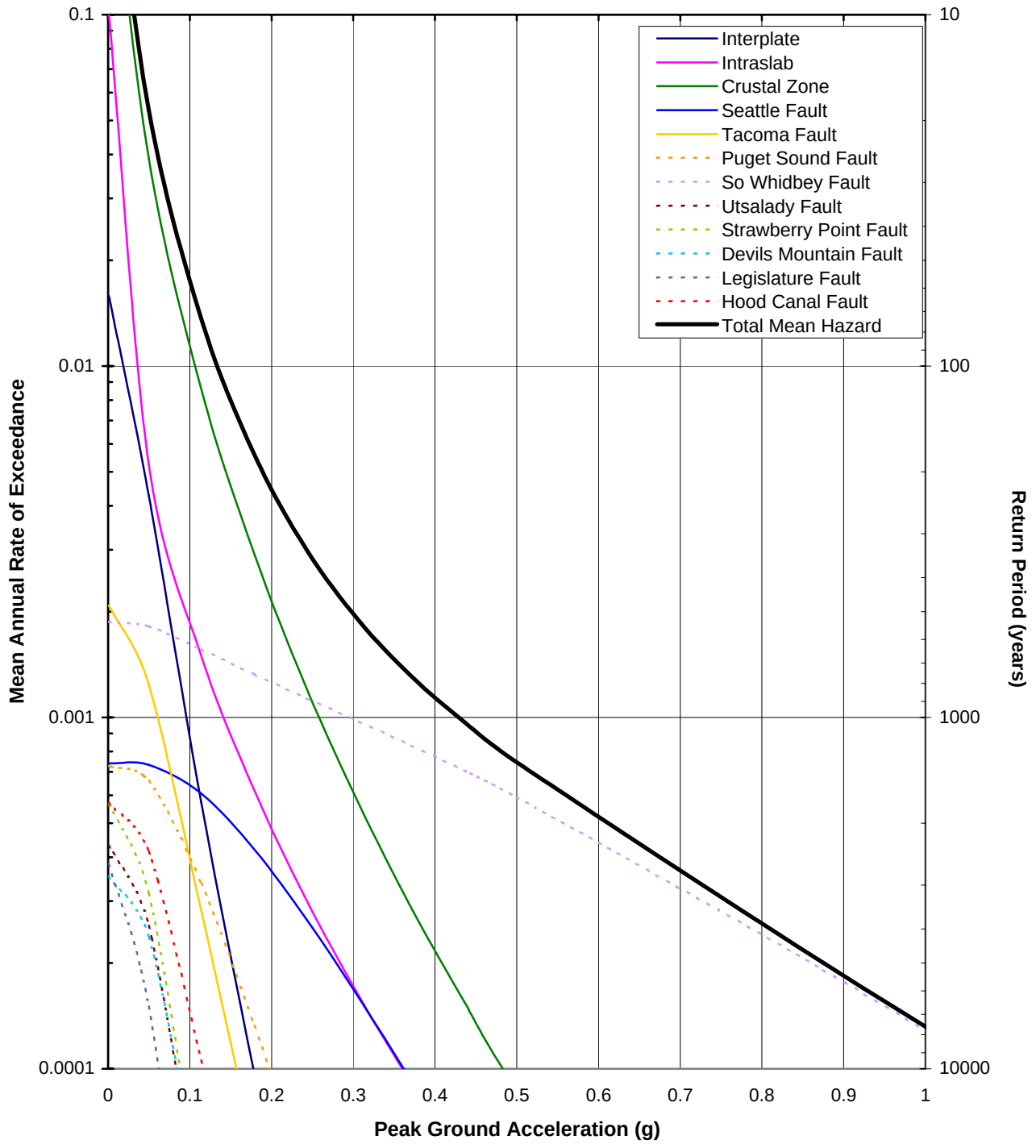

NOTE:
Fault model used to produce these hazard curves includes the extension of the South Whidbey Island Fault.

Brightwater Project
Seismic Hazard Analysis
King County Department of Natural Resources

SEISMIC SOURCE CONTRIBUTIONS TO PEAK GROUND ACCELERATION

January 2005

FIG. 4-2

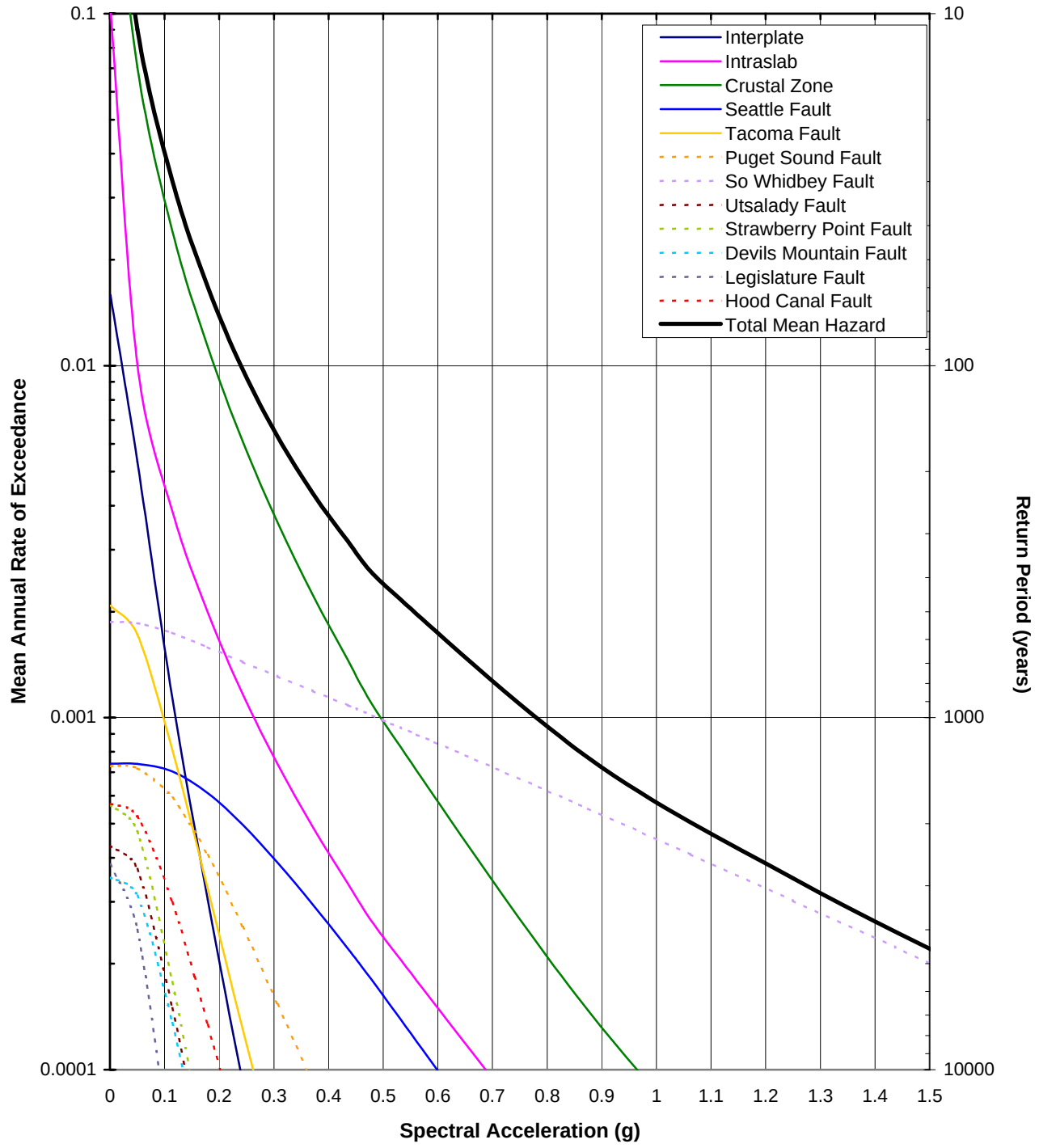

NOTE:
Fault model used to produce these hazard curves includes the extension of the South Whidbey Island Fault.

Brightwater Project
Seismic Hazard Analysis
King County Department of Natural Resources

SEISMIC SOURCE CONTRIBUTIONS TO 0.1 SECOND ACCELERATION

January 2005

FIG. 4-3

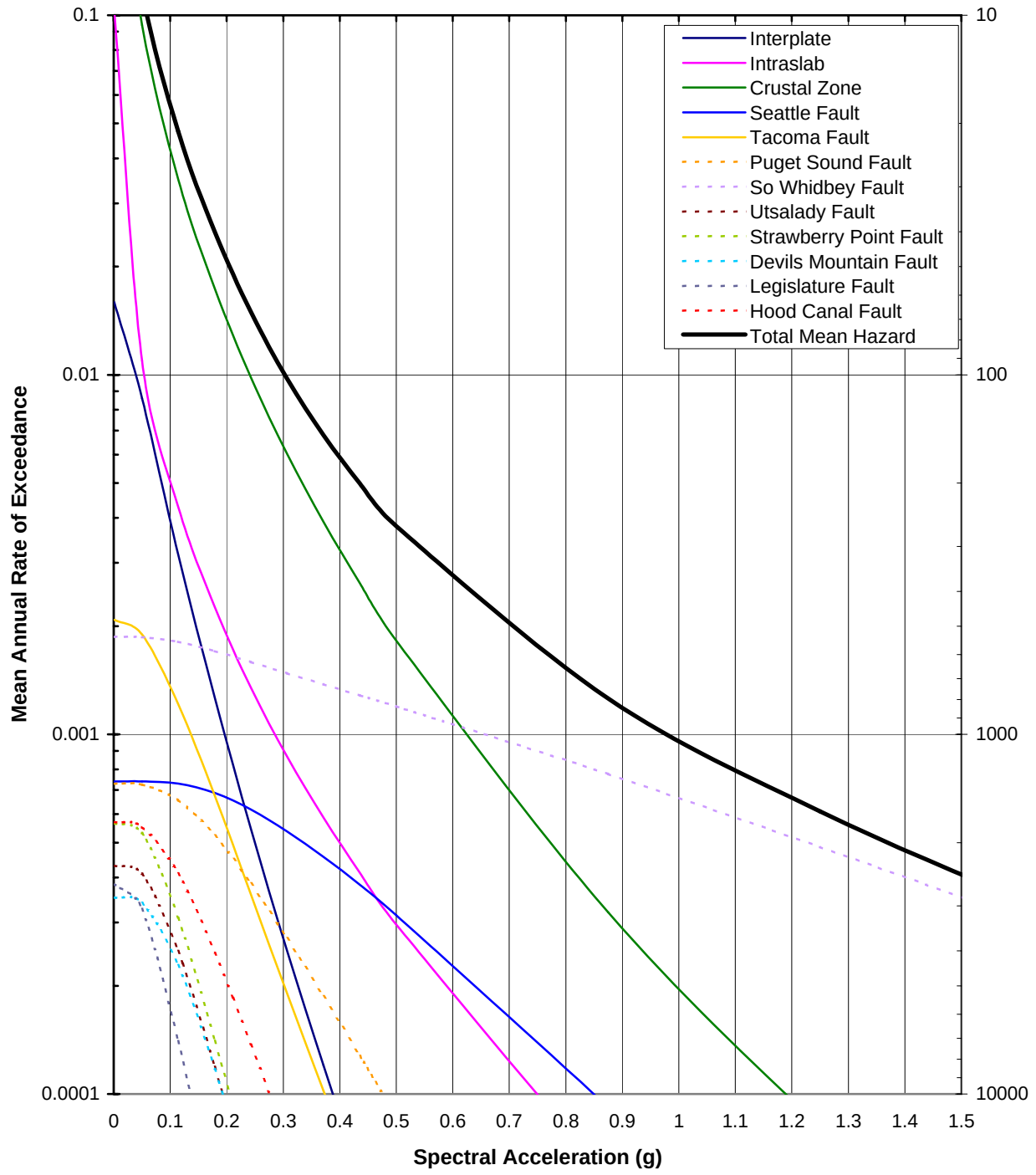

NOTE:
Fault model used to produce these hazard curves includes the extension of the South Whidbey Island Fault.

Brightwater Project
Seismic Hazard Analysis
King County Department of Natural Resources

SEISMIC SOURCE CONTRIBUTIONS TO 0.2 SECOND ACCELERATION

January 2005 | **FIG. 4-4**

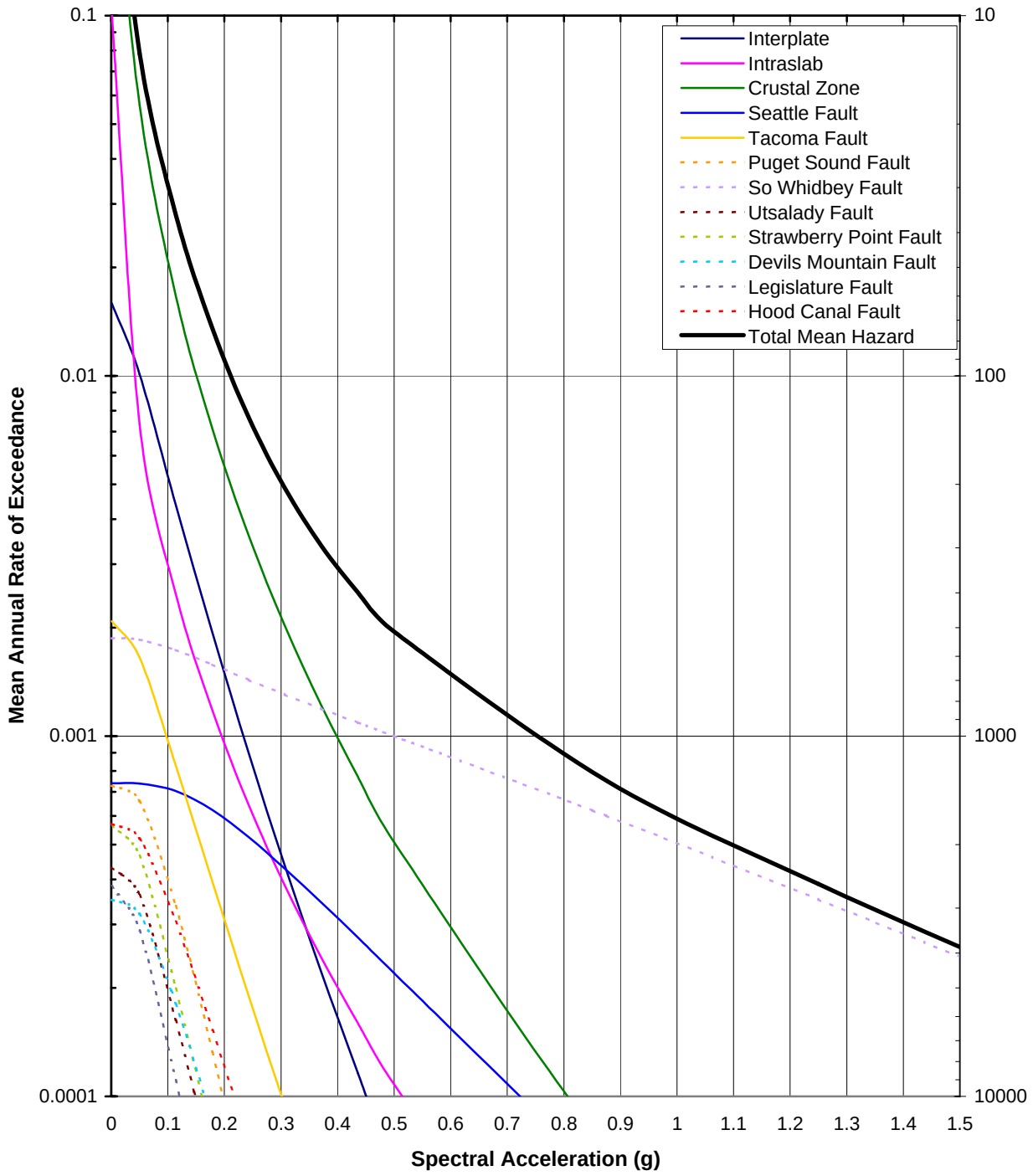

NOTE:
Fault model used to produce these hazard curves includes the extension of the South Whidbey Island Fault.

Brightwater Project
Seismic Hazard Analysis
King County Department of Natural Resources

SEISMIC SOURCE CONTRIBUTIONS TO 0.5 SECOND ACCELERATION

January 2005 | **FIG. 4-5**

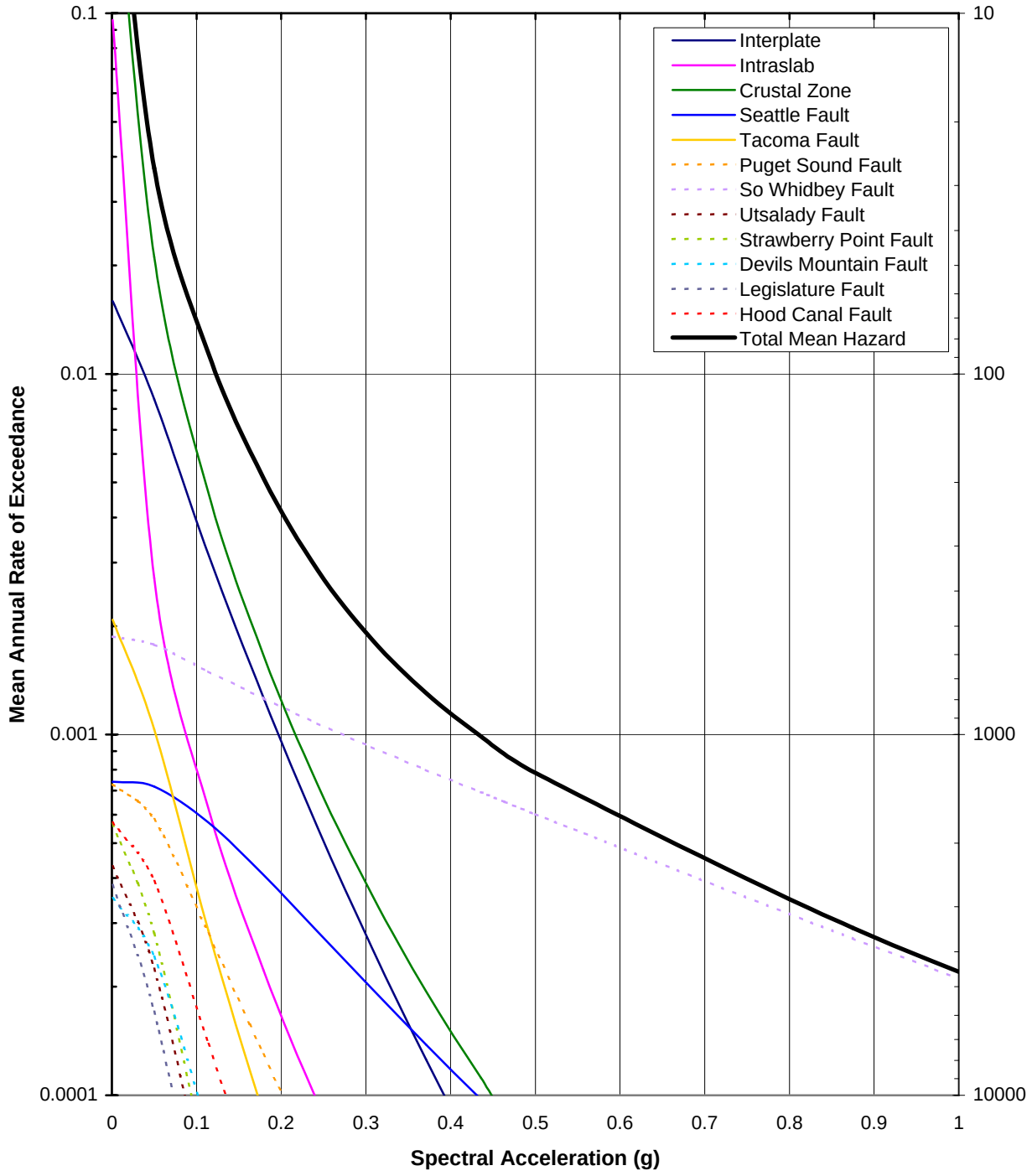

NOTE:
Fault model used to produce these hazard curves includes the extension of the South Whidbey Island Fault.

Brightwater Project
Seismic Hazard Analysis
King County Department of Natural Resources

SEISMIC SOURCE CONTRIBUTIONS TO 1.0 SECOND ACCELERATION

January 2005

FIG. 4-6

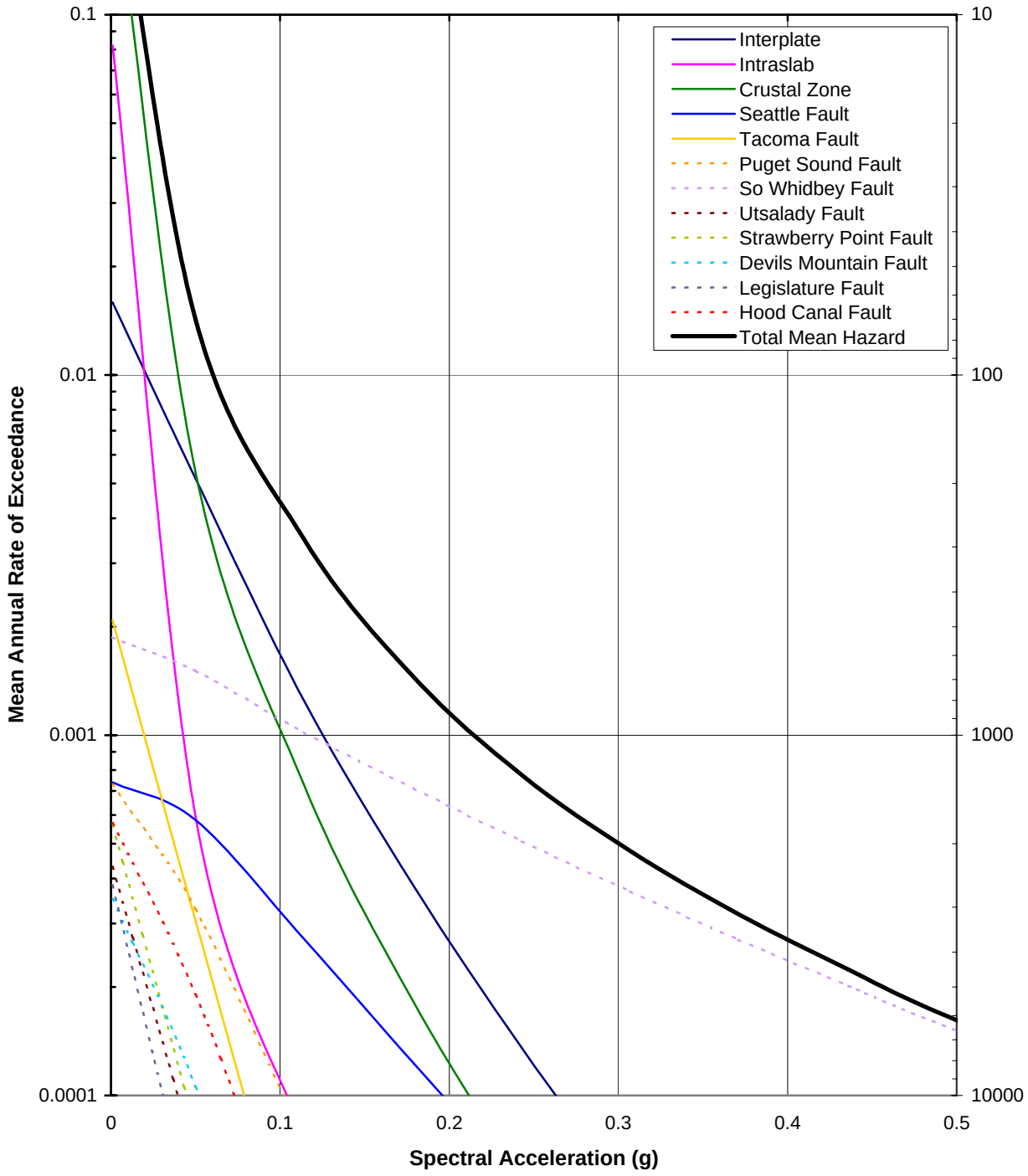

NOTE:
Fault model used to produce these hazard curves includes the extension of the South Whidbey Island Fault.

Brightwater Project
Seismic Hazard Analysis
King County Department of Natural Resources

SEISMIC SOURCE CONTRIBUTIONS TO 2.0 SECOND ACCELERATION

January 2005 | **FIG. 4-7**

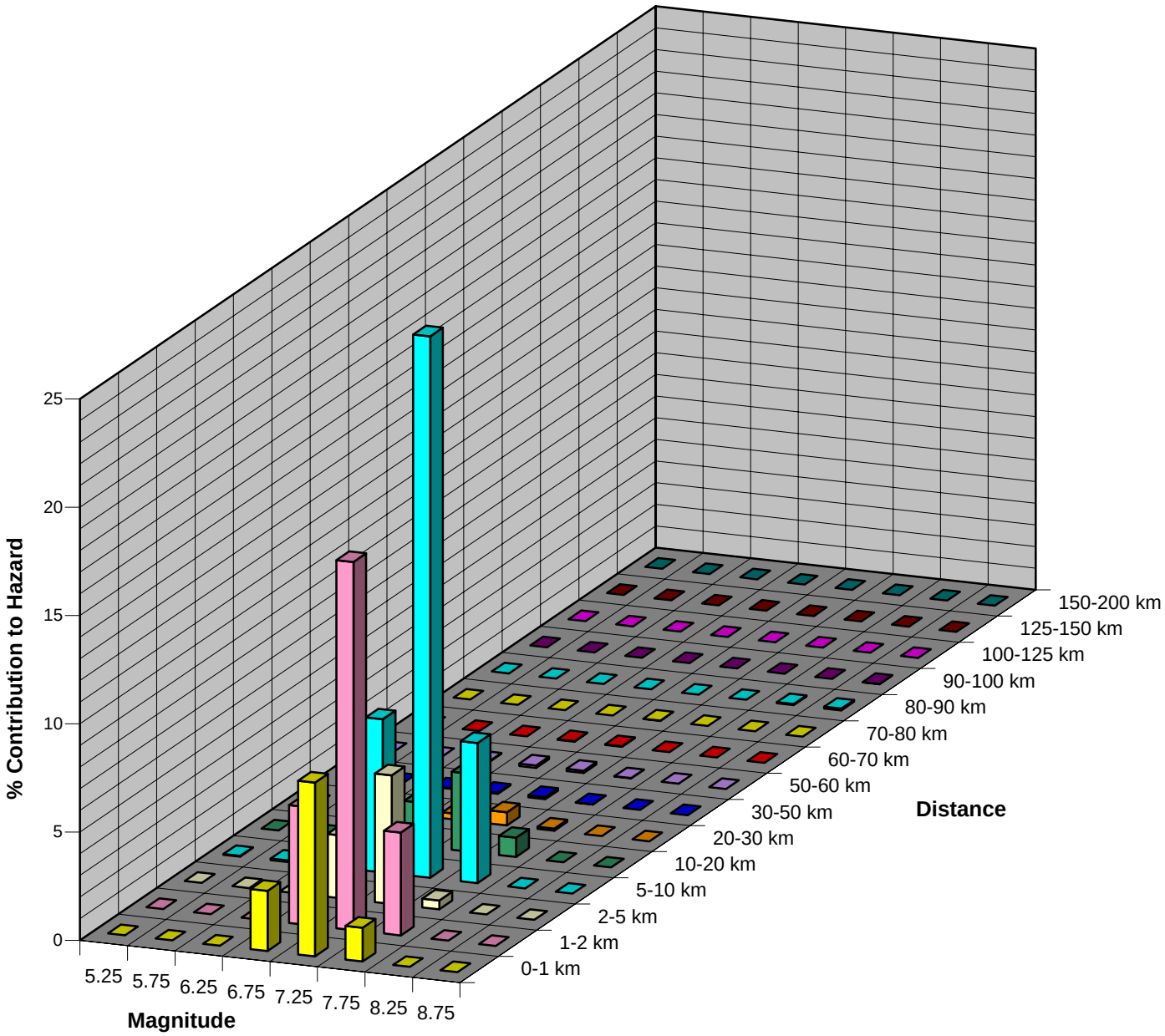

Magnitude Bar	6.9
Distance Bar	8
Epsilon Bar	0.30

Brightwater Treatment Plant
Seismic Hazard Analysis
King County Department of Natural Resources

MAGNITUDE & DISTANCE CONTRIBUTION
PEAK GROUND ACCELERATION
2500-YEAR EARTHQUAKE

January 2005

FIG. 4-8

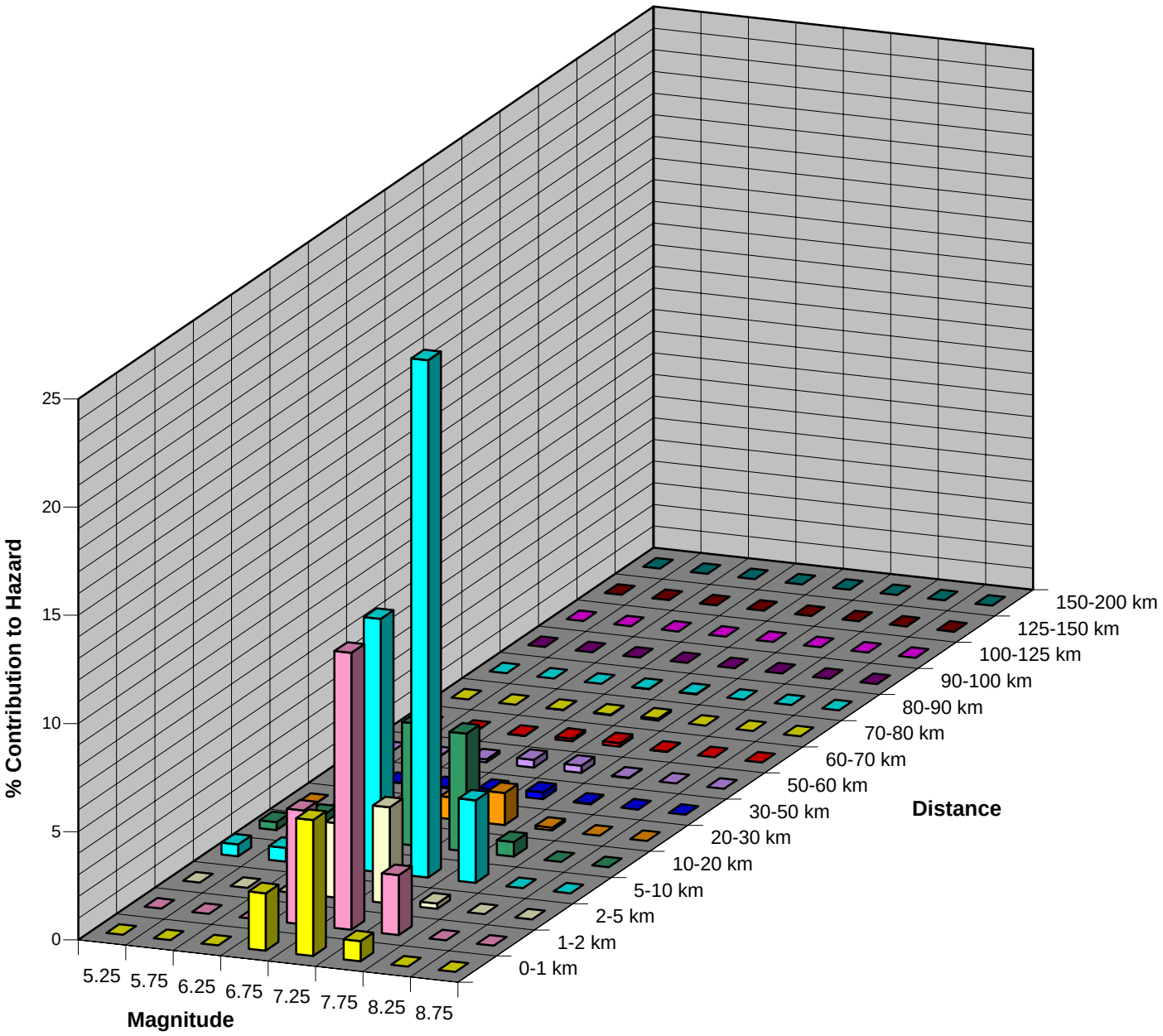

Magnitude Bar	6.8
Distance Bar	9
Epsilon Bar	0.56

Brightwater Treatment Plant
Seismic Hazard Analysis
King County Department of Natural Resources

MAGNITUDE & DISTANCE CONTRIBUTION
0.1 SECOND ACCELERATION
2500-YEAR EARTHQUAKE

January 2005

FIG. 4-9

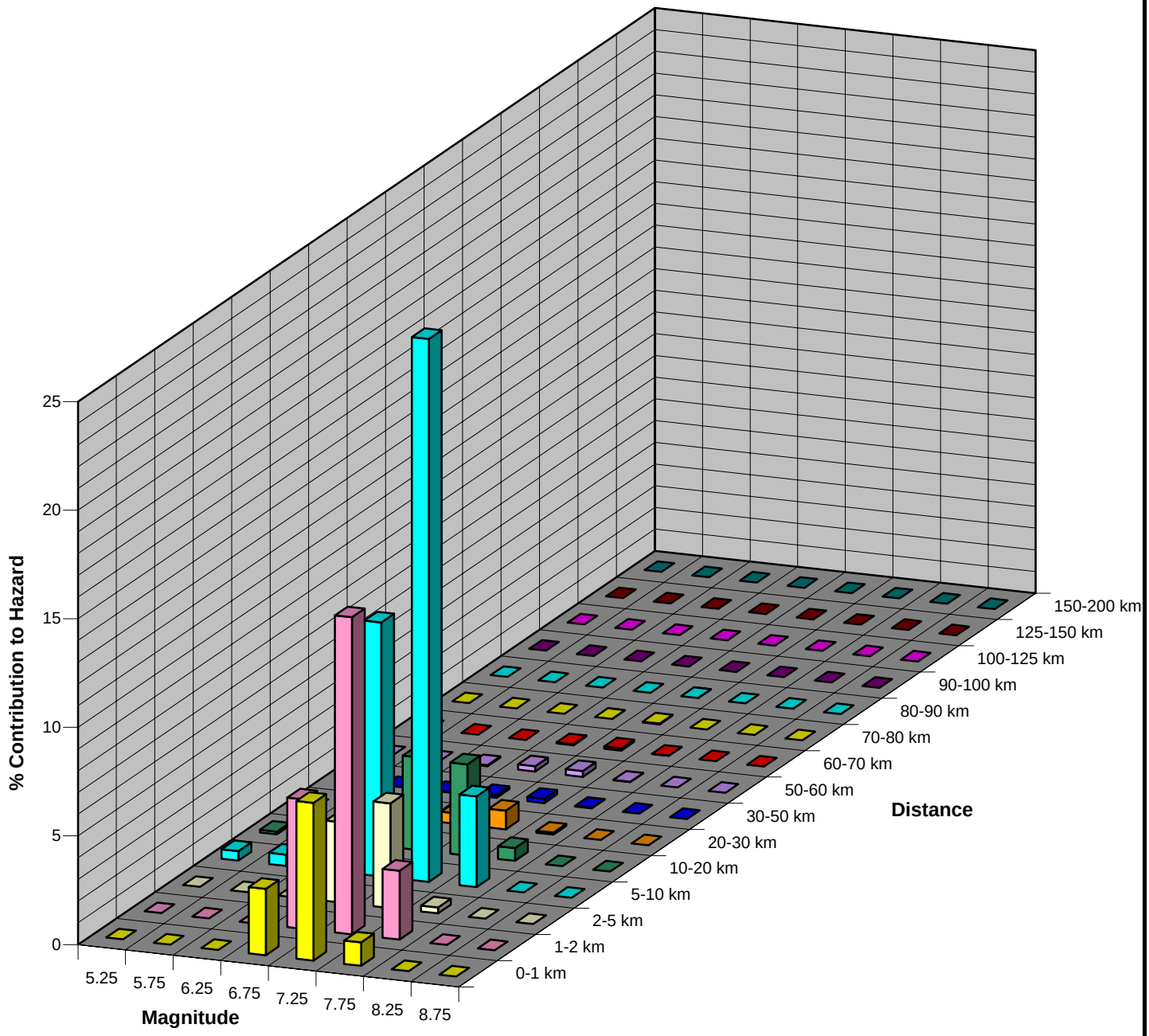

Magnitude Bar	6.9
Distance Bar	7
Epsilon Bar	0.48

Brightwater Treatment Plant
Seismic Hazard Analysis
King County Department of Natural Resources

MAGNITUDE & DISTANCE CONTRIBUTION
0.2 SECOND ACCELERATION
2500-YEAR EARTHQUAKE

January 2005

FIG. 4-10

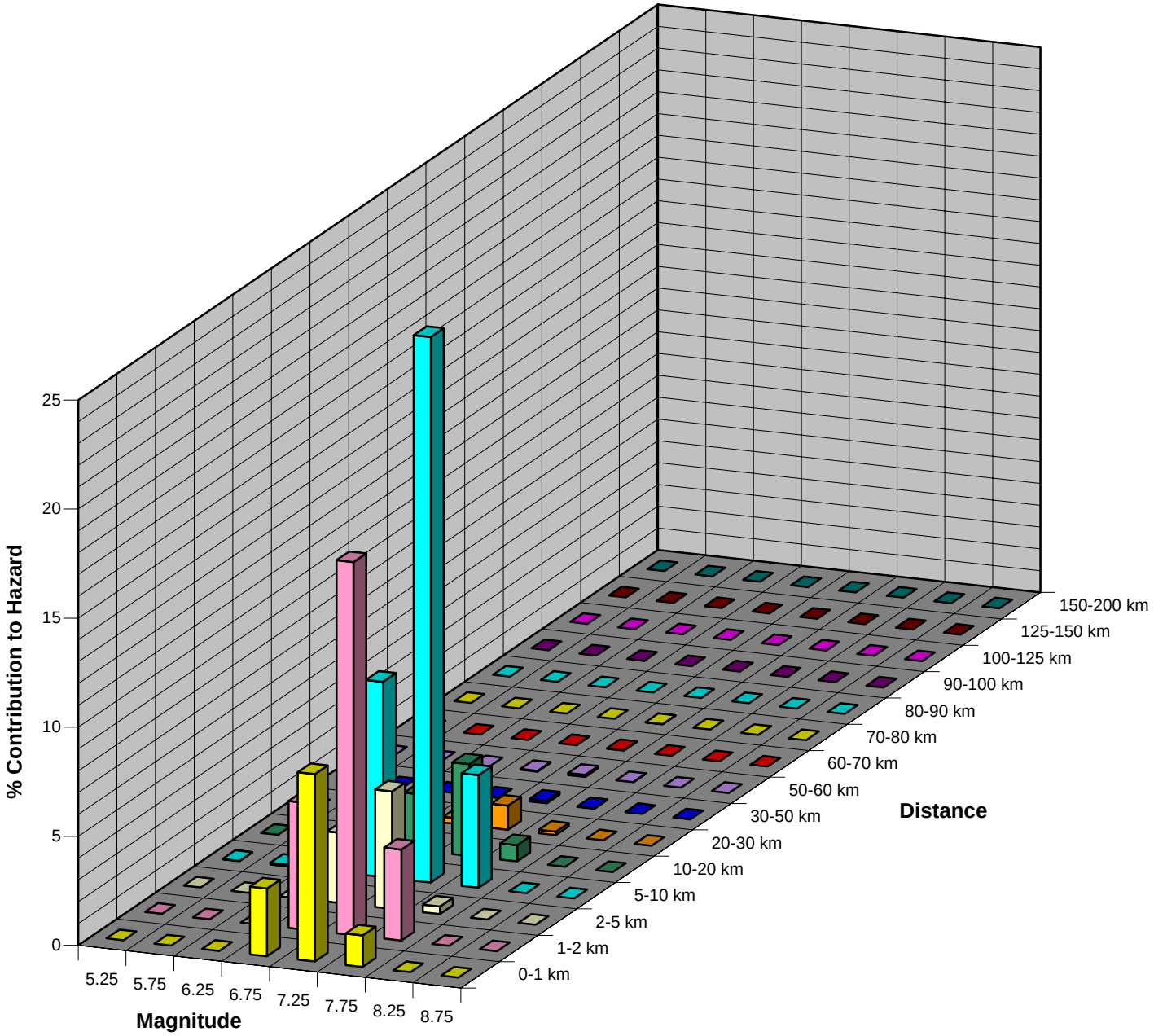

Magnitude Bar	6.9
Distance Bar	6
Epsilon Bar	0.31

Brightwater Treatment Plant
Seismic Hazard Analysis
King County Department of Natural Resources

MAGNITUDE & DISTANCE CONTRIBUTION
0.5 SECOND ACCELERATION
2500-YEAR EARTHQUAKE

January 2005 | **FIG. 4-11**

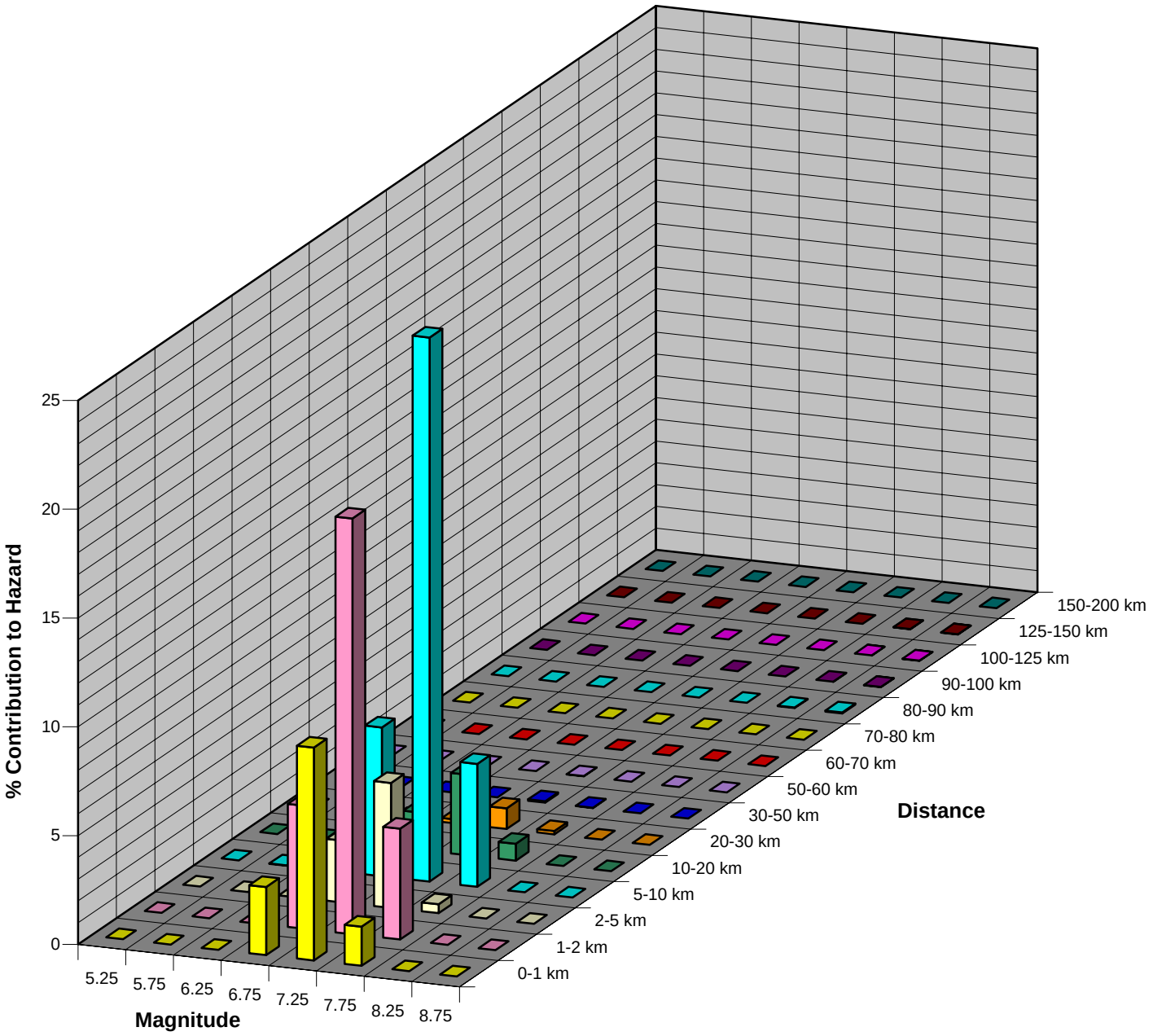

Magnitude Bar	6.9
Distance Bar	9
Epsilon Bar	0.31

Brightwater Treatment Plant
Seismic Hazard Analysis
King County Department of Natural Resources

MAGNITUDE & DISTANCE CONTRIBUTION
1.0 SECOND ACCELERATION
2500-YEAR EARTHQUAKE

January 2005

FIG. 4-12

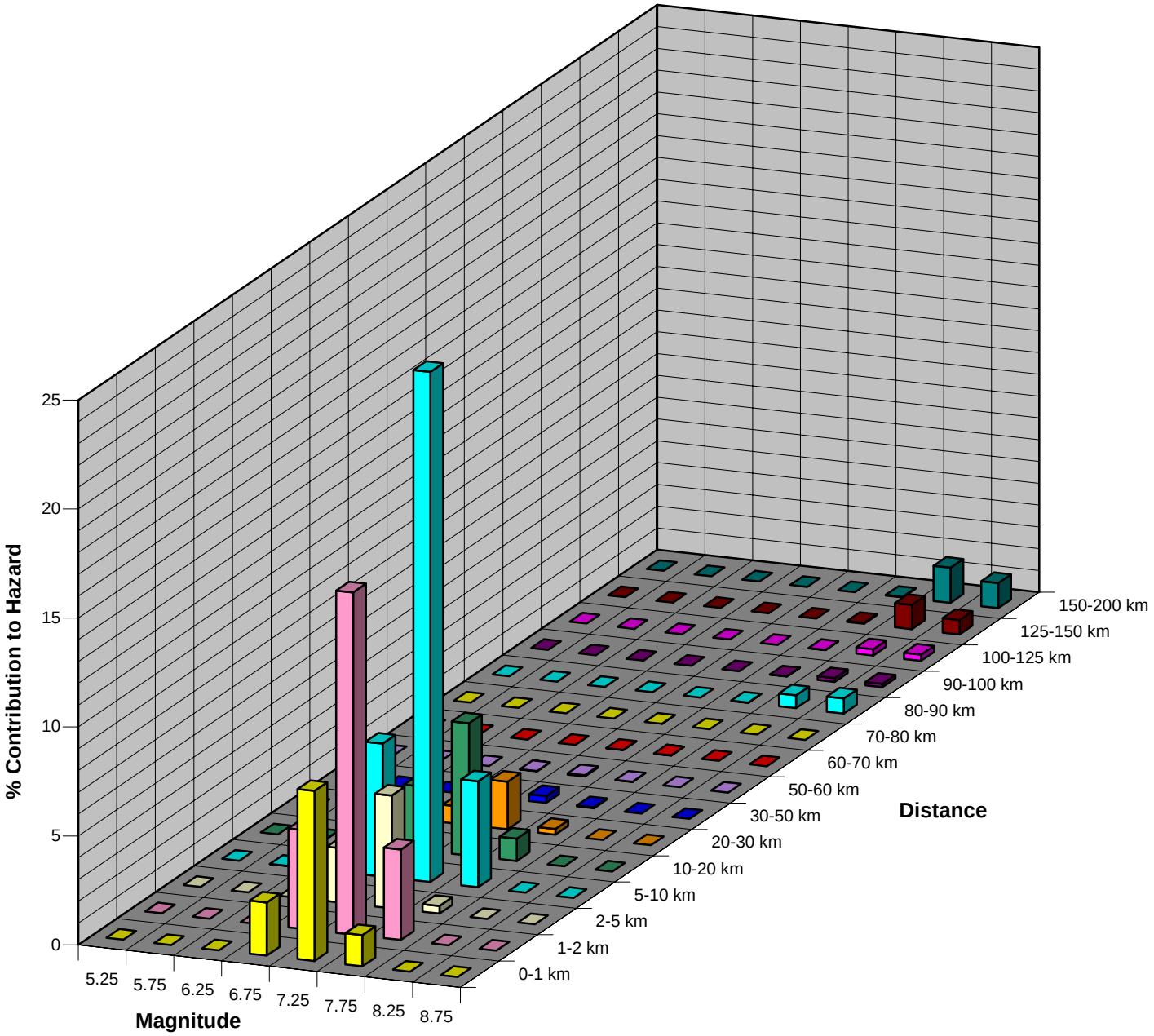

Magnitude Bar	7.0
Distance Bar	21
Epsilon Bar	0.59

Brightwater Treatment Plant
Seismic Hazard Analysis
King County Department of Natural Resources

MAGNITUDE & DISTANCE CONTRIBUTION
2.0 SECOND ACCELERATION
2500-YEAR EARTHQUAKE

January 2005

FIG. 4-13

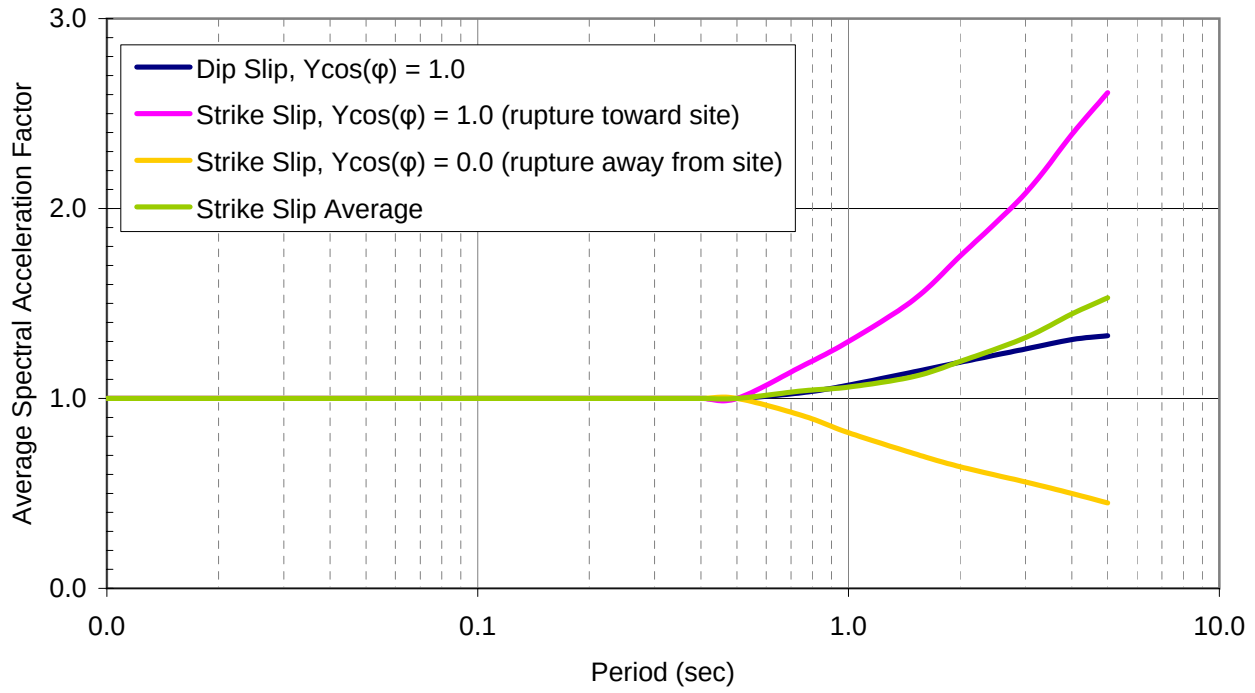

NOTES

1. Deterministic Average Spectral Acceleration Factors based on Somerville et al (1997).
2. Directivity factors taken as the maximum of Dip Slip for Ycos(φ) = 1.0 and Strike Slip Average.

Brightwater Project
Seismic Hazard Analysis
King County Department of Natural Resources

SPECTRAL ACCELERATION FACTORS
AVERAGE DIRECTIVITY EFFECTS

January 2005 | **FIG. 4-14**

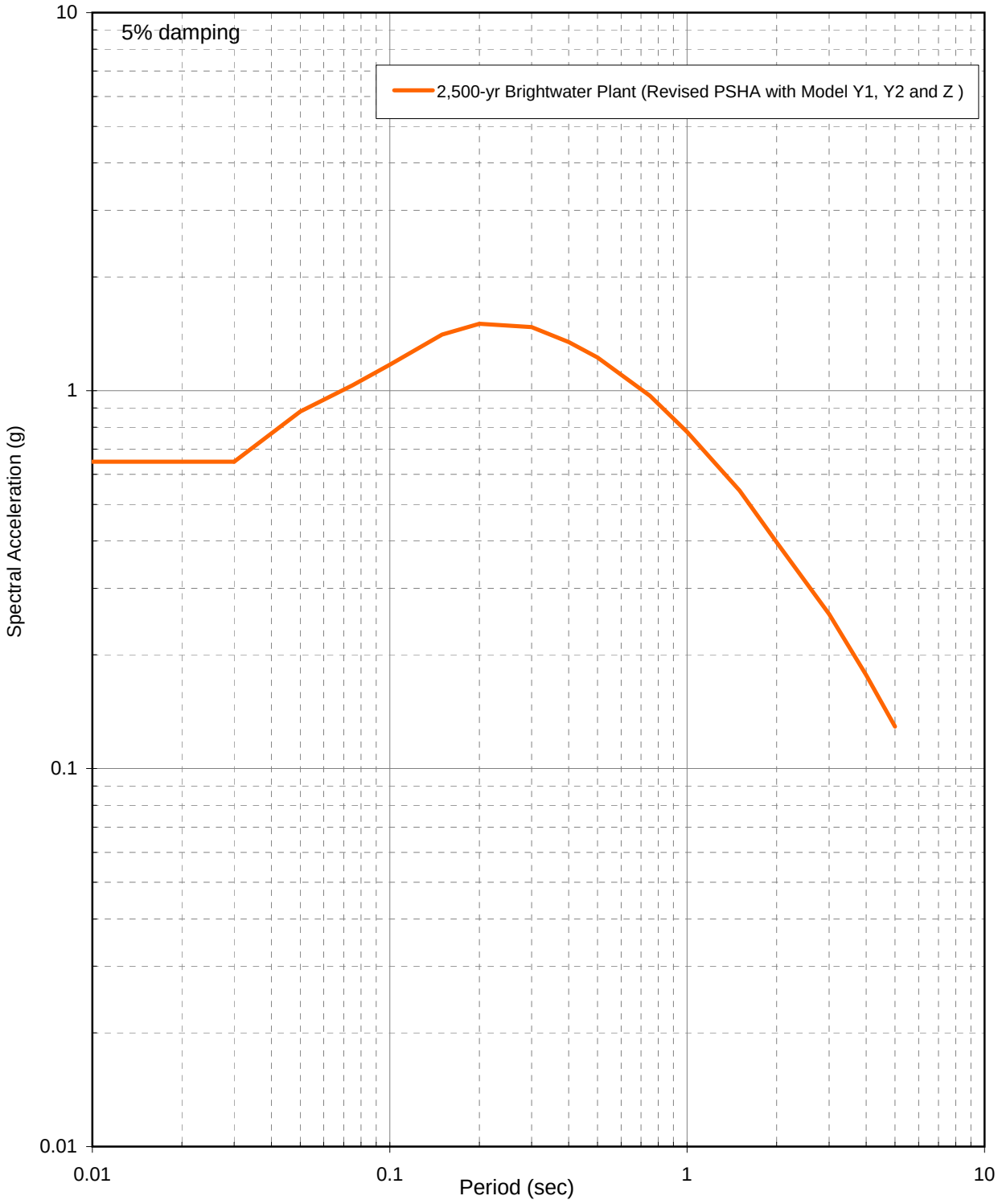

NOTE:
1. Spectrum corresponds to a 2500-year return period ground motion.

Brightwater Project
Seismic Hazard Analysis
King County Department of Natural Resources

SOFT ROCK ACCELERATION SPECTRUM WITH AVERAGE DIRECTIVITY EFFECTS

January 2005

FIG. 4-15

Appendix A

Tectonics and Seismicity

Appendix A

Tectonics and Seismicity

TABLE OF CONTENTS

Page

A.1 TECTONICS A-1
- A.1.1 Province 1, Juan De Fuca Plate A-1
- A.1.2 Province 2, Fore-Arc A-2
- A.1.3 Province 3, Volcanic Arc A-3

A.2 SEISMICITY A-3
- A.2.1 Historical Seismicity A-4
- A.2.2 Holocene Paleoseismicity A-5
  - A.2.2.1 Cascadia Subduction Zone Interplate Seismicity A-5
  - A.2.2.2 Seattle Fault Seismicity A-6
  - A.2.2.3 Tacoma Fault Seismicity A-7
  - A.2.2.4 Southern Whidbey Island Fault Seismicity A-7
  - A.2.2.5 Utsalady Point Fault Seismicity A-8

A.3 REFERENCES A-9

LIST OF TABLES

Table No.

A-1 Largest Historic Earthquakes Felt in Washington (2 pages)
A-2 Historic Earthquakes in or Near Western Washington, $M \geq 4$ (14 pages)

LIST OF FIGURES

Figure No.

A-1 North American Plate Tectonic Provinces in Western Washington
A-2 Major Crustal Structures in the Central Puget Sound and Adjacent Areas
A-3 Historic Earthquakes in or Near Western Washington

Appendix A
Tectonics and Seismicity

A.1 Tectonics

The tectonics and seismicity of the region are the result of ongoing, oblique, relative northeastward subduction of the Juan de Fuca Plate beneath the North American Plate between northern California and southern British Columbia and dextral strike-slip motion on the transform boundary between the North American and Pacific Plates farther south. The relative motion among these plates not only results in east-west compressive strain, but also results in dextral shear, clockwise rotation, and north-south compression of accreted crustal blocks that form the leading edge of the North American Plate (Wells et al., 1998) above the subduction zone. As in most active convergence zones, the Cascadia Subduction Zone (CSZ) contains a continental fore-arc consisting of accreted sedimentary and volcanic rocks in front of a landward mountainous, active volcanic arc. Unlike most active subduction zones, there is a conspicuous absence of an oceanic trench near the juncture of the two plates.

Within the framework of the subduction zone, the region is divided into four primary tectonic provinces: (1) the Juan de Fuca Plate, (2) the continental fore-arc on the western edge of the North American Plate, (3) the landward continental volcanic arc (Cascade Mountains), and (4) the back arc east of the Cascade Mountains. The three provinces on the North American Plate in and adjacent to western Washington (fore-arc, volcanic arc, and back arc) are illustrated in Figure A-1. The Juan de Fuca Plate is located at depth below the crustal provinces and is not shown in Figure A-1. As shown in Figure A-1, the crustal tectonic provinces can be further subdivided into subprovinces based on structural deformation styles, seismicity, rock types, and geomorphology.

The Brightwater Plant and Portal sites are situated within the eastern half of continental fore-arc (province 2) near the Cascade Mountains (province 3) and is underlain at depth by the subducted portion of the Juan de Fuca Plate (province 1). Because of the location of the facilities within, near, or above these tectonic provinces, the following provides a brief description of these provinces as a basis for discussion of seismicity and earthquake sources that could significantly affect the site.

A.1.1 Province 1, Juan De Fuca Plate

Province 1 is the Juan de Fuca Plate oceanic crust. This province can be divided into two subprovinces: the portion of the plate west of the subduction zone and the portion of the slab

subducted beneath the North American Plate. Of the subducted portion of the Juan de Fuca Plate, the shallower western part is undergoing north-south compression to accommodate the relative movement and regional geometry of the North American Plate and the subduction zone (Weichert and Hyndman, 1983). The north-south compression produces an arch or an east-west-trending, east-plunging anticlinal structure in the subducting plate (Crosson and Owens, 1987, and Stanley et al., 1999). The crest of the arch corresponds approximately with the center of the Olympic Mountains in the overlying continental crust. As the plate dives deeper to the east, downdip (i.e., east-west) tensional forces dominate.

A.1.2 Province 2, Fore-Arc

Province 2, the fore-arc region on the western edge of the North American Plate, is composed of imbricated slabs of Tertiary oceanic sediment and basaltic crust that have been accreted or underplated onto the leading edge of the continental crust. These sedimentary and volcanic strata are exposed in the coastal mountains, including the Olympic Mountains and the Willapa Hills. The accretion and underplating at the continental margin is particularly well illustrated in the Olympic Mountains, which contain sequences of steeply dipping and overturned, thrust-faulted sedimentary and volcanic rock around the metamorphic core of Tertiary rock.

Geophysical, geodetic, and geologic evidence support the hypothesis that the fore-arc (western leading edge of the North American Plate) consists of two primary crustal blocks that are being dragged and pulled to the north parallel to the arc (Wells et al., 1998). These blocks include the coastal areas of Oregon and Washington and extend east to the Cascade Mountains. The southern block, consisting of the Coast Range and Willamette Lowland subprovinces in Oregon and southern Washington, is moving northward and rotating clock-wise relative to a pole or pivot point located in eastern Washington. This motion translates into north-south compression and dextral shear in the northern block, consisting of the Olympic Mountains, Willapa Hills, and Central Puget Sound subprovinces, as it is compressed between the southern block and the North Puget Sound and North Cascades subprovinces and the relatively stationary Canadian Coastal Mountains to the north. It is estimated that the compression rate across these terrains is about 0.4 to 1.0 centimeters per year, and it is postulated that most of the compression and shearing is occurring within the more fractured, Central Puget Sound subprovince (Wells and Johnson, 2001, and Wells et al., 1998). This hypothesis is supported by the observation that the rate of historical shallow crustal seismicity is much greater in the Central Puget Sound subprovince than in the Willapa Hills or Olympic Mountains, and substantial evidence for Late Quaternary movement on structures within the Central Puget Sound Province.

While the underlying bedrock structure of the Puget Sound subprovinces is largely concealed by thick Quaternary deposits and repeated glaciation, it has been the subject of recent and on-going scientific research to understand the seismic hazards and to identify seismogenic sources in the region (e.g., ten Brink et al., 2002; Blakely et al., 2002; Brocher et al., 2004; Brocher et al., 2001; Gower et al., 1985; Johnson et al., 1994, 1996, 1999, and 2001; Ma et al.,

1996; Pratt et al., 1997; Yount and Gower, 1991; and Yount et al., 1985). This on-going research suggests that the north-south compression of this terrain is being accommodated primarily beneath the Central Puget Sound by a series of west and northwest trending faults or structures that may extend to depths of about 14 to 28 kilometers. These structures extend from the Doty Fault near Chehalis, north to the Devils Mountain Fault near Anacortes and include the Olympia Fault, the Tacoma Fault, Seattle Fault, Kingston Arch, South Whidbey Fault, Utsalady Point Fault, and Strawberry Point Fault (Figure A-2). Conclusive geologic evidence of Holocene ground surface fault rupture has been observed to date for the Seattle and Utsalady Point Faults, and Late Quaternary (possibly Holocene) movement has been detected on the remainder of these, with the exception of the Kingston Arch and Doty Fault.

The west- to northwest-trending structures are presumably bounded on the east near the Cascade Mountains (province 3) by strike-slip or shear zones and on the west along Hood Canal at the foot of the Olympic Mountains (Hood Canal Fault, Figure A-2). South and east of the Central Puget Sound, active shear zones are observed in en echelon, northwest-southeast-trending zones around Mount St. Helens and Mount Rainier (Figure A-2). Shear from the Mount St. Helens and Mount Rainier zones could be transferred north, along the east side of the Central Puget Sound subprovince to the south Whidbey Fault Zone by an as of yet unrecognized master fault(s) or a zone of small faults and folds characterized by a zone of diffuse seismicity. A zone of small faults and folds may be the most likely of these two hypotheses as seismicity appears diffuse, and to date, there is no direct geologic or geophysical evidence of the existence of a master fault(s) along the east side of the province. Dextral shear may also be accommodated within the Central Puget Sound subprovince based on recent assessments of geophysical explorations (Johnson et al., 1999) that tentatively identify north-south-orientated dextral shear zones or strike-slip faults (Puget Sound Fault – see Figure A-2) beneath Puget Sound, extending from south of Vashon Island to north of Kingston.

A.1.3 Province 3, Volcanic Arc

Province 3, the landward continental volcanic arc, encompasses the Cascade Mountains and is further divided into a North Cascades subprovince of mostly metamorphosed Cretaceous and older rocks that are intruded by igneous rocks, and a South Cascades subprovince of younger sedimentary and igneous rocks that predominate in the mountains south of Snoqualmie Pass. Superimposed on this mountain range are relatively young volcanoes, resulting from partial melting of the subducted oceanic crust beneath. Cascade volcanoes in Washington include Mount Rainier, Mount Baker, Mount St. Helens, Mount Adams, and Glacier Peak.

A.2 Seismicity

The project site is located in a moderately active seismic region that in the brief 170-year historical record in the Pacific Northwest has been subjected to numerous earthquakes of low to

moderate strength and occasionally to stronger shocks. Geologic evidence indicates that large earthquakes have also occurred in the region during the Holocene but prior to written historical records (i.e., Holocene paleoseismicity). The following presents a review of both the historical seismicity and Holocene paleoseismicity.

In discussing the historical seismicity, both earthquake magnitude and intensity are used. Prior to the 1940s, historical events were primarily recorded using the Modified Mercalli intensity scale. The Modified Mercalli intensity scale reflects ground shaking effects on people and objects using a closed-end scale having numbers ranging from I to XII to represent the severity of ground shaking. Roman numerals are used exclusively with the Modified Mercalli scale. Magnitudes reported prior to the 1940s in the northwest are typically estimated from the Modified Mercalli intensity.

Since the 1940s, earthquakes have generally been reported using magnitude scales. Earthquake magnitudes may correspond to several different scales including surface waves (M_s), body waves (m_b), and "Richter" or local magnitude (M_L). The preferred measure is the moment magnitude (M_W), which is a measure of the total energy (seismic moment) released by an earthquake. Unless otherwise noted in this report, use of moment magnitude is implied. All earthquake magnitude scales use Arabic numerals to represent the size of the event.

A.2.1 Historical Seismicity

The largest historic earthquakes felt in Washington are listed in Table A-1. Table A-2 lists earthquakes of magnitude 4 or larger that have occurred in western Washington or adjacent regions in British Columbia, Canada and Oregon. Figure A-3 shows the locations of the earthquakes listed in Table A-2.

The largest historic earthquakes to affect the site include the magnitude (M_s) 7.1 Olympia earthquake of April 13, 1949; the magnitude (m_b) 6.5 Seattle-Tacoma earthquake of April 29, 1965; and the magnitude (M_W) 6.8 Nisqually earthquake of February 28, 2001. These events were located at epicentral distances of approximately 88 kilometers south-southwest (1949), 46 kilometers south (1965), and 82 kilometers south-southwest (2001) of the Portal and Plant sites. Ground shaking in the project area was reported as intensity VII (1949), VII (1965), and IV to V (2001), respectively. All three events were located in the subducted Juan de Fuca slab (Province 1) beneath the Puget Sound Lowland at depths of 53, 63, and 52 kilometers, respectively. The 1949 and 2001 events occurred in the subducted Juan de Fuca slab at nearly the same location. The level of ground shaking that occurred during these three events are likely the maximum vibratory ground motions that would have occurred in project area during the 170 years of historical record.

Other large historic earthquakes in the region include the 1872 North Cascades earthquake and two other events in western British Columbia, Canada. The North Cascades earthquake of December 15, 1872, appears to have been one of the largest crustal earthquakes in

the Pacific Northwest, with a maximum reported intensity of IX. Although the epicentral location of this event is uncertain, owing to the sparse population of the area at that time, it apparently was a shallow crustal event located about 190 to 230 kilometers (epicentral distance) northeast of Seattle, in the general vicinity of the southeast end of Lake Chelan (near the eastern edge of the North Cascades subprovince). The estimated magnitude for this event ranges from 6.8 (Bakun et al., 2002) to 7.4 (Malone and Bor, 1979). In Canada, major earthquakes occurred on Vancouver Island on June 23, 1946, and in the Queen Charlotte Islands on August 21, 1949 (Coffman and von Hake, 1973). These events had local magnitudes of 7.3 and 8.1, respectively. Because of the large distances of these earthquakes from the Puget Sound area (over 150 kilometers), there were no reports of significant ground shaking or damage in the area.

A.2.2 Holocene Paleoseismicity

Paleoseismic studies have demonstrated the occurrence of large Holocene earthquakes in the region prior to written historical records. The interface between the Juan de Fuca and North American Plates within the CSZ has been identified by these studies as producing multiple events during the Holocene Epoch. There are also several shallow crustal structures within or adjacent to the Central Puget Sound that appear to have late Quaternary movement. On four of these structures, the Seattle, Tacoma, Southern Whidbey Island, and Utsalady Faults, evidence of Holocene rupture has been observed. The following provides a description of Holocene paleoseismicity on these structures.

A.2.2.1 Cascadia Subduction Zone Interplate Seismicity

Evidence has been found by several researchers to support the potential occurrence of interplate earthquakes on the CSZ. Paleoseismological investigations have revealed compelling evidence of a number of instances of sudden coastal subsidence at numerous locations along the length of the CSZ (e.g., Atwater, 1987 and 1992; Grant, 1989; Darienzo and Peterson, 1990; Clarke and Carver, 1992; and Atwater and Hemphill-Haley, 1997). Other evidence of large earthquakes along this zone includes the presence of turbidites in deep-sea channels off the coast of Washington and Oregon (Adams, 1990 and 1996), the presence of buried soils at Humboldt Bay (Clarke and Carver, 1992) and in northern Oregon (Darienzo and Peterson, 1995, and Peterson and Darienzo, 1996), interbedded peat and mud at Coos Bay, Oregon (Nelson et al., 1996), buried scarps near Willapa Bay (Meyers et al., 1996), and buried soils at Grays Harbor (Shennan et al., 1996). Taken together, these different observations represent strong evidence that the CSZ has produced, and remains capable of producing, strong earthquakes.

Multiple interplate earthquakes have occurred on the CSZ during the Holocene Epoch. Based on historical tsunami records in Japan (Satake et al., 1996) the most

recent interplate event on the CSZ was a magnitude 9 event on January 26, 1700. Adams (1990) interpreted the occurrence of turbidites from failures of submarine canyon heads 50 km west of Willapa Bay (Griggs and Kulm, 1970), which is an area directly above the shallow rupture zone of the CSZ, as the result of rupture on the CSZ. Adams interpreted the ages of the turbidites from the relatively uniform thicknesses of interbedded pelagic clay layers. The estimated ages of five distinct events, interpreted to be the result of rupture on the CSZ, were 250 to 360 years, 570 to 830 years, 1,000 to 1,400 years, 1,730 to 2,640 years, and 2,270 to 3,300 years. Atwater and Hemphill-Haley (1997) also reported ranges of age for seven distinct seismic events based on buried soils in Willapa Bay. The estimated ages of these events were 290 to 310 years, 900 to 1,300 years, 1,110 to 1,350 years, 1,500 to 1,700 years, 2,390 to 2,780 years, 2,800 to 3,320 years, and 3,320 to 3,500 years.

A.2.2.2 Seattle Fault Seismicity

Until the 1990s, crustal seismicity generally had not been correlated with known or inferred structures within the fore-arc, and with the exception of two small minor scarps at the southeast corner of the Olympic Mountains, surface expression of Holocene fault ground surface rupture within western Washington had not been observed. Until the late 1980s, it had generally been accepted that shallow crustal events within the Lowland would have a maximum magnitude of about 6. However, geologic evidence developed during the 1990s (Bucknam et al., 1992; Atwater and Moore, 1992; Karlin and Abella, 1992; Schuster et al., 1992; Jacoby et al., 1992; Johnson et al., 1996; Pratt et al., 1997; Johnson et al., 1999; and Brocher et al., 2001) and tectonic models (Wells et al., 1998) suggest that the geophysical lineament/ crustal block boundary beneath the Puget Sound Basin are potentially seismogenic and capable of producing shallow crustal events of magnitudes up to 7.5.

Many of the recent studies regarding the potential for large earthquakes have focused on the Seattle Fault Zone. This zone is characterized as a 60 to 65 kilometers long (east-west) south-dipping reverse or thrust master fault at depth that produces a series of strands as it approaches the ground surface. Evidence of recent movement on the Seattle Fault includes raised bedrock terraces south of the inferred Seattle Fault, tsunami deposits north of the fault, and landslide deposits into Lake Washington, which have correlative dates of about 1,100 years before present (Bucknam et al., 1992; Atwater and Moore, 1992; Karlin and Abella, 1992; Schuster et al., 1992; and Jacoby et al., 1992). It has been postulated that these events were the result of reverse movement of the Seattle Fault, with the south side moving up approximately 7 meters relative to the north.

Analyses of seismic reflection data (Pratt et al., 1997, and Johnson et al., 1999) provide additional evidence of recent movement on the Seattle Fault. Johnson et al. (1999) analyzed high-resolution and conventional industry marine seismic reflection data and subsequently characterized the Seattle Fault as a 4 to 6 kilometer-wide (north-south) zone consisting of a series of east-west-trending fault strands as shown in Figure A-2. Folds in the Quaternary section of the seismic reflection profile indicate that movement has occurred on at

least some of the strands through the Holocene. Johnson et al. (1999) also identify a north trending strike-slip zone in the center of Puget Sound (Puget Sound Fault) that offsets the east-west trending strands of the Seattle Fault (Figure A-2). While there is no paleoseismological evidence of rupture on this structure, based on the observed offset of the Seattle Fault, Johnson et al. (1999) indicate that the Puget Sound Fault is also likely to be active.

Fault trenching studies by the U.S. Geological Survey (USGS) on the Toe Jam Hill (on Bainbridge Island) and Waterman Point (Kitsap Peninsula near Port Orchard) strands of the Seattle Fault Zone also indicate that movement in the zone has ruptured the ground surface during the Holocene. The trenching studies completed thus far suggest that at least four events ruptured the ground surface on this strand of the fault over the last 16,000 years (Nelson et al., 2003a and 2003b).

A.2.2.3 Tacoma Fault Seismicity

In the shallow crustal structure model for the Puget Lowland by Pratt et al. (1997), the previously observed geophysical lineament noted by Gower et al. (1985) or Tacoma "Fault" shown on Figure A-2 was interpreted as the down-dip extent of the Seattle Fault. However, the results of recent tomographic studies of the shallow crustal structure in the Puget Lowland (Brocher et al., 2001) suggest that this structure could be a steep, north dipping reverse fault. In September 2002, the USGS acquired light distance and ranging data (LIDAR) of the center segment and identified what appeared to be a surface scarp (Sherrod et al., 2004). A test trench was excavated and logged by the USGS across a portion of the scarp in September and October 2002. A south vergent monoclinal fold appeared to present in the Late Pleistocene Vashon Till at the site with up to about 1 foot of displacement on possible slip planes within the fold (Sherrod, 2004).

A.2.2.4 Southern Whidbey Island Fault Seismicity

The Southern Whidbey Island Fault Zone (SWIF) is described (Johnson et al., 1996) as a 6 to 11 kilometer-wide, northwest-trending, northeast dipping zone with inferred reverse, thrust and strike slip (dextral) displacement on different splays within the zone, with a length of at least 70 km (Figure A-2).

Kelsey et al. (2004) describe 1 to 2 meters of vertical displacement (north side up) between two coastal marshes located within 1.5 kilometers of the inferred fault trace. While no surface fault rupture has been observed between the two marshes, LIDAR images indicate a break in topography that they interpret to be surface deformation above the tip of a blind fault. Kelsey et al. (2004) note that folded Holocene marine strata observed in marine seismic reflection data offshore are consistent with a blind fault. Based on a 60-degree fault dip,

they postulate that the observed surface deformation approximately 2,800 to 3,200 years ago was the result of 1.2 to 2.3 meters of slip or more (horizontal motion parallel to the fault (strike-slip) could not be determined) from a magnitude 6 ½ to 7 earthquake on this fault.

Recently, possible onshore extensions of the SWIF have been identified using aeromagnetic, LIDAR, and borehole data (Blakely et al., 2004). The USGS has subsequently begun trenching studies on some of the more likely possible onshore extensions. To date, trenching studies have been conducted at Blakely et al.'s (2004) LIDAR Scarps 10 and 11 near Crystal Lake and at LIDAR Lineament 4 at or near the Plant site. The SWIF Cottage Lake Extension modeled in the PSHA is located along Scarps 10 and 11; the Bear Creek Extension in the PSHA model is located along Lineament 4. The analyses of these trench excavations are ongoing by the USGS. However, to date one late Pleistocene or early Holocene seismic event is recognized by folding in Vashon recessional outwash in two trenches excavated at Scarps 10 and 11 along the Cottage Lake Extension (personal communication with USGS investigators as documented in Shannon & Wilson, 2004b). One to two meters of vertical displacement are observed in these trenches; the horizontal component parallel to the scarp (strike-slip component) could not be determined. In the trenches excavated at Lineament 4 at or near the Plant site along the Bear Creek Extension (AMEC, 2005; personal communication with USGS investigators as documented in Shannon & Wilson, 2004b), strong evidence is observed for two ground-deforming seismic events, weak evidence is noted for a third, and liquefaction features potentially not associated with any of the ground-deforming events could be evidence for a fourth event. While dating has not been complete, all of these appear to have occurred during or after the retreat of glacial ice (i.e., younger than about 16,000 calibrated years before present) with some events that appear to be late Holocene. Vertical ground deformations observed in the Lineament 4 trenches range from 1 to 2 meters to about 0.3 meters; the horizontal component parallel to the lineament (strike-slip component) could not be determined.

These recently completed and on-going paleoseismic studies (e.g., Kelsey et al., 2004; AMEC, 2005) have identified up to 5 or 6 instances of ground deformation or ground shaking that could be associated with seismic events on the SWIF over approximately the last 16,000 years. While a single seismic event could be responsible for more than one of the identified instances of ground deformation/shaking, the possibility that each instance of ground deformation/shaking are from separate seismic events can not be precluded.

A.2.2.5 Utsalady Point Fault Seismicity

The Utsalady Point Fault is described (Johnson et al., 2001) as a northwest-trending, subvertical, oblique-slip, transpressional fault with a length of approximately 28 kilometers. Its location is shown on Figure A-2. On Camano Island, it appears that the south side is up, whereas to the west on the west side of Whidbey Island, the north side is up (Johnson, et al., 2001). The USGS recently excavated two fault trenches across scarps on the west side of Whidbey Island. Results from these trenches identified possibly two events that caused Holocene ground surface rupture or deformation; one approximately 100 to 500 years before

present and the other approximately 1,100 to 2,200 years before present (Johnson et al., 2003). Reported vertical ground surface rupture for both events was approximately 1 meter whereas the younger event 2 meters of left-lateral movement was also observed in one of the trenches.

A.3 References

Adams, J., 1990, Paleoseismicity of the Cascadia Subduction Zone: evidence from turbidities off the Oregon-Washington margin: Tectonics, v. 9, no. 4, p. 569-583.

Adams, J., 1996, Great earthquakes recorded by turbidities off the Oregon-Washington coast, *in* Rogers, A.M., Walsh, T.J., Kockelman, W.J., and Priest, G.R., eds., Assessing Earthquake Hazards and Reducing Risk in the Pacific Northwest, U.S. Geological Survey Professional Paper 1560, p. 147-158.

Atwater, B.F., 1987, Evidence for great Holocene earthquakes along the outer coast of Washington State: Science, v. 236, p. 942-944.

Atwater, B.F., 1992, Geologic evidence for earthquakes during the past 2000 years along the Copalis River, Southern Coastal Washington: Journal of Geophysical Research, v. 97, p. 1901-1919.

Atwater, B.F., and Hemphill-Haley, E., 1997, Recurrence intervals for great earthquakes of the past 3500 years at Northeastern Willapa Bay, Washington: U.S. Geological Survey Professional Paper 1576.

Atwater, B.F., and Moore, A.L., 1992, A tsunami about 1000 years ago in Puget Sound, Washington: *Science*, v. 236, p. 942-944.

Bakun, W.H., Haugerud, R.A., Hopper, M.G., and Ludwin, R.S.. 2002, The December 1872 Washington State earthquake: Bulletin of the Seismological Society of America, 92(8), p. 3239-3258.

Blakely, R.J., Sherrod, B.L., Wells, R.E., Weaver, C.S., McCormack, D.H., Troost, K.G., and Haugerud, R.A., 2004, The Cottage Lake aeromagnetic lineament-A possible onshore extension of the southern Whidbey Island fault, Washington: U.S. Geological Survey Open-File Report 2004-1204, 60 p.

Blakely, R.J., Wells, R.E., Weaver, C.S., and Johnson, S.Y., 2002, Location, structure, and seismicity of the Seattle fault, Washington: Evidence from aeromagnetic anomalies, geologic mapping, and seismic-reflection data: Geological Society of America Bulletin, v. 114, p. 169-177.

Brocher, T. M., Blakely, R. J., and Wells, R. E., 2004, Interpretation of the Seattle uplift, Washington, as a passive-roof duplex: Bulletin of the Seismological Society of America, v. 94, no. 4, p. 1379-1401.

Brocher, T.M., Parsons, T., Blakely, R.J., Christensen, N.I., Fisher M.A., Wells, R.E., and the SHIPS Working Group, 2001, Upper crustal structure in Puget Lowland, Washington, results from the 1998 Seismic Hazards Investigation in Puget Sound: Journal of Geophysical Research, v. 106, no. B7, p. 13,541-13,564, July 10.

Bucknam, R.C., Hemphill-Haley, E., and Leopold, E.B., 1992, Abrupt uplift within the past 1700 years of the southern Puget Sound, Washington: *Science*, v. 258, p. 1611-1613.

Clarke, S.H., Jr., and Carver, G.A., 1992, Late Holocene tectonics and paleoseismicity, southern Cascadia Subduction Zone: Science, v. 255, p. 188-192.

Coffman, J.L., and von Hake, C.A., 1973, Earthquake history of the United States (revised, ed.): U.S. National Oceanic and Atmospheric Administrative Publication 41-1.

Crosson, R.S., and Owens, T.J., 1987, Slab geometry of the Cascadia Subduction Zone beneath Washington from earthquake hypocenters and teleseismic converted waves: Geophysical Research Letters, v. 14, p. 824-827.

Darienzo, M., and Peterson, C., 1990, Investigation of coastal neotectonics and paleoseismicity of the southern Cascadia margin as recorded in coastal marsh systems," *in* Jacobson, M.L. ed., National Earthquake Hazards Reduction Program, Summaries of Technical Reports, Volume XXXI, U.S. Geological Survey Open File Report 90-680, p. 131-139.

Darienzo, M.E., and Peterson, C.D., 1995, Magnitude and frequency of subduction-zone earthquakes at four estuaries in Northern Oregon: Journal of Coastal Research, v. 10, p. 850-876.

Gower, H.D., Yount, J.D., and Crosson, R.S., 1985, Seismotectonic map of the Puget Sound region, Washington: U.S. Geological Survey Miscellaneous Investigations Series Map I-1613, scale 1:250,000.

Grant, W.C., 1989, More evidence from tidal-marsh stratigraphy for multiple late Holocene subduction earthquakes along the northern Oregon Coast: Geological Society of America Abstracts with Programs, v. 21, no. 4, p. 86.

Griggs, G.B., and Kulm, L.D., 1970, Sedimentation in Cascadia deep-sea channel: Geological Society of America Bulletin, v. 81, p. 1361-1384.

Jacoby, G.C., Williams, P.L., and Buckley, B.M., 1992, Tree ring correlation between prehistoric landslides and abrupt tectonic events in Seattle, Washington: Science, v. 258, p. 1621-1623.

Johnson, S.Y., Potter, C.J., and Armentrout, J.M., 1994, Origin and evolution of the Seattle Basin and Seattle Fault: Geology, v. 22, p. 71-74.

Johnson, S.Y., Potter, C.J., Armentrout, J.M., and others, 1996, The Southern Whidbey Island Fault, an active structure in the Puget Lowland, Washington: Geological Society of America Bulletin, v. 108, p. 334-354.

Johnson, S.Y., Dadisman, S.V., Childs, J.R., and Stanley, W.D., 1999, Active tectonics of the Seattle Fault and Central Puget Sound, Washington--implications for earthquake hazards: Geological Society of America Bulletin, v. 111, No. 7, July, p. 1042-1053.

Johnson, S.Y., Dadisman, S.V., Mosher, D.C., Blakely, R.J., and Childs, J.R., 2001, Active tectonics of the Devils Mountain Fault and related structures, northern Puget Lowland and eastern Strait of Juan de Fuca Region, Pacific Northwest: U.S. Geological Society Professional Paper 1643.

Johnson, S.Y., and others, 2003, Evidence for one or two late Holocene earthquakes on the Utsalady Point fault, Northern Puget Lowland, Washington: Abstracts with Program, Annual National Meeting, Geological Society of America.

Karlin, R.E., and Arbella, S.E.B., 1992, Paleoearthquakes in the Puget Sound Region recorded in sediments from Lake Washington, USA: Science, v. 258, p. 1617-1620.

Kelsey, H. M., Sherrod, Brian, Johnson, S. Y., and others, 2004, Land-level changes form a late Holocene earthquake in the northern Puget Lowland, Washington: Geology, v. 32, no. 6, p. 469-472.

Ma, L., Crosson, R.S., and Ludwin, R.S., 1996, Western Washington focal mechanisms and their relationship to regional tectonic stress: U.S. Geological Survey Professional Paper 1560, p. 257-284.

Malone, S.D., and Bor, S.S., 1979, Attenuation patterns in the Pacific Northwest based on intensity data and location of the 1872 North Cascades earthquake: Bulletin of the Seismological Society of America, 69, p. 531-546.

Meyers, R.A., Smith, D.G., Jol, H.M., and Peterson, C.D., 1996, Evidence for eight great earthquake-subsidence events detected with ground penetrating radar, Willapa Barrier, Washington: Geology, v. 24, p. 99-102.

Nelson, A.R., Shennan, I., and Long, A.J., 1996, Identifying coseismic subsidence in tidal-wetland stratigraphic sequences at the Cascadia Subduction Zone of western North America: Journal of Geophysical Research, v. 101, p. 6115-6135.

Nelson, A.R, Johnson, S.Y., Kelsey, H.M., Sherrod, B.L., Wells, R.E., Bradley, L.-A., Okumura, K., and Bogar, R., 2003a, Late Holocene earthquakes on the Waterman Point reverse fault, another ALSM-discovered fault scarp in the Seattle fault zone, Puget Lowland, Washington: Geological Society of America Abstracts with Program, (Abstract for talk in topical session on "Earthquake geology in reverse faulting terrains" at the Nov 03 Annual Meeting of The Geological Society of America in Seattle Washington).

Nelson, A.R., Johnson, S.Y., Kelsey, H.M., Wells, R.E., Sherrod, B.L., Pezzopane, S.K., Bradley, L.-A., and Koehler, R.D., III, 2003b, Late Holocene earthquakes on the Toe Jam Hill fault, Seattle fault zone, Bainbridge Island, Washington: Geological Society of America Bulletin, v. 115, p. 1388-1403.

Peterson, C.D., and Darienzo, M.E., 1996, Discrimination of climatic, oceanic, and tectonic mechanisms of cyclic marsh burial, Alsea Bay, Oregon: *in* Rogers, A.M., Walsh, T.J., Kockelman, W.J., and Priest, G.R., eds., Assessing earthquake hazards and reducing risk in the Pacific Northwest: U.S. Geological Survey Professional Paper 1560, p. 115-146.

Pratt, T.L., Johnson, S.Y., Potter, C.J., and others, 1997, Seismic-reflection images beneath Puget Sound, Western Washington State: Journal of Geophysical Research, v. 102, p. 469-490.

Satake, K.; Shimazaki, K.; Tsuji, Y.; and Ueda, K., 1996, Time and size of a giant earthquake in Cascadia inferred from Japanese tsunami records of January 1700: Nature, v. 378, no. 18, January, p. 246-249.

Schuster, R.L., Laiger, R.L., and Pringle, P.T., 1992, Prehistoric rock avalanches in the Olympic Mountains, Washington: Science, v. 258, p. 1620-1621.

Shannon & Wilson, Inc., 2004b, Proposed revisions to the SWIF model for the revised Brightwater PSHA based on recent USGS/project team fault studies and reviews: Report by Shannon & Wilson, Inc., Seattle, Wash., 21-1-20150-002, for CH2M Hill, Bellevue, Wash., November 17.

Shennan, I., Long, A.J., Rutherford, M.M., Green, F.M., Innes, J.B., Lloyd, J.M., Zong, Y., and Walker, K.J., 1996, Tidal marsh stratigraphy, sea-level change and large earthquakes, I: a 5000 year record in Washington, USA: Quaternary Science Reviews, v. 15, p. 1023-1059.

Sherrod, B.L., Brocher, T.M., Weaver, C.S., Bucknam, R.C., Blakely, R.J., Kelsey, H.M., Nelson, A.R., and Haugerud, R., 2004, Holocene fault scarps near Tacoma, Washington, USA: Geology, v. 32, no. 1, p. 912.

Stanley, D., Villasenor, A., and Benz, H., 1999, Subduction zone and crustal dynamics of Western Washington: a tectonic model for earthquake hazards evaluation: U.S. Geological Survey Open-File Report 99-311 on-line edition, 66 p.

ten Brink U.S., P.C. Molzer, M.A. Fisher, R.J. Blakely, R.C. Bucknam, T. Parsons, R.S. Crosson and K.C. Creager, 2002, Subsurface geometry and evolution of the Seattle fault zone and the Seattle basin, Washington: Bulletin of the Seismological Society of America, v. 92, p. 1737-1753.

Weichert, D.H., and Hyndman, R.D., 1983, A comparison of the rate of seismic activity and several estimates of deformation in the Puget Sound Area: Proceedings of Workshop XIV, Earthquake Hazards of the Puget Sound Region, U.S. Geological Survey Open-File Report 83-19, p. 105-130.

Wells, R.E., Weaver, C.S., and Blakeley, R.J., 1998, Fore-arc migration in Cascadia and its neotectonic significance: Geology, v. 26, p. 759-762.

Wells, R.E., and Johnson, S.Y., 2001, Deformations of Western Washington resulting from northward migration of the Cascadia Forearc: Seismological Research Letters, v. 72, no. 2, March/April.

Yount, J.C., and Gower, H.D., 1991, Bedrock geologic map of the Seattle 30' x 60' Quadrangle, Washington: U.S. Geological Survey Open-File Report 91-147.

Yount, J.C., Dandorff, G.R., and Barats, G.M., 1985, Map showing depth to bedrock in the Seattle 30' x 60' Quadrangle, Washington: U.S. Geological Survey Miscellaneous Field Studies Map MF-1692, 1 sheet.

Table A-1. Largest Historic Earthquakes Felt in Washington

Year	Date	Time (PST)	North Latitude	West Longitude	Depth (km)	Mag (felt)[1]	Mag (inst)[2]	Maximum Modified Mercalli Intensity	Felt Area (sq km)	Location
1872	Dec. 14	21:40	47° 45'00"	119° 52'00"	Shallow	6.8	None	IX	1,010,000	North Cascades
1877	Oct. 12	13:53	45° 30'00"	122° 30'00"	Shallow	5.3	None	VII	48,000	Portland, Oregon
1880	Dec. 12	20:40	47° 30'00"	122° 30'00"	?	?	None	VII	?	Puget Sound
1891	Nov. 29	15:21	48° 00'00"	123° 30'00"	?	?	None	VII	?	Puget Sound
1893	Mar. 06	17:03	45° 54'00"	119° 24'00"	Shallow	4.7	None	VII	21,000	Southeastern Washington
1896	Jan. 03	22:15	48° 30'00"	122° 48'00"	?	5.7	None	VII	?	Puget Sound
1904	Mar. 16	20:20	47° 48'00"	123° 00'00"	?	5.3	None	VII	50,000	Olympic Peninsula, eastside
1909	Jan. 11	15:49	48° 42'00"	122° 48'00"	Deep	6.0	None	VII	150,000	Puget Sound
1915	Aug. 18	06:05	48° 30'00"	121° 24'00"	?	5.6	None	VI	77,000	North Cascades
1918*	Dec. 06	00:41	49° 37'00"	125° 55'00"	?	7.0	7.0	VIII	650,000	Vancouver Island
1920	Jan. 23	23:09	48° 36'00"	123° 00'00"	?	5.5	None	VII	70,000	Puget Sound
1932	July 17	22:01	47° 45'00"	121° 50'00"	Shallow	5.2	None	VII	41,000	Central Cascades
1936	July 15	23:08	46° 00'00"	118° 18'00"	Shallow	6.4	5.75	VII	270,000	Southeastern Washington
1939	Nov. 12	23:46	47° 24'00"	122° 36'00"	Deep	6.2	5.75	VII	200,000	Puget Sound
1945	April 29	12:16	47° 24'00"	121° 42'00"		5.9	5.5	VII	128,000	Central Cascades
1946	Feb. 14	19:18	47° 18'00"	122° 54'00"	40 (Deep)	6.4	6.3	VII	270,000	Puget Sound
1946*	June 23	09:13	49° 48'00"	125° 18'00"	Deep	7.4	7.3	VIII	1,096,000	Vancouver Island
1949	April 13	11:55	47° 06'00"	122° 42'00"	54 (Deep)	7.0	7.1	VIII	594,000	Puget Sound
1949*	Aug. 21	20:01	53° 37'20"	133° 16'20"		7.8	8.1	VIII	2,220,000	Queen Charlotte Is, B.C.
1959	Aug. 05	19:44	47° 48'00"	120° 00'00"	35 (Deep)	5.5	5.0	VI	64,000	North Cascades, east side
1959*	Aug. 17	22:37	44° 49'59"	111° 05'	10-12 (Shallow)	7.6	7.5	X	1,586,00	Hebgen Lake, Montana
1962*	Nov. 05	19:36	45° 36'30"	122° 35'54"	18 (Shallow)	5.3	5.5	VII	51,000	Portland, Oregon
1965	April 29	07:28	47° 24'00"	122° 24'00"	63 (Deep)	6.8	6.5	VIII	500,000	Puget Sound
1976	May 16	00:35	48° 45'36"	123° 19'48"	Deep		5.1			Friday Harbor, San Juan Isl, WA
1981	Feb. 13	22:09	46° 21'01"	122° 14'66"	7 (Shallow)	5.8	5.5	VII	104,000	South Cascades

Table A-1 (cont.)
Largest Historic Earthquakes Felt in Washington

Year	Date	Time (PST)	North Latitude	West Longitude	Depth (km)	Mag (felt)[1]	Mag (inst)[2]	Maximum Modified Mercalli Intensity	Felt Area (sq km)	Location
1981	May 28	01:11	46° 30'36"	121° 22'48"	Shallow		5.0			Goat Rocks
1983*	Oct. 28	06:06	44° 03'29"	113° 51'25"	14 (Shallow)	7.2	7.3	VII	800,000	Borah Peak, Idaho
1989	Dec 24	00:46	46° 39'00"	122° 06'00"	Shallow		4.9			Morton
1990	April 14	21:33	48° 49'48"	122° 09'00"	Shallow		5.0			Deming
1995	Jan. 28	07:11	47° 23'17"	122° 21'54"	16 (Shallow)	--	5.0	V	--	Robinson Point, Washington
1996	May 2	20:04	47° 45'36"	121° 52'34"	7 (Shallow)	--	5.1	V	--	Duvall, Washington
1997	June 23	11:13	47° 35'56"	122° 32'26"	7 (Shallow)	--	4.9	VI		Bremerton, Washington
1999	July 2	05:43	47° 04'33"	123° 46'35"	41 (Deep)	--	5.9	VII	--	Satsop, Washington
2001	Feb 28	10:55	47° 12'00"	122° 42'00"	52 (Deep)	--	6.8		--	Nisqually, Washington

a. Mag (felt) = an estimate of magnitude, based on felt area; unless otherwise indicated, it is calculated from Mag (felt) = -1.88+1.53 logA, where A is the total felt area; from Toppozada 1975.
b. Mag (inst) = instrumentally determined magnitude; refer to reference listed in the original Table 2 of Noson et al (1988) (or NGDC (1999) [post 1983]).
* Located outside the state of Washington.

Source: Noson et al. (1988) and NGDC (1999).

Table A-2. Historic Earthquakes in or Near Western Washington, M ≥ 4[1]

Year	Month	Day	Time (GMT)	North Latitude (degrees)	West Longitude (degrees)	Depth (kilometers)	Magnitude[2]	Source
1841	12	2	16:00:00	45.6	122.7	–	4.3	GSC
1859	4	2	02:30:00	47	123	–	4.3	GSC
1864	10	29	18:10:00	48.5	123.5	–	5	GSC
1865	8	25	21:00:00	48.5	123.5	–	5	GSC
1872	12	15	05:37:00	47.8	119.9	–	6.8	GSC
1877	10	12	17:00:00	45.5	122.5	–	5.33	DNA
1885	10	9	08:00:00	47	123	–	4.3	GSC
1885	12	8	22:40:00	47.5	122.5	–	4.3	GSC
1891	9	21	13:00:00	48	123.5	–	4.3	OSU
1891	9	22	03:40:00	48	123.5	–	4.3	GSC
1891	11	29	23:21:00	48.11	123.45	–	5	OSU
1892	2	3	20:30:00	45.5	122.8	–	5	GSC
1892	4	17	14:50:00	47	123	–	5	GSC
1895	2	25	04:47:00	46.5	122.4	–	4.3	GSC
1895	4	16	00:02:00	48	123	–	4.6	GSC
1896	2	6	21:55:00	48.3	124.3	–	5	GSC
1896	4	2	03:17:00	45.3	123.3	–	5	GSC
1896	4	2	11:17:00	45.2	123.2	–	5	OSU
1903	3	14	02:15:00	47.7	122.2	–	4.3	GSC
1904	3	17	04:21:00	47.5	124	–	5.3	GSC
1909	1	11	23:49:00	48.7	122.8	–	6	DNA
1909	5	24	17:20:00	47.6	120	–	4	GSC
1911	9	29	02:39:00	48.8	122.7	–	4.3	GSC
1913	7	29	16:15:00	47	122	–	4.3	GSC
1913	12	25	14:40:00	47.7	122.5	–	4.3	GSC
1914	9	5	09:35:00	47	123	–	4.3	GSC
1915	5	18	19:00:00	45.5	122.7	–	4.3	GSC
1915	5	20	03:00:00	45.5	122.7	–	4.3	GSC
1915	8	18	14:05:00	48.53	121.43	–	5.5	GSC
1915	8	18	18:00:00	48.5	121.4	–	4.3	GSC
1916	1	2	00:52:00	47.3	122.3	–	4.3	GSC
1916	2	22	11:45:00	48.8	122.6	–	4.3	GSC
1917	3	28	17:05:00	46.8	122	–	4.3	GSC
1917	6	9	14:30:00	46.8	122	–	4.3	GSC
1917	11	12	10:47:00	46.8	121.8	–	4.3	GSC
1918	2	28	23:45:00	46.5	120.5	–	4.3	GSC
1918	6	21	06:47:00	46.5	121.7	–	4.3	GSC
1920	1	24	07:10:00	48.7	123	–	5	GSC
1923	2	12	18:30:00	49	122.7	–	4.3	GSC
1926	9	17	23:14:40	49	124	–	5.5	GSC
1926	12	4	13:55:00	48.5	123	–	4.3	GSC
1926	12	30	17:57:00	47.7	120.2	–	5	DNA

Table A-2 (cont.)
Historic Earthquakes in or Near Western Washington, M ≥ 4[1]

Year	Month	Day	Time (GMT)	North Latitude (degrees)	West Longitude (degrees)	Depth (kilometers)	Magnitude[2]	Source
1928	2	2	12:52:00	47.8	121.7	–	5	DNA
1930	7	19	02:38:00	45	123.2	–	5	DNA
1931	4	18	03:55:00	48.7	122.2	–	5	DNA
1931	12	31	15:25:00	47.5	123	–	5	DNA
1932	1	5	23:13:00	48	121.8	–	4.3	GSC
1932	7	18	06:01:00	48	121.8	–	5.7	DNA
1932	8	6	22:16:00	47.7	122.3	–	5	DNA
1934	5	5	04:06:00	48	123	–	4.3	GSC
1934	9	18	08:00:00	47	121	–	4.3	GSC
1934	9	27	00:15:00	47	121	–	4.3	GSC
1934	10	20	07:31:00	47	121	–	4.3	GSC
1934	11	1	15:28:00	47	121	–	4.3	GSC
1934	11	2	23:17:00	47	121	–	4.3	GSC
1934	11	3	14:50:00	48	121	–	4	GSC
1935	7	9	21:45:00	47.7	120	–	4.3	GSC
1938	1	6	13:11:00	47.8	122.4	–	4.3	GSC
1939	11	13	07:45:54	47.4	122.6	–	6.2	DNA
1940	10	27	22:29:18	47.2	123.4	–	4.6	GSC
1941	12	29	18:37:00	45.535	122.62	–	5	DNA
1942	10	14	11:30:00	48.3	120.6	–	4.3	GSC
1943	4	24	00:10:46	47.3	120.6	–	5	DNA
1943	11	29	00:43:00	48.4	122.9	–	5	DNA
1944	3	5	13:00:00	45	123.41	–	4.3	OSU
1944	3	31	22:15:00	47	123	–	4.3	GSC
1944	10	31	12:34:00	47.8	120.6	–	4.3	GSC
1944	12	7	04:48:00	46.977	123.89	–	5	DNA
1945	1	28	05:06:08.1	48.242	122.377	–	5	DNA
1945	4	29	20:16:17	47.4	121.7	–	5.7	DNA
1945	4	30	07:45:45	47.4	121.7	–	5	DNA
1945	5	1	20:46:00	47.4	121.7	–	4.3	GSC
1945	6	15	22:24:21	49	123.5	–	4.2	GSC
1945	11	12	04:05:00	48	122.5	–	5	DNA
1946	2	15	03:17:47	47.3	122.9	25	5.8	DNA
1946	2	15	12:17:15	46.87	122.268	–	5	DNA
1946	2	23	08:54:53	47.045	122.89	–	5	DNA
1948	9	24	22:35:00	47.855	122.587	–	5	DNA
1949	4	13	19:55:43	47.1	122.75	54	7.1	DNA
1949	6	1	08:23:15	47.5	124.5	–	4	GSC
1950	4	14	11:03:48	48	122.5	–	5	DNA
1950	12	3	01:57:00	48	122.3	–	4.3	GSC
1952	8	6	17:32:17	47.5	122.4	–	4.3	GSC

Table A-2 (cont.)
Historic Earthquakes in or Near Western Washington, M ≥ 4[1]

Year	Month	Day	Time (GMT)	North Latitude (degrees)	West Longitude (degrees)	Depth (kilometers)	Magnitude[2]	Source
1953	12	16	04:32:12	45.5	122.7	–	5	DNA
1954	3	16	15:56:00	47.1	121.8	–	4.3	GSC
1954	4	23	19:19:26	45.1	122.9	–	4	GSC
1954	5	5	01:42:00	47.3	122.4	–	4.3	GSC
1954	5	15	13:02:32	47.4	122.5	–	5	DNA
1955	3	26	06:56:51	48.1	122	–	5	DNA
1957	1	26	01:16:07.4	48.29	122.6	–	5	DNA
1957	2	11	17:05:56	47.5	121.7	–	5	DNA
1957	11	1	10:12:02	46.7	121.5	–	4.2	GSC
1957	11	16	22:00:00	45.3	123.8	–	5	GSC
1957	11	17	06:00:29	45.3	123.8	–	5	DNA
1958	4	12	22:37:11	48	120	–	5	DNA
1958	5	22	20:13:01	48.02	121.6	–	4.2	GSC
1958	10	7	05:07:56	46.7	124	–	5	DNA
1959	8	4	23:53:30	45.68	122.27	–	4.7	GSC
1959	11	23	18:15:25	46.67	121.75	–	4.8	GSC
1959	12	12	06:24:17	48.7	123.3	–	4.5	DNA
1960	9	10	15:06:34	47.7	123.15	–	5.2	DNA
1961	9	16	03:24:58	46	122.2	–	4.3	GSC
1961	9	17	15:55:55.9	46.023	122.122	7	5.1	DNA
1961	10	31	02:35:00	48.4	120	–	4.3	GSC
1961	11	7	01:29:08.4	45.7	122.866	–	5.1	DNA
1961	11	7	21:30:00	45.5	122.6	–	4.3	GSC
1962	1	15	05:29:13	47.833	120.216	–	4.4	DNA
1962	8	11	16:53:00	46	123.5	–	5	OSU
1962	11	6	03:36:43	45.608	122.598	18	5.5	DNA
1962	12	31	20:49:30.8	47.25	122.08	2	5.2	DNA
1963	1	24	21:43:09.8	47.57	122.03	–	5.1	DNA
1963	12	27	02:36:22.5	45.78	123.35	35	5	DNA
1964	1	15	23:06:36.2	45.9	120	33	4.2	PDE
1964	1	26	21:41:00	46.1	122.4	–	4.3	GSC
1964	4	26	01:42:49	48.7	120.5	–	4.4	DNA
1964	7	14	15:50:03.3	48.9	122.5	–	5	DNA
1964	10	1	12:31:24.6	45.7	122.8	–	4.5	DNA
1964	10	12	04:31:00	45.7	122.8	–	4.3	GSC
1964	10	14	06:33:00	47.7	122.1	–	4.3	GSC
1964	10	15	14:32:37.7	47.6	122.1	–	4.4	DNA
1965	4	29	15:28:43.3	47.4	122.4	57	6.5	DNA
1965	10	23	16:27:59.3	47.5	122.4	–	4.8	DNA
1967	1	18	06:58:21	47.295	122.571	22	4	DNA
1967	3	7	03:51:8.8	47.84	122.68	34	4.5	DNA

Table A-2 (cont.)
Historic Earthquakes in or Near Western Washington, M ≥ 4[1]

Year	Month	Day	Time (GMT)	North Latitude (degrees)	West Longitude (degrees)	Depth (kilometers)	Magnitude[2]	Source
1967	5	16	01:01:00	49	122.5	–	4	DNA
1967	5	25	23:22:34.5	48.2	122.81	33	4.5	DNA
1967	8	5	01:11:54.7	46.1	120	33	4.4	DNA
1968	1	27	08:28:23.7	45.61	122.605	34	4	DNA
1968	6	19	05:51:43	47.2	122.5	–	4.69	DNA
1968	9	6	12:16:30.8	48.1	122.76	34	4.7	DNA
1968	11	30	14:40:11	46.68	122.4	13	4.1	DNA
1969	2	14	8:33:36.1	48.94	123.07	52	4.7	DNA
1969	6	11	21:45:08	48.8	122.1	33	4	DNA
1969	10	9	17:07:55	46.766	121.716	–	4.3	DNA
1969	11	1	15:44:24.4	47.89	121.81	5	4.5	DNA
1969	11	10	07:38:44.7	48.55	121.51	33	5.1	DNA
1969	11	28	09:51:32.6	47.4	122.7	33	4.1	DNA
1970	5	18	05:29:54	48.6	122.7	18	4	GSC
1970	10	24	22:32:08.4	47.34	122.374	13	4.2	DNA
1971	11	23	02:12:17.3	48.178	121.37	18	4.14	DNA
1971	12	28	07:50:00.8	47.576	122.216	20	4.1	DNA
1972	11	9	04:19:19.9	48.394	123.23	42	4.12	DNA
1973	7	18	21:58:05.9	46.827	121.814	6	4	DNA
1974	4	20	03:00:10.3	46.774	121.567	–	4.9	DNA
1974	5	16	13:04:36.9	48.101	122.974	49	4.33	DNA
1974	12	13	03:28:54.2	45.265	121.599	22	4	DNA
1974	12	13	03:30:39	45.37	121.707	5	4.1	DNA
1975	4	16	19:09:29.4	47.548	122.909	42	4	DNA
1975	4	23	01:03:42.7	47.082	122.672	45	4.5	DNA
1976	4	13	00:47:15	45.154	120.861	15	4.8	DNA
1976	4	13	00:47:17.1	45.221	120.771	15	4.8	PDE
1976	4	17	02:11:46	45.168	120.801	15	4.2	DNA
1976	5	16	08:35:15	48.8	123.351	60	5.1	DNA
1976	9	2	13:36:11.4	48.193	122.768	20	4.5	DNA
1976	9	8	08:21:02	47.379	123.098	46	4.5	DNA
1976	10	14	21:39:18.2	46.697	122.384	5	4	DNA
1977	6	17	06:16:02.4	47.761	122.72	18	4	DNA
1977	7	10	07:19:30.2	48.583	122.398	13	4.3	DNA
1978	3	5	18:13:36.5	48.054	122.954	53	4	DNA
1978	3	11	15:52:11.6	47.422	122.718	24	4.8	DNA
1978	3	31	08:03:00.4	47.42	122.721	23	4.2	DNA
1978	8	19	01:51:19	48.63	123.55	32	4.3	DNA
1978	8	23	10:37:19	48.349	123.212	18	4.4	DNA
1978	12	31	03:23:46.9	47.595	121.847	19	4.1	DNA
1979	3	11	14:39:33.2	46.444	122.406	17	4.2	DNA

Table A-2 (cont.)
Historic Earthquakes in or Near Western Washington, M ≥ 4[1]

Year	Month	Day	Time (GMT)	North Latitude (degrees)	West Longitude (degrees)	Depth (kilometers)	Magnitude[2]	Source
1979	11	9	16:02:09	48.82	124.66	16	4.3	DNA
1979	11	26	23:18:27.3	48.549	122.396	17	4.1	DNA
1980	3	20	23:47:43.4	46.192	122.204	1	4.2	SEA
1980	3	22	22:22:42.5	46.204	122.221	–	4.2	SEA
1980	3	24	21:56:49.4	46.199	122.173	–	4.4	SEA
1980	3	25	07:08:46.1	46.197	122.183	–	4.1	SEA
1980	3	25	21:50:51.2	46.202	122.205	–	4.1	SEA
1980	3	25	22:53:01.6	46.2	122.18	–	4.3	SEA
1980	3	26	01:06:29.9	46.202	122.189	–	4	SEA
1980	3	26	02:03:18.3	46.206	122.206	–	4.4	SEA
1980	3	26	02:35:59.9	46.202	122.187	–	4.1	SEA
1980	3	26	05:00:04.3	46.203	122.184	–	4.3	SEA
1980	3	26	05:13:40.4	46.205	122.196	–	4.1	SEA
1980	3	26	05:30:09.8	46.2	122.195	–	4.2	SEA
1980	3	26	05:30:26.4	47.563	122.061	–	4	ISC
1980	3	26	07:17:21.8	46.205	122.183	–	4.1	SEA
1980	3	26	09:10:07.8	46.206	122.176	–	4.1	SEA
1980	3	26	09:44:02.5	46.201	122.169	–	4.4	SEA
1980	3	26	14:47:26.1	46.256	122.177	–	4.1	SEA
1980	3	26	17:07:10.8	46.192	122.206	2	4.4	SEA
1980	3	26	20:37:49	46.209	122.187	–	4	SEA
1980	3	27	03:40:05.6	46.218	122.18	–	4.2	SEA
1980	3	27	03:48:58.4	46.209	122.188	–	4.1	SEA
1980	3	27	04:26:10.3	46.194	122.182	4	4	SEA
1980	3	27	06:33:23.8	46.197	122.218	–	4.3	SEA
1980	3	27	07:39:15.5	46.207	122.178	–	4	SEA
1980	3	27	14:55:54.5	46.205	122.191	–	4.3	SEA
1980	3	27	15:55:03.7	46.209	122.201	1	4	SEA
1980	3	27	18:55:44.8	46.205	122.192	–	4	SEA
1980	3	27	20:16:43	46.204	122.186	–	4.3	SEA
1980	3	27	22:00:05.4	46.215	122.194	–	4.7	SEA
1980	3	28	01:51:12.6	46.206	122.187	2	4.3	SEA
1980	3	28	03:35:50.8	46.203	122.19	–	4	SEA
1980	3	28	08:28:25.6	46.214	122.178	–	4.9	SEA
1980	3	28	12:51:19.3	46.209	122.18	1	4.4	SEA
1980	3	28	13:59:38.4	46.207	122.189	–	4.1	SEA
1980	3	28	15:18:43.2	46.205	122.204	–	4	SEA
1980	3	28	22:50:28.4	46.21	122.201	2	4.1	SEA
1980	3	29	05:48:47.3	46.205	122.193	2	4.4	SEA
1980	3	29	08:36:56.7	46.203	122.176	1	4.4	SEA
1980	3	29	10:34:40.3	46.214	122.185	–	4.3	SEA

Table A-2 (cont.)
Historic Earthquakes in or Near Western Washington, M ≥ 4[1]

Year	Month	Day	Time (GMT)	North Latitude (degrees)	West Longitude (degrees)	Depth (kilometers)	Magnitude[2]	Source
1980	3	29	11:51:48.1	46.203	122.196	2	4.4	SEA
1980	3	29	13:01:50.7	46.199	122.204	–	4.3	SEA
1980	3	29	15:05:24.7	46.202	122.187	–	4.5	SEA
1980	3	29	15:35:39.6	46.214	122.176	1	4.4	SEA
1980	3	29	19:01:01.7	46.215	122.178	–	4	SEA
1980	3	29	20:55:51.8	46.207	122.19	–	4.4	SEA
1980	3	29	23:20:40.5	46.204	122.189	–	4.3	SEA
1980	3	30	02:56:19.6	46.211	122.192	–	4.3	SEA
1980	3	30	03:53:55	46.192	122.169	–	4.4	SEA
1980	3	30	07:42:17.1	46.206	122.183	–	4.1	SEA
1980	3	30	09:16:53.1	46.203	122.193	2	4.5	SEA
1980	3	30	12:39:57.6	46.21	122.177	–	4.1	SEA
1980	3	30	13:32:25.3	46.21	122.193	–	4.6	SEA
1980	3	30	17:55:10	46.208	122.183	–	4.6	SEA
1980	3	30	22:47:11.7	46.211	122.195	–	4.7	SEA
1980	3	31	02:44:6.1	46.208	122.193	–	4.5	SEA
1980	3	31	07:49:42	46.21	122.188	–	4.7	SEA
1980	3	31	08:12:51.9	46.213	122.199	–	4.2	SEA
1980	3	31	11:34:9.8	46.21	122.194	–	4.6	SEA
1980	3	31	14:49:01.2	46.215	122.191	–	4.5	SEA
1980	3	31	14:49:01.2	46.212	122.193	–	4.5	SEA
1980	3	31	19:29:11.3	46.224	122.171	–	4.2	SEA
1980	4	1	04:24:30.5	46.215	122.18	–	4.9	SEA
1980	4	1	08:54:25.4	46.213	122.187	–	4.9	SEA
1980	4	1	12:30:46.6	46.208	122.182	1	4.9	SEA
1980	4	1	23:14:38.5	46.209	122.193	–	4.9	SEA
1980	4	2	09:37:12.9	46.21	122.191	–	4.9	SEA
1980	4	2	18:48:20.6	46.208	122.183	–	4.6	SEA
1980	4	3	02:43:19.3	46.208	122.189	–	4.8	SEA
1980	4	3	09:35:26.8	46.227	122.172	–	5.1	SEA
1980	4	3	15:30:20.1	46.203	122.186	–	4.3	SEA
1980	4	3	21:51:58.5	46.212	122.181	–	4	SEA
1980	4	3	23:57:51.9	46.212	122.187	–	5	SEA
1980	4	4	09:42:35.3	46.212	122.206	1	4.3	SEA
1980	4	4	09:49:56.1	46.221	122.193	–	4	SEA
1980	4	4	13:45:05.6	46.209	122.181	–	4.9	SEA
1980	4	4	21:40:44.7	46.222	122.186	–	4.9	SEA
1980	4	5	06:39:3.1	46.204	122.183	–	4.3	SEA
1980	4	5	08:49:17.3	46.21	122.177	1	4.4	SEA
1980	4	5	10:58:49.2	46.203	122.191	–	4.1	SEA
1980	4	5	13:46:55.9	46.206	122.2	1	4.5	SEA

Table A-2 (cont.)
Historic Earthquakes in or Near Western Washington, M ≥ 4[1]

Year	Month	Day	Time (GMT)	North Latitude (degrees)	West Longitude (degrees)	Depth (kilometers)	Magnitude[2]	Source
1980	4	5	16:42:05.5	46.216	122.2	2	4.7	SEA
1980	4	6	06:58:04.3	46.211	122.187	–	5.1	SEA
1980	4	6	17:18:46.6	46.213	122.174	–	4	SEA
1980	4	6	20:26:12.2	46.201	122.194	–	4.1	SEA
1980	4	6	23:22:56	46.205	122.174	–	4	SEA
1980	4	6	23:26:00.8	46.206	122.192	–	4.4	SEA
1980	4	7	01:57:44.8	46.207	122.196	–	4.1	SEA
1980	4	7	04:52:53.9	46.185	122.168	2	4	SEA
1980	4	7	06:45:18.9	46.213	122.182	–	4.8	SEA
1980	4	7	09:42:01.5	46.213	122.176	–	4	SEA
1980	4	7	11:32:31.6	46.21	122.177	–	4	SEA
1980	4	7	11:51:43.5	46.205	122.178	–	4	SEA
1980	4	7	15:05:32.7	46.217	122.182	3	5.1	SEA
1980	4	8	02:18:46.8	46.202	122.189	–	4	SEA
1980	4	8	04:46:58.2	46.211	122.178	–	4.1	SEA
1980	4	8	06:07:04.5	46.206	122.18	–	4.8	SEA
1980	4	8	13:42:26.9	46.201	122.183	–	4.1	SEA
1980	4	8	19:29:02.9	46.21	122.196	–	5.1	SEA
1980	4	8	22:10:15.2	46.225	122.188	–	4.2	SEA
1980	4	8	22:13:49.8	46.203	122.193	–	4.4	SEA
1980	4	9	05:40:50.6	46.481	122.324	–	4.2	SEA
1980	4	9	09:01:44.2	46.202	122.184	2	4.5	SEA
1980	4	9	10:13:19.8	46.192	122.185	–	4.7	SEA
1980	4	9	18:19:26.9	46.214	122.173	–	4.7	SEA
1980	4	9	22:29:03.3	46.207	122.183	–	4.1	SEA
1980	4	10	00:25:47.8	46.215	122.168	–	4.8	SEA
1980	4	10	00:25:51.8	46.332	122.099	4	4.3	ISC
1980	4	10	00:44:15.5	46.222	122.185	–	4.9	SEA
1980	4	10	00:44:18.7	46.309	122.075	4	4.8	SEA
1980	4	10	14:16:15.1	46.209	122.183	–	4.7	SEA
1980	4	10	21:08:26	46.206	122.18	–	4.2	SEA
1980	4	11	04:45:22	46.218	122.178	1	4.7	SEA
1980	4	11	07:42:01.6	46.207	122.195	–	4.1	SEA
1980	4	11	14:52:25	46.209	122.188	–	4.1	SEA
1980	4	11	18:01:10.3	46.205	122.183	–	4.3	SEA
1980	4	11	19:15:08.3	46.2	122.152	–	4.1	SEA
1980	4	11	21:56:30.9	46.208	122.18	–	4	SEA
1980	4	11	23:51:59.8	46.208	122.168	–	5	SEA
1980	4	12	05:16:22.2	46.217	122.174	–	4.7	SEA
1980	4	12	15:08:11.7	46.204	122.186	–	4.3	SEA
1980	4	12	20:45:33.9	46.208	122.191	–	4	SEA

Table A-2 (cont.)
Historic Earthquakes in or Near Western Washington, M ≥ 4[1]

Year	Month	Day	Time (GMT)	North Latitude (degrees)	West Longitude (degrees)	Depth (kilometers)	Magnitude[2]	Source
1980	4	12	20:47:42	46.213	122.18	–	4	SEA
1980	4	12	22:29:12	46.219	122.198	1	4.6	SEA
1980	4	13	01:25:55.9	46.203	122.189	–	4.2	SEA
1980	4	13	03:03:22.7	46.245	122.188	–	4	SEA
1980	4	13	04:45:26.9	46.208	122.186	–	4	SEA
1980	4	13	06:13:18.4	46.204	122.188	–	4.2	SEA
1980	4	13	08:36:18.7	46.212	122.18	1	4.8	SEA
1980	4	13	09:40:46.3	46.213	122.185	–	4	SEA
1980	4	13	12:06:20.5	46.207	122.195	–	4.1	SEA
1980	4	13	17:35:41.6	46.204	122.193	–	4.5	SEA
1980	4	13	18:58:21.6	46.21	122.183	–	4.9	SEA
1980	4	14	03:01:02.4	46.203	122.188	–	4.1	SEA
1980	4	14	06:53:38.8	46.215	122.178	–	4.3	SEA
1980	4	14	06:59:22.3	46.21	122.192	2	4.9	SEA
1980	4	14	12:28:43.5	46.212	122.187	1	4.4	SEA
1980	4	14	13:49:03.7	46.203	122.197	1	5.2	SEA
1980	4	14	15:30:30.6	46.207	122.189	–	4	SEA
1980	4	14	22:28:53.1	46.214	122.2	–	4	SEA
1980	4	15	00:37:5.3	46.209	122.184	2	4.5	SEA
1980	4	15	02:26:17.9	46.197	122.196	–	4.3	SEA
1980	4	15	06:58:22.2	46.211	122.201	1	4.7	SEA
1980	4	15	07:15:31.8	46.201	122.19	1	4	SEA
1980	4	15	11:53:53.9	46.207	122.188	1	4.1	SEA
1980	4	15	16:12:04.6	46.207	122.187	–	4.1	SEA
1980	4	15	17:54:54.1	46.213	122.181	–	5	SEA
1980	4	15	21:55:49	46.427	121.929	5	4	SEA
1980	4	16	04:58:57.4	46.205	122.184	1	4	SEA
1980	4	16	11:47:28.6	46.203	122.189	1	4.1	SEA
1980	4	16	15:22:05.5	46.212	122.186	–	4.8	SEA
1980	4	16	15:40:23.5	46.214	122.176	3	4.6	SEA
1980	4	16	22:46:24.7	46.207	122.188	–	4.2	SEA
1980	4	17	04:26:15.9	46.208	122.182	–	4.7	SEA
1980	4	17	07:06:47.3	46.193	122.202	2	4	SEA
1980	4	17	17:43:22.5	46.213	122.186	–	5	SEA
1980	4	18	00:51:05.7	46.208	122.187	–	4	SEA
1980	4	18	00:53:40.4	46.213	122.184	–	4.7	SEA
1980	4	18	02:24:37.4	46.287	121.596	3	4.1	SEA
1980	4	18	09:23:38.9	46.201	122.188	–	4	SEA
1980	4	18	10:45:22.2	46.201	122.184	1	4	SEA
1980	4	18	13:03:55.2	46.212	122.178	–	4.2	SEA
1980	4	18	13:08:29.3	46.204	122.186	–	4	SEA

Table A-2 (cont.)
Historic Earthquakes in or Near Western Washington, M ≥ 4[1]

Year	Month	Day	Time (GMT)	North Latitude (degrees)	West Longitude (degrees)	Depth (kilometers)	Magnitude[2]	Source
1980	4	18	19:16:25.3	46.205	122.184	2	4	SEA
1980	4	18	21:16:02.1	46.208	122.183	–	5	SEA
1980	4	18	22:27:14.4	46.208	122.178	1	4.6	SEA
1980	4	19	02:37:26.1	46.203	122.185	–	4.1	SEA
1980	4	19	06:03:12.4	46.204	122.193	–	4.1	SEA
1980	4	19	08:07:17.9	46.206	122.189	–	4.3	SEA
1980	4	19	14:53:14.2	46.207	122.182	–	4	SEA
1980	4	19	17:48:35.5	46.216	122.174	–	4.4	SEA
1980	4	19	22:28:28.2	46.21	122.181	1	4.8	SEA
1980	4	20	04:53:02.4	46.206	122.185	–	4.1	SEA
1980	4	20	05:04:50.2	46.209	122.192	1	4	SEA
1980	4	20	08:08:08.5	46.218	122.192	–	4	SEA
1980	4	20	10:25:25	46.209	122.181	1	4.3	SEA
1980	4	20	17:53:34	46.202	122.191	–	4	SEA
1980	4	20	19:19:32.8	46.211	122.179	1	5.1	SEA
1980	4	20	22:03:48.7	46.211	122.176	–	4.4	SEA
1980	4	21	03:23:33.6	46.203	122.189	–	4.1	SEA
1980	4	21	05:17:52.1	46.209	122.181	–	4.3	SEA
1980	4	21	15:13:54.6	46.208	122.174	–	4.8	SEA
1980	4	21	19:52:08.5	46.211	122.167	–	4.4	SEA
1980	4	22	03:11:33	46.203	122.184	–	4	SEA
1980	4	22	6:11:55.8	46.211	122.181	1	4.4	SEA
1980	4	22	06:46:20	46.221	122.194	–	4	SEA
1980	4	22	10:25:05.4	46.209	122.189	–	4.4	SEA
1980	4	22	16:36:17.9	46.204	122.186	–	4	SEA
1980	4	22	19:28:18.7	46.203	122.182	–	5	SEA
1980	4	22	22:04:11	46.206	122.17	2	4.4	SEA
1980	4	23	13:08:15.3	46.207	122.202	1	4	SEA
1980	4	23	15:18:01	46.208	122.18	–	4.5	SEA
1980	4	24	09:50:9.4	46.209	122.179	–	4.4	SEA
1980	4	24	10:50:42.6	46.212	122.191	–	4	SEA
1980	4	24	13:32:07.7	46.196	122.18	2	4.1	SEA
1980	4	24	17:34:10.3	46.213	122.183	–	4.8	SEA
1980	4	24	23:07:53.5	46.211	122.182	–	4.2	SEA
1980	4	25	00:27:57.5	46.202	122.205	–	4	SEA
1980	4	25	11:00:21.7	46.203	122.188	–	4.1	SEA
1980	4	25	23:20:27.9	46.257	122.18	5	4.6	SEA
1980	4	26	12:16:55.6	46.204	122.187	–	4	SEA
1980	4	26	14:26:00.2	46.212	122.179	–	4	SEA
1980	4	26	15:53:59.7	46.207	122.183	–	4.1	SEA
1980	4	27	01:15:41.6	46.207	122.189	1	4.3	SEA

Table A-2 (cont.)
Historic Earthquakes in or Near Western Washington, M ≥ 4[1]

Year	Month	Day	Time (GMT)	North Latitude (degrees)	West Longitude (degrees)	Depth (kilometers)	Magnitude[2]	Source
1980	4	27	01:59:56	46.205	122.187	–	4.2	SEA
1980	4	27	07:15:17.4	46.203	122.186	3	4	SEA
1980	4	27	07:26:21	46.211	122.179	–	4.9	SEA
1980	4	27	12:34:37.3	46.208	122.188	–	4	SEA
1980	4	27	14:48:20.2	46.21	122.178	–	4.2	SEA
1980	4	28	03:49:33.5	46.208	122.189	1	4.9	SEA
1980	4	28	05:15:53.9	46.215	122.181	–	4.4	SEA
1980	4	28	12:30:54.6	46.199	122.188	–	4	SEA
1980	4	28	12:39:38.5	46.209	122.19	–	4.1	SEA
1980	4	28	15:09:07.5	46.202	122.182	–	4.1	SEA
1980	4	28	23:52:35.4	46.206	122.181	–	4.1	SEA
1980	4	29	04:24:30	46.214	122.18	1	4.8	SEA
1980	4	29	06:22:38.5	46.216	122.183	–	4.6	SEA
1980	4	29	12:41:36.3	46.21	122.18	–	4.2	SEA
1980	4	30	00:34:10.3	46.193	122.16	–	4.2	SEA
1980	4	30	05:09:02.5	46.21	122.172	–	4.9	SEA
1980	4	30	05:09:02.5	46.211	122.169	–	4.9	SEA
1980	4	30	07:42:09.1	46.211	122.184	1	4.5	SEA
1980	4	30	07:42:09.2	46.212	122.189	1	4.5	SEA
1980	4	30	07:54:58.9	46.204	122.171	–	4	SEA
1980	4	30	20:50:38.4	46.202	122.186	–	4	SEA
1980	5	1	04:46:15.4	46.209	122.182	–	4.6	SEA
1980	5	1	04:46:15.4	46.207	122.182	–	4.6	SEA
1980	5	1	06:18:32.1	46.203	122.189	–	4.1	SEA
1980	5	1	10:59:03.5	46.192	122.196	1	4	SEA
1980	5	1	19:27:15.6	46.189	122.199	–	4.6	SEA
1980	5	1	21:31:09.4	46.21	122.175	–	4.1	SEA
1980	5	2	05:12:18.9	46.209	122.183	2	4.4	SEA
1980	5	2	08:36:31.4	46.202	122.196	–	4.1	SEA
1980	5	2	12:52:17.7	46.206	122.176	6	4.3	SEA
1980	5	2	13:02:29.4	46.215	122.19	–	4.8	SEA
1980	5	3	05:00:46.4	46.204	122.179	–	4.5	SEA
1980	5	3	05:05:30.2	46.21	122.19	–	4.4	SEA
1980	5	3	06:47:50.5	46.2	122.187	–	4.1	SEA
1980	5	3	15:40:57	46.207	122.2	–	4.2	SEA
1980	5	3	20:45:37.8	46.199	122.173	–	4.2	SEA
1980	5	4	11:58:27.4	46.217	122.186	1	4.9	SEA
1980	5	4	21:39:22	46.201	122.189	–	4	SEA
1980	5	5	01:53:30.3	46.207	122.194	–	4	SEA
1980	5	5	05:43:04	46.21	122.179	1	4.7	SEA
1980	5	5	07:27:30.3	46.196	122.182	–	4	SEA

Table A-2 (cont.)
Historic Earthquakes in or Near Western Washington, M ≥ 4[1]

Year	Month	Day	Time (GMT)	North Latitude (degrees)	West Longitude (degrees)	Depth (kilometers)	Magnitude[2]	Source
1980	5	5	09:12:54.4	46.211	122.18	1	4.3	SEA
1980	5	5	13:19:08.4	46.211	122.19	4	4	SEA
1980	5	5	16:13:51.9	46.213	122.176	–	4	SEA
1980	5	6	00:03:31.5	46.209	122.18	–	4.3	SEA
1980	5	6	08:15:01.6	46.206	122.198	–	4	SEA
1980	5	6	15:30:44.8	46.383	121.9	1	4	PDE
1980	5	6	17:04:49.1	46.21	122.174	1	4.6	SEA
1980	5	6	17:53:13.2	46.221	122.247	–	4	SEA
1980	5	6	19:22:28.3	46.211	122.178	1	4.4	SEA
1980	5	7	03:44:42.6	46.204	122.188	–	4.2	SEA
1980	5	7	08:52:32.9	46.205	122.187	–	4	SEA
1980	5	7	11:09:17.9	46.217	122.195	1	4.7	SEA
1980	5	7	12:33:20.8	46.204	122.181	–	4	SEA
1980	5	8	01:19:58.8	46.2	122.187	–	4.2	SEA
1980	5	8	07:46:50	46.207	122.191	1	4.4	SEA
1980	5	8	07:48:46.2	46.21	122.177	–	4.7	SEA
1980	5	8	08:47:55.4	46.203	122.191	–	4	SEA
1980	5	8	09:03:39.9	46.214	122.179	1	4.6	SEA
1980	5	8	10:05:38	46.206	122.193	–	4.3	SEA
1980	5	9	00:55:2.3	46.201	122.187	1	4	SEA
1980	5	9	04:31:58	46.203	122.179	–	4	SEA
1980	5	9	07:01:01.1	46.216	122.174	–	4.7	SEA
1980	5	9	14:10:37.2	46.207	122.182	1	4	SEA
1980	5	9	18:06:26.5	46.214	122.174	1	4.6	SEA
1980	5	9	21:29:35.6	46.201	122.181	–	4	SEA
1980	5	10	01:14:10.5	46.204	122.187	1	4	SEA
1980	5	10	05:50:3.9	46.206	122.19	1	4.1	SEA
1980	5	10	09:25:55.3	46.18	122.119	–	4.1	SEA
1980	5	10	11:15:54.8	46.207	122.183	–	4	SEA
1980	5	10	12:31:47.5	46.213	122.178	1	4.5	SEA
1980	5	10	17:35:20.5	46.207	122.191	2	4.3	SEA
1980	5	11	01:19:29.4	46.202	122.189	2	4.1	SEA
1980	5	11	04:00:17.9	46.211	122.179	2	4.6	SEA
1980	5	11	08:09:48.3	46.203	122.185	1	4.1	SEA
1980	5	11	13:29:53.9	46.211	122.18	1	4.4	SEA
1980	5	11	15:00:52.1	46.199	122.166	1	4	SEA
1980	5	11	22:46:24.4	46.207	122.191	1	4.3	SEA
1980	5	12	12:11:25.2	46.207	122.194	–	4.2	SEA
1980	5	12	16:26:29.6	46.209	122.177	1	4.3	SEA
1980	5	12	16:46:50.2	46.203	122.182	1	4.3	SEA
1980	5	12	17:24:11.7	46.206	122.191	–	4.1	SEA

Table A-2 (cont.)
Historic Earthquakes in or Near Western Washington, M ≥ 4[1]

Year	Month	Day	Time (GMT)	North Latitude (degrees)	West Longitude (degrees)	Depth (kilometers)	Magnitude[2]	Source
1980	5	12	18:42:09.9	46.211	122.17	–	4	SEA
1980	5	12	20:33:39.6	46.212	122.176	–	4.8	SEA
1980	5	13	01:30:50.1	46.217	122.173	–	4.4	SEA
1980	5	13	11:12:12.8	46.184	122.194	5	4.1	SEA
1980	5	14	02:18:57.7	46.213	122.177	1	4.6	SEA
1980	5	14	09:43:51.7	46.203	122.186	1	4.2	SEA
1980	5	14	14:08:16.3	46.21	122.171	1	4.1	SEA
1980	5	14	18:48:01.8	46.196	122.178	–	4.1	SEA
1980	5	14	23:45:58.4	46.203	122.181	–	4	SEA
1980	5	15	06:48:24.6	46.199	122.183	1	4.1	SEA
1980	5	15	17:29:16.7	46.207	122.167	1	4	SEA
1980	5	16	03:31:04.6	46.199	122.182	–	4.3	SEA
1980	5	16	12:34:54.1	46.213	122.197	1	4.7	SEA
1980	5	16	13:27:13.5	46.2	122.184	1	4.1	SEA
1980	5	16	14:22:00.2	46.207	122.179	1	4.3	SEA
1980	5	16	16:17:44.4	46.198	122.196	–	4.1	SEA
1980	5	17	08:31:53	46.197	122.205	3	4.2	SEA
1980	5	17	21:42:07.4	46.209	122.177	2	4.3	SEA
1980	5	18	01:50:52	46.198	122.184	2	4.1	SEA
1980	5	18	14:36:10.7	46.205	122.182	2	4.1	SEA
1980	5	18	15:32:11.4	46.207	122.188	2	5.7	SEA
1980	5	18	20:24:05.3	46.166	122.162	–	4.1	SEA
1980	5	18	21:07:11.5	46.202	122.21	5	4.3	SEA
1980	5	18	21:10:06.9	46.203	122.194	3	4	SEA
1980	5	18	21:52:14.1	46.205	122.188	3	4.1	SEA
1980	5	18	21:54:40.9	46.203	122.176	2	4	SEA
1980	5	18	21:59:00.9	46.203	122.192	2	4	SEA
1980	5	18	22:18:08.8	46.199	122.177	1	4.1	SEA
1980	5	18	22:27:12.7	46.189	122.198	6	4.1	SEA
1980	5	18	22:35:49.9	46.209	122.207	10	4.2	SEA
1980	5	18	22:37:08	46.203	122.186	2	4	SEA
1980	5	18	22:38:34.2	46.195	122.189	1	4.1	SEA
1980	5	18	22:48:08.9	46.164	122.194	12	4.2	SEA
1980	5	18	22:49:04.4	46.199	122.191	2	4.2	SEA
1980	5	18	22:50:54.9	46.182	122.211	5	4.3	SEA
1980	5	18	22:54:01.3	46.227	122.18	–	4.5	SEA
1980	5	18	22:59:04.3	46.201	122.192	3	4.2	SEA
1980	5	18	23:00:49.9	46.208	122.193	6	4	SEA
1980	5	18	23:03:17.6	46.204	122.179	1	4	SEA
1980	5	18	23:07:21.5	46.127	122.15	–	4.3	SEA
1980	5	18	23:09:41.3	46.149	122.171	27	4.1	SEA

Table A-2 (cont.)
Historic Earthquakes in or Near Western Washington, M ≥ 4[1]

Year	Month	Day	Time (GMT)	North Latitude (degrees)	West Longitude (degrees)	Depth (kilometers)	Magnitude[2]	Source
1980	5	18	23:14:19.5	46.211	122.184	3	4.1	SEA
1980	5	19	00:18:02.7	46.204	122.187	1	4	SEA
1980	5	21	16:02:31.8	46.196	122.205	14	4.3	SEA
1980	5	24	23:01:23.6	46.333	122.213	2	4.1	SEA
1980	5	28	14:15:31.6	46.336	122.213	1	4.1	SEA
1980	5	28	14:18:30.2	46.335	122.206	3	4	SEA
1980	6	8	22:40:10.6	47.968	123.017	48	4.2	SEA
1981	2	2	01:23:18.3	46.263	120.989	1	4	SEA
1981	2	14	06:09:27.2	46.349	122.236	7	5.2	SEA
1981	2	18	06:09:38.7	47.197	120.893	3	4.2	SEA
1981	5	13	05:00:36.1	46.363	122.248	10	4.5	SEA
1981	5	28	08:56:02.5	46.53	121.398	2	4.6	SEA
1981	5	28	09:10:45.9	46.525	121.394	3	5	SEA
1982	3	1	17:40:04.7	46.346	122.247	11	4.4	SEA
1983	10	31	21:47:58.8	47.337	123.243	43	4.3	SEA
1984	4	11	03:07:42	47.535	120.186	8	4.3	SEA
1987	12	2	07:12:57.4	46.675	120.684	18	4.1	SEA
1987	12	2	09:02:24.2	46.679	120.673	17	4.3	SEA
1988	3	11	10:01:26	47.191	122.322	65	4.3	PDE
1988	7	29	04:59:47	46.855	121.914	11	4.1	SEA
1989	2	14	21:41:10	48.429	122.228	–	4	SEA
1989	3	5	06:42:00	47.813	123.357	46	4.5	SEA
1989	3	6	03:09:54	48.429	122.231	1	4.2	SEA
1989	6	18	20:38:37.3	47.41	122.776	45	4.4	PDE
1989	12	24	08:45:58	46.65	122.116	18	4.9	SEA
1990	4	2	11:13:22	48.832	122.188	–	4.3	SEA
1990	4	3	02:18:20	48.836	122.175	2	4	SEA
1990	4	14	05:33:26	48.845	122.161	12	5	SEA
1990	4	14	05:40:07	48.822	122.189	3	4	SEA
1990	6	9	17:12:16	46.268	122.055	10	4	SEA
1990	6	11	11:44:90	48.268	121.761	4	6	SEA
1990	12	20	22:16:12	46.201	122.186	1	6	SEA
1990	12	21	02:45:33	46.204	122.187	–	5	SEA
1991	5	3	23:12:36	46.267	122.21	7	6	SEA
1993	3	25	13:34:35	45.035	122.607	20	5.6	SEA
1994	6	15	08:22:19.8	47.411	123.161	45	4	SEA
1994	6	18	07:01:07.3	47.621	121.27	–	4.3	SEA
1995	5	20	12:48:48.2	46.881	121.943	13	4.1	SEA
1996	5	3	04:04:22	47.76	121.88	4	5.5	PDE
1997	6	23	19:13:27	47.6	122.57	7	5	PDE
1997	6	24	14:23:12	48.38	119.89	7	4.6	PDE

Table A-2 (cont.)
Historic Earthquakes in or Near Western Washington, M ≥ 4[1]

Year	Month	Day	Time (GMT)	North Latitude (degrees)	West Longitude (degrees)	Depth (kilometers)	Magnitude[2]	Source
1998	10	9	16:43:08	46.2	120.7	3.2	4	SEA
1999	7	3	01:43:54	47.07	123.46	40	5.8	PDE
2000	1	30	19:10:23	45.19	120.12	–	4.1	SEA
2001	2	28	18:54:32	47.14	122.72	51.9	6.8	SEA
2001	6	10	13:19:11	47.16	123.50	40.7	5.0	SEA
2001	7	22	15:13:52	47.08	122.68	52.4	4.3	SEA
2001	11	11	16:00:29	47.68	117.40	4.7	4.0	SEA
2002	6	29	14:36:04	45.33	121.68	6.2	4.5	SEA
2002	9	21	00:55:20	48.48	123.12	23.4	4.1	SEA
2003	4	25	10:02:12	47.67	123.25	51.3	4.8	SEA

a. Data from National Geographic Data Center, Boulder, Colorado.
b. M_S, M_L, m_b or based on felt area or Maximum Modified Mercalli Intensity. Maximum reported magnitudes are listed on the table.
DNA = Decade of North American Geology
GSC = Geological Survey of Canada
OSU = Oregon State University
PDE = Preliminary Determination of Epicenters from NEIS/CGS
SEA = University of Washington, Seattle

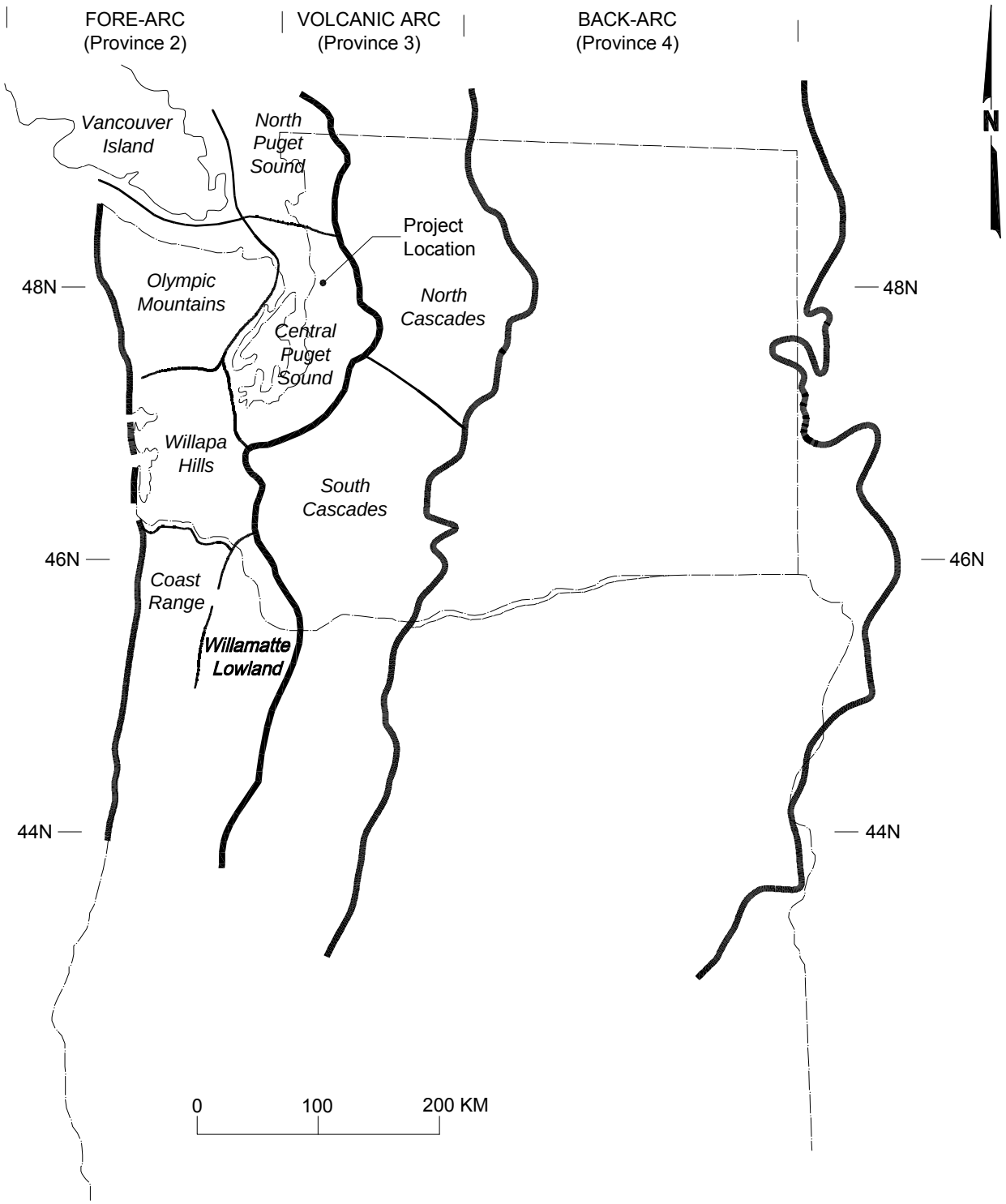

LEGEND

Province Boundary

Subprovince Boundary

NOTE

Figure adapted from McCrumb et al., 1989.

Brightwater Project
Seismic Hazard Analysis
King County Department of Natural Resources

NORTH AMERICAN PLATE TECTONIC PROVINCES IN WESTERN WASHINGTON

January 2005

FIG. A-1

File: I:\Drafting\211\20150-002\21-1-20150-002 Fig A-1.dwg Date: 12-28-2004 Author: SAC Shannon & Wilson, Inc.

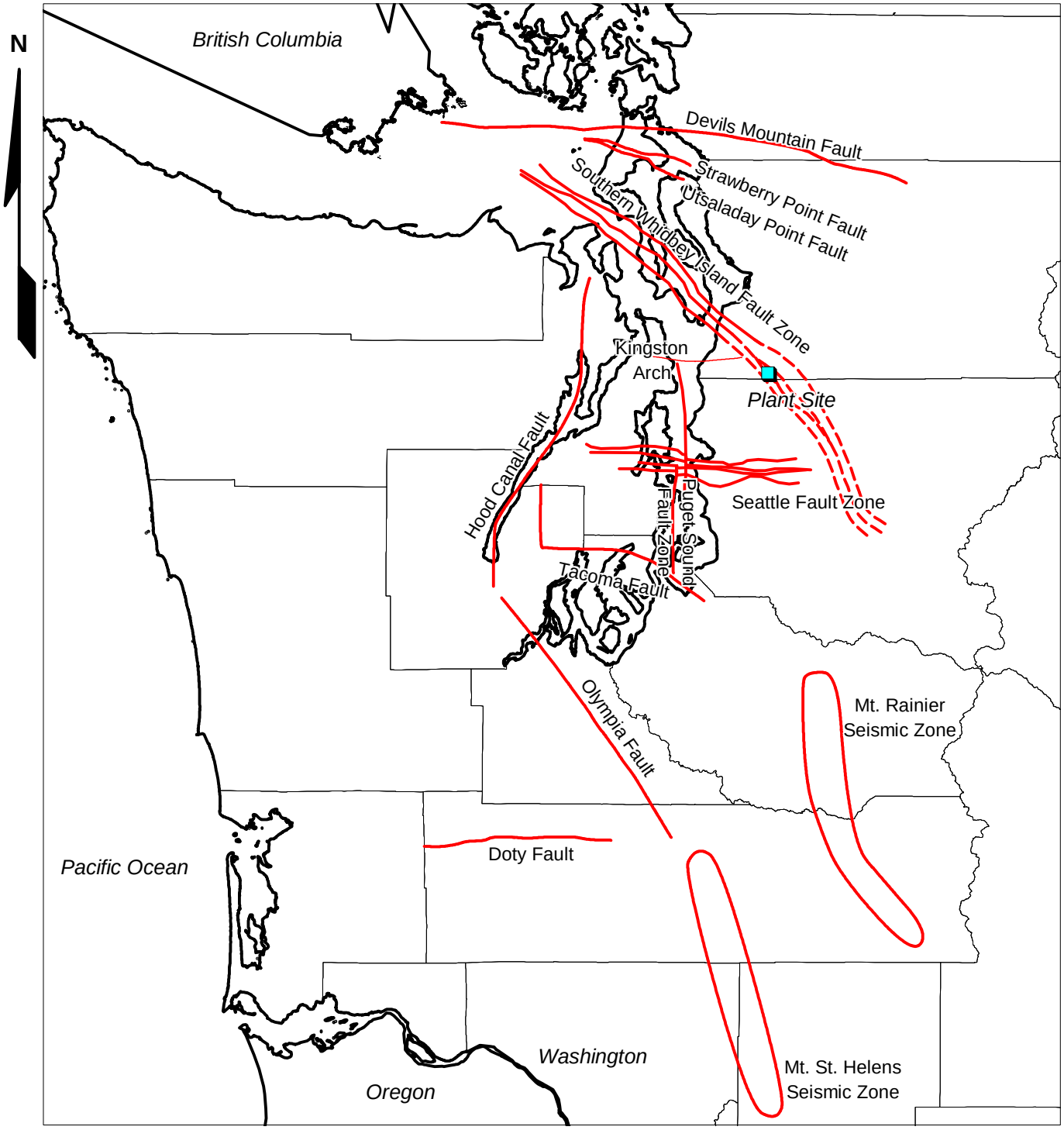

NOTES

1. Figure shows major crustal structures in and adjacent to the Central Puget Sound that are or may be associated with current tectonic stresses with known or possible Quaternary movement.
2. Structural features after Gower et al. (1985), Johnson et al. (1999), Johnson et al. (2000), Johnson et al. (2001), Brocher et al. (2001), Dragovich et al. (2002), Blakely et al. (2004).
3. Mainland extensions of the Southern Whidbey Island Fault Zone modeled in the revised PSHA and described in this report are indicated with dashed lines.

Brightwater Project
Seismic Hazard Analysis
King County Department of Natural Resources

MAJOR CRUSTAL STRUCTURES IN THE CENTRAL PUGET SOUND AND ADJACENT AREAS

Janaury 2005

FIG. A-2

File: 21-1-20150-002, Fig A-2 Major Crustal Structures.WOR Date: 01/04/05 Author: Shannon & Wilson (WJP)

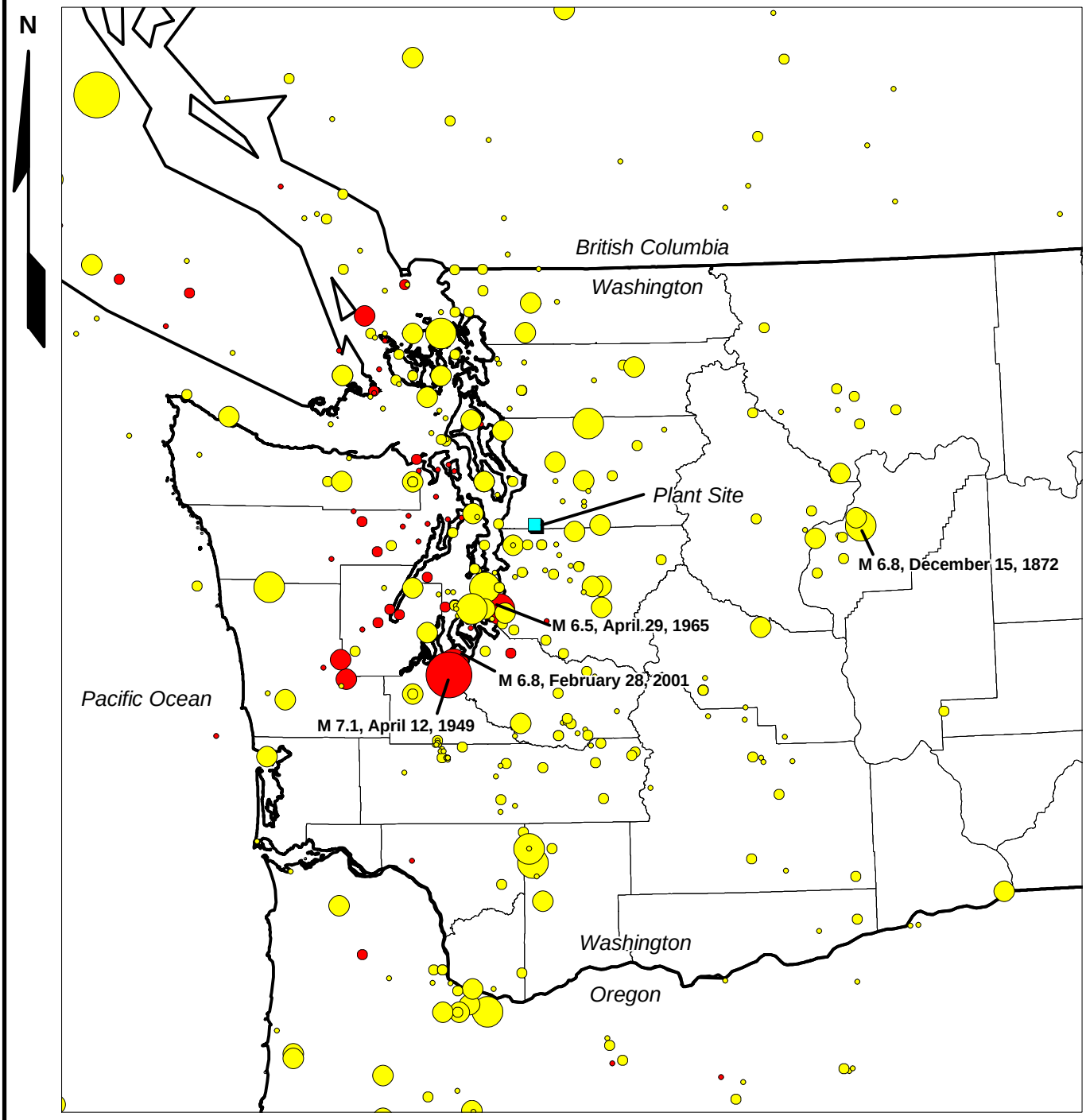

0 80 160

Scale in Kilometers

LEGEND

EARTHQUAKE MAGNITUDES

Shallow Crustal Earthquakes (Depth < 30 km)	Deep Intraslab Earthquakes (Depth > 30 km)
7 to 7.5	7 to 7.5
6 to 7	6 to 7
5 to 6	5 to 6
4 to 5	4 to 5
3.5 to 4	3.5 to 4

Brightwater Project
Seismic Hazard Analysis
King County Department of Natural Resources

HISTORIC EARTHQUAKES IN OR NEAR WESTERN WASHINGTON

Janaury 2005

FIG. A-3

File: 21-1-20150-002, Fig A-3 Historical seismicity.WOR Date: 01/04/05 Author: Shannon & Wilson (WJP)

Appendix B

Seismicity Catalog and Earthquake Recurrence

Appendix B

Seismicity Catalog and Earthquake Recurrence

TABLE OF CONTENTS

Page

B.1 Seismicity Catalog B-1

B.2 Earthquake Recurrence B-2

B.3 References B-3

LIST OF TABLES

Table No.

B-1 Seismicity Catalog

B-2 Estimated Catalog Completeness From Ludwin et al., 1991

B-3 Catalog Completeness for Brightwater Treatment Plant Probabilistic Seismic Hazard Analysis (PSHA)

LIST OF FIGURES

Figure No.

B-1 Lower Magnitude Earthquake Catalog Completeness Versus Year

B-2 Recurrence Curve for Intraslab Zone

B-3 Recurrence Curve for Vancouver Island Zone

B-4 Recurrence Curve for Olympic Mountains, Willapa Hills, & Coastal Range Zones

B-5 Recurrence Curve for Willamette Lowland Zone

B-6 Recurrence Curve for North Puget Sound Zone

B-7 Recurrence Curve for Central Puget Sound Zone

B-8 Recurrence Curve for North Cascades Zone

B-9 Recurrence Curve for South Puget Sound Zone

Appendix B

Seismicity Catalog and Earthquake Recurrence

B.1 Seismicity Catalog

The seismicity catalog developed for the probabilistic seismic hazard analysis (PSHA) is a compilation of several separate catalogs shown in Table B-1. The seismicity catalog contained pre-instrumental and instrumental seismicity between 1841 and June 2003. The catalog records from the various sources were combined for the Puget Sound region and duplicate events were removed.

Duplicate records and dependent events, such as foreshocks and aftershocks, were removed from the catalog, and the catalog was corrected for completeness prior to determination of the Gutenberg-Richter parameters. Dependent events in this catalog were identified and removed using empirical criteria given by Gardner and Knopoff (1974), Uhrhammer (1986), and Wyss (1979). These references define a spatial and temporal window that is a function of magnitude. Events that fall within the window are considered dependent events and were then removed from the catalog. Foreshock or aftershock sequences were also determined using this procedure.

The Pacific Northwest Seismograph Network (PNSN), the Cascadia earthquake, and the U.S. Geological Survey (USGS) catalogs were the primary sources of data for the Plant site PSHA. Duplicate events of small magnitude (typically less than M4) that were recorded by the sources in Table B-1 were occasionally assigned different magnitude and locations. The magnitudes and locations in the PNSN and Cascadia catalog were given precedence over the other catalogs. If the event in an alternate catalog was not present in the PNSN or Cascadia catalog, the larger magnitude and location closer to the Plant site were assumed. The 1872 North Cascades earthquake was located according to Bakun et al. (2002).

Ludwin et al. (1991) and Brocher et al. (2003) estimate catalog completeness intervals of the University of Washington Regional Catalog (now called the PNSN catalog) for all of Oregon and Washington. The completeness intervals shown in Table B-2 and Figure B-1 are from Ludwin et al. (1991) and Brocher et al. (2003), respectively.

The completeness intervals in Table B-3 were used in the development of recurrence relations for this analysis and are conservative compared to those presented in Brocher et al. (2003). The values in Table B-3 were implemented as a step function when computing the earthquake recurrence.

B.2 Earthquake Recurrence

The magnitude-frequency recurrence equations used for each of the source zones describe the expected distribution of the magnitudes of earthquakes produced by that source zone. Two forms of the recurrence equation were considered: the truncated exponential (Gutenberg-Richter) distribution and the characteristic earthquake distribution.

The Gutenberg-Richter model is typically applied to zones where the observed seismicity includes contributions from multiple sources. The basic Gutenberg-Richter recurrence equation expresses the average number of earthquakes per year, N, that exceed some magnitude, M, using the form:

$$\log \mathbf{N} = \mathbf{a} - \mathbf{b}M$$

where **a** is equal to the annual number of earthquakes of M > 0 and **b** describes the relative likelihood of large and small earthquakes.

The Gutenberg-Richter relations were used to describe the earthquake recurrence for the crustal areal zones and the intraslab zone. The values of **a** and **b** were determined by maximum likelihood regression analysis using historical seismicity data for all the crustal areal zones except the Intraslab Cascadia Subduction Zone (CSZ). Linear regression of the Intraslab CSZ historical seismicity data was used because the seismic hazard computed using the maximum likelihood regression fit did not match the observed seismicity.

The Gutenberg-Richter equation is commonly modified to consider earthquakes above some minimum magnitude (taken as M = 5.0 in this study) and below some maximum value. However, considering the small amount of observed seismicity in most crustal zones, the values of **a** and **b** were typically computed using the data from M>4. The Willamette Lowland has a very small amount observed seismicity, and the values of **a** and **b** were computed using the data from M>3.5.

Plots of the Gutenberg-Richter recurrence equations and the data from which they were obtained are shown in Figures B-2 through B-9.

Magnitude-frequency relations for large earthquakes are typically based on interpolation and extrapolation of smaller events from recorded seismicity catalogs. Hyndman et al. (2003) obtained an estimate of the Gutenberg-Richter magnitude-frequency relations using the seismic moment rate required to accommodate the rate of deformation obtained from global positioning system measurements and geological data in the central Puget Sound. Hyndman et al. (2003) obtained **a** and **b** values equal to 2.63 and 0.72, respectively, for a zone with a geometry very similar to our modeled Central Puget Sound. These values are in good agreement with the **a** and **b** obtained from the seismicity catalog used for the Plant and Portal PSHA.

For all crustal sources and the intraslab, our **a** and **b** values are only based on observed seismicity in the Pacific Northwest. The 1996 USGS PSHA (Frankel et al., 1996) used a **b**-value equal to

0.8 for the Intraslab CSZ. The 1996 USGS ground motion hazard mapping project **b**-value was based on all deep events including Northern California. However, the 2002 USGS ground motion hazard mapping project (Frankel et al., 2002) uses deep events only from the Puget Lowland and the Georgia Strait. As a result of this significant modification, the 2002 USGS uses a **b**-value equal to 0.4 (this fit may be from only M>=5 events similar to the areal sources) for the Intraslab CSZ. The **b**-value obtained for this study for the Intraslab CSZ is 0.5 and is based on fitting between M=4 to approx M=7.1.

Studies have shown that individual faults tend to produce repeated earthquakes of similar magnitude. This behavior is described by the characteristic earthquake model, the magnitude distribution of which is generally applied to specific faults. In this study, the characteristic magnitude distribution of Youngs and Coppersmith (1985) was used to describe earthquake recurrence for the Interplate CSZ and the nine shallow crustal fault sources.

For the SWIF both characteristic and exponential distributions were used. The exponential distribution was used to allow for the possibility of smaller, non-characteristic events on the SWIF as the recent fault trenching studies by the King County design team (AMEC, 2005) and the USGS (Shannon & Wilson, 2004b) have found some evidence that could indicated that there may be a significant difference in the size of earthquakes that have occurred on the SWIF. For the exponential distribution, the **b**-value was taken to be the same as **b**-value calculated from the observed crustal seismicity in the Central Puget Sound Zone (Figure B-7), the areal source zone in which the SWIF is located. The **a**-value was set such that the moment rate for the exponential distribution corresponds to the moment rate for the characteristic recurrence model and a maximum magnitude of 7.5.

B.3 References

AMEC Earth & Environmental, Inc., 2005, Draft report: surface-fault-rupture hazard evaluation, Brightwater Wastewater Treatment Plant site, Snohomish County, Washington: Report by AMEC Earth & Environmental, Anaheim, Calif., 4-212-102100, for Bob Peterson, King County – Wastewater Treatment Division, Seattle, Wash., January.

Bakun, W.H., Haugerud, R.A., Hopper, M.G., and Ludwin, R.S., 2002, The December 1872 Washington State earthquake: Bulletin of the Seismological Society of America, 92(8), p. 3239-3258.

Brocher, T.M., Weaver, C., and Ludwin, R., 2003, Assessing hypocentral accuracy and lower magnitude completeness in the Pacific Northwest using seismic refraction detonations and cumulative frequency-magnitude relationships: Seismological Research Letters, 74(6), p. 773-790.

Frankel, A., Mueller C., Barnhard, T., Perkins, D., Leyendecker, E.V., Dickman, N., Hanson, S., and Hopper, M., 1996, National seismic hazard maps, June 1996 Documentation: U.S. Geological Survey Open-File Report 96-532.

Frankel, A., Petersen, M., Mueller, C., Haller, K., Wheeler, R., Leyendecker, E., Wesson, R., Harmsen, S., Cramer, C., Perkins, D., and Rukstales, K., 2002, Documentation for the 2002 update of the national seismic hazard maps: U.S. Geological Survey Open-File Report 02-420, 39 p.

Gardner, J.K., and Knopoff, L., 1974, Is the sequence of earthquakes in Southern California, with aftershocks removed, Poissonian?: Bulletin of the Seismological Society of America, v. 64, no. 5, p. 1363-1367.

Hyndman, R.D, Mazozotti, S , Weichert, D., and Rogers, G..C., 2003, Frequency of large crustal earthquakes in Puget Sound-Southern Georgia Strait predicted from geodetic and geological deformation rates: Journal of Geophysical Research , v. 108.

Ludwin, R.S., Weaver, C.S., and Vrosson, R.S., 1991, Seismicity of Washington and Oregon *in* Slemmons, D.B., E.R. Engdahl, M.D. Zoback, and D.D. Blackwell (eds.), Neotectonics of North America, p. 77-98.

Shannon & Wilson, Inc., 2004b, Proposed revisions to the SWIF model for the revised Brightwater PSHA based on recent USGS/project team fault studies and reviews: Report by Shannon & Wilson, Inc., Seattle, Wash., 21-1-20150-002, for CH2M Hill, Bellevue, Wash., November 17.

Uhrhammer, R.A., 1986, Characteristics of northern and central California seismicity [abs.]: Earthquake Notes, v. 57, no. 1, p. 21.

Wyss, M., 1979, Estimating maximum expectable magnitude of earthquakes from fault dimensions: Geology, v. 7, no. 7, p. 336-340.

Youngs, R.R., and Coppersmith, K.J., 1985, Implications of fault slip rates and earthquake recurrence models to probabilistic seismic hazard estimates: Bulletin of the Seismological Society of America 75(4), p. 939-964.

Table B-1. Seismicity Catalog
(region of interest = 44° – 51.5° N, 116° – 129° W
Minimum Magnitude = 3.5)

Catalog	Host	Time Period
Pacific Northwest Seismological Network (PNSN)	University of Washington www.geophys.washington.edu/SEIS/PNSN/CATALOG_SEARCH/cat.search.html	1970 – 6/2003
The Cascadia Earthquake Catalog	University of Washington www.geophys.washington.edu/SEIS/PNSN/HIST_CAT/histcat.html	1793-1929
National Earthquake Information Center (NEIC)	USGS wwwneic.cr.usgs.gov/neis/epic/epic_rect.html	1973 – 6/2003
Advanced National Seismic System (ANSS)	Northern California Earthquake Data Center quake.geo.berkeley.edu/cnss/	1898 –6/2003
Significant Worldwide Earthquakes by National Geophysical Data Center	USGS wwwneic.cr.usgs.gov/neis/epic/epic_rect.html	2150 B.C. – 1994 A.D.
Significant U.S. Earthquakes by Stover & Coffman, 1993.	USGS wwwneic.cr.usgs.gov/neis/epic/epic_rect.html	1568 – 1989
Canada by the Earth Physics Branch of Canada.	USGS wwwneic.cr.usgs.gov/neis/epic/epic_rect.html	1568-1992
National Earthquake Database of Canada	Canada www.seismo.nrcan.gc.ca/nedb/eq_db_e.php	1980 - 6/2003

Table B-2. Estimated Catalog Completeness From Ludwin et al., 1991

Date	Minimum Magnitude	Estimated Magnitude Completeness Level
Before 1917	5.75	6.5 (before 1900)
1917 – 1939	5.25	6.0
1940 - 1955	4.75	5.5
1956 – 1964	4.25	5.0
1965 – 1970	3.75	4.25
1970 – Present	2.5	4.0

Table B-3. Catalog Completeness for Brightwater Treatment Plant Probabilistic Seismic Hazard Analysis (PSHA)

Minimum Magnitude	Completeness Level (years)	Inclusive Completeness Dates
3.5	34	1970 – 2003
4.25	39	1965 – 2003
5.0	48	1956 – 2003
5.5	64	1940 – 2003
6.0	103	1901 – 2003
>6.5	134	1870 – 2003

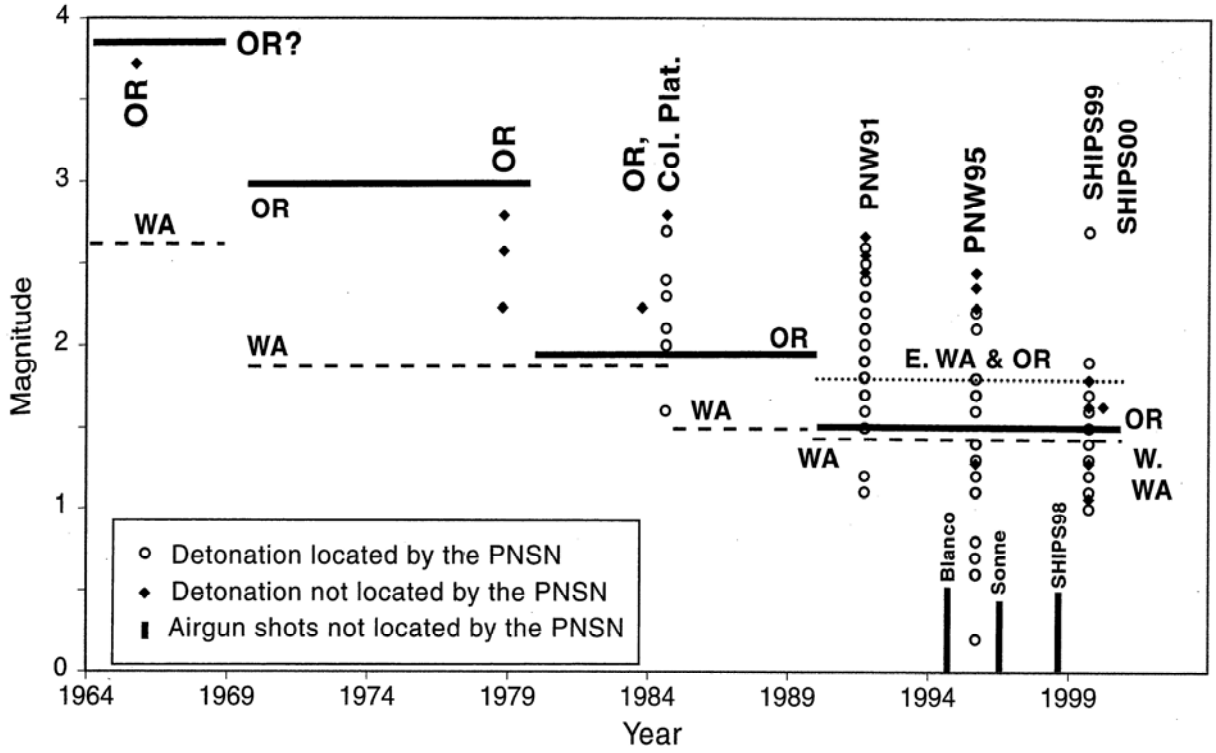

from Brocher et al. (2003)

Brightwater Project
Seismic Hazard Analysis
King County Department of Natural Resources

LOWER MAGNITUDE EARTHQUAKE CATALOG COMPLETENESS VERSUS YEAR

January 2005 | **FIG. B-1**

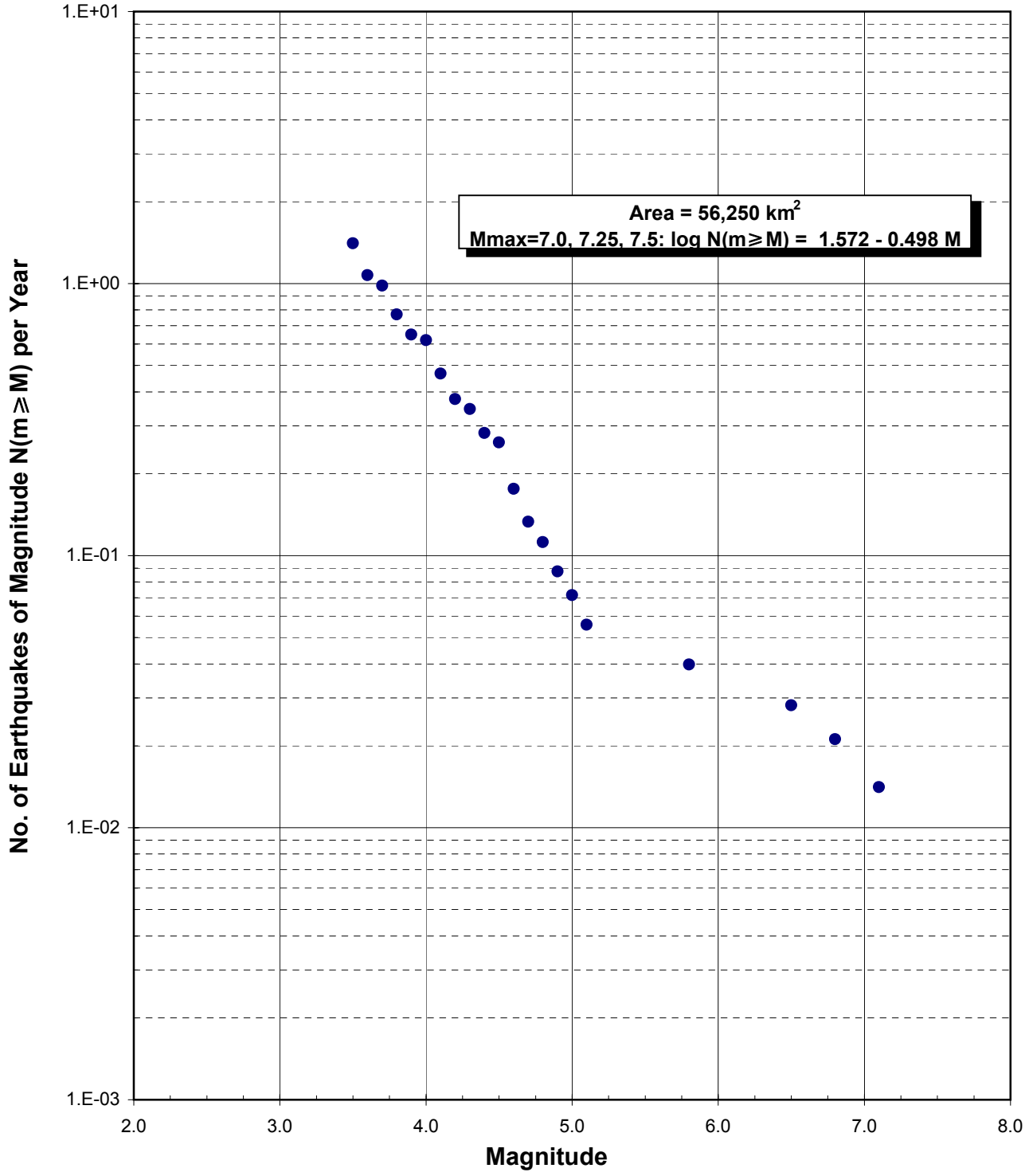

NOTE:
Events smaller than M 4.0 were not used in the regression analysis.

Brightwater Project
Seismic Hazard Analysis
King County Department of Natural Resources

RECURRENCE CURVE FOR INTRASLAB ZONE

January 2005

FIG. B-2

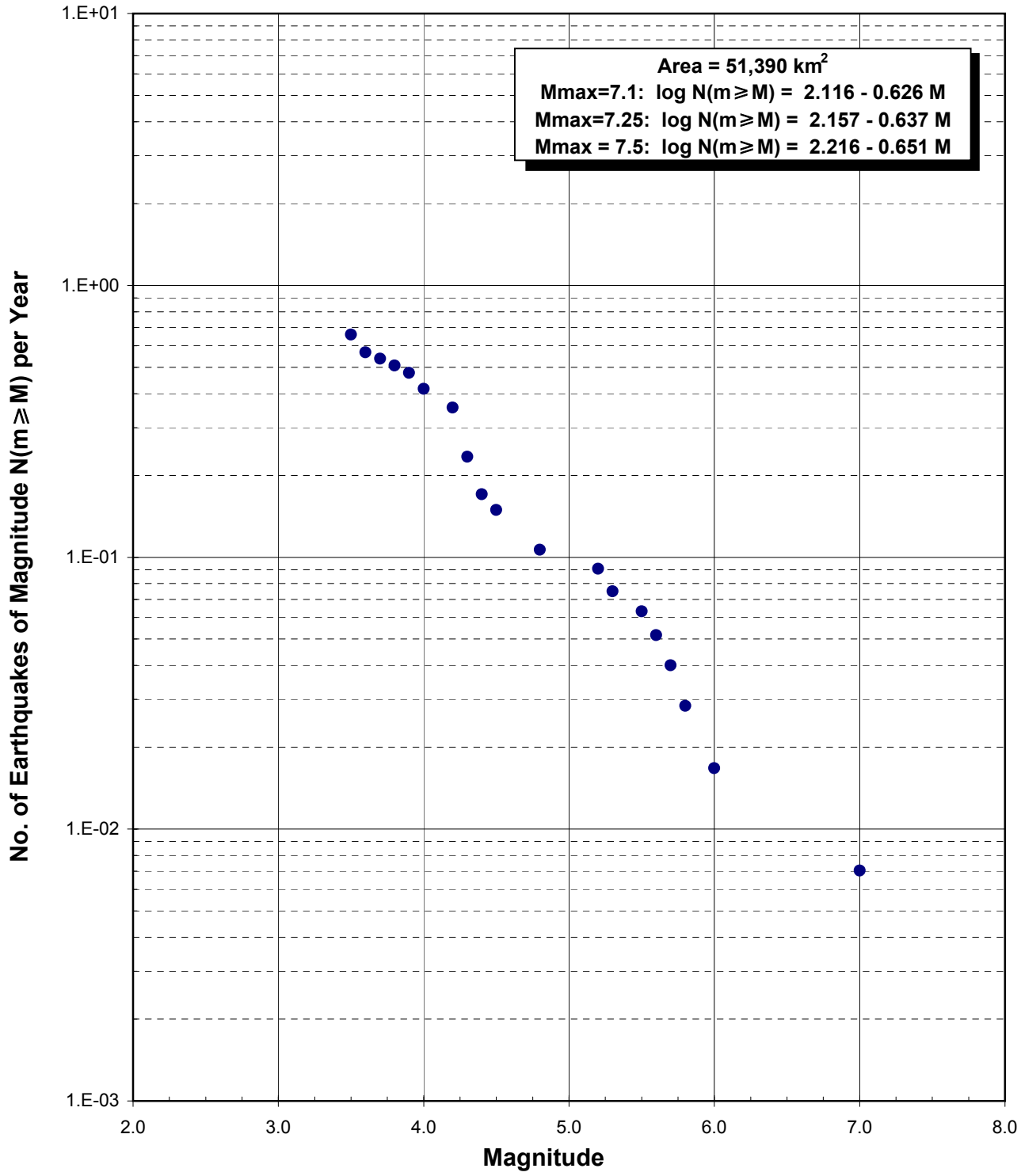

NOTE:
Events smaller than M 4.0 were not used in the regression analysis.

Brightwater Project
Seismic Hazard Analysis
King County Department of Natural Resources

RECURRENCE CURVE FOR VANCOUVER ISLAND ZONE

January 2005

FIG. B-3

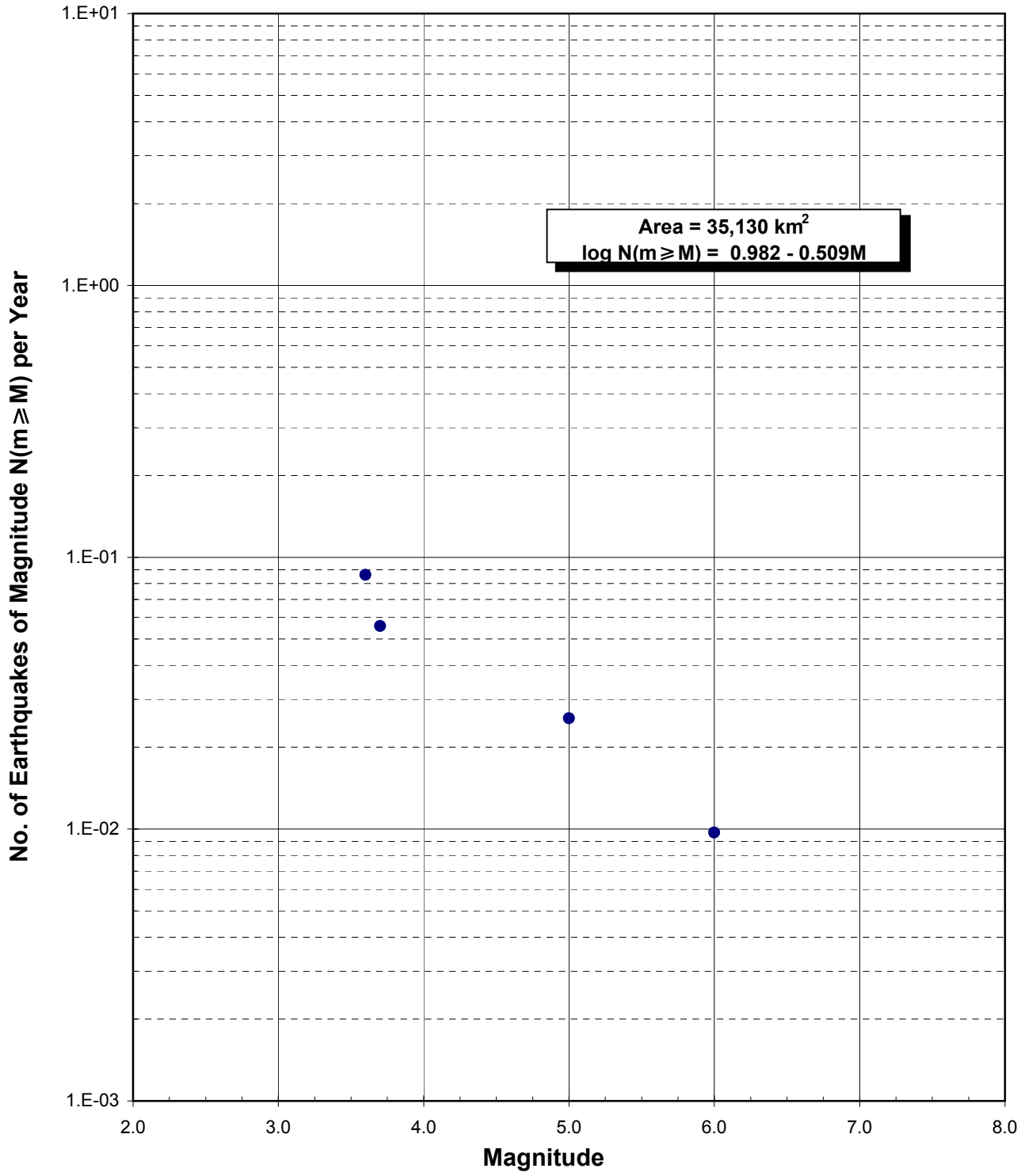

NOTE:
Events smaller than M 4.0 were not used in the regression analysis.

Brightwater Project
Seismic Hazard Analysis
King County Department of Natural Resources

RECURRENCE CURVE FOR OLYMPIC MOUNTAINS, WILLAPA HILLS, & COASTAL RANGE ZONES

January 2005

FIG. B-4

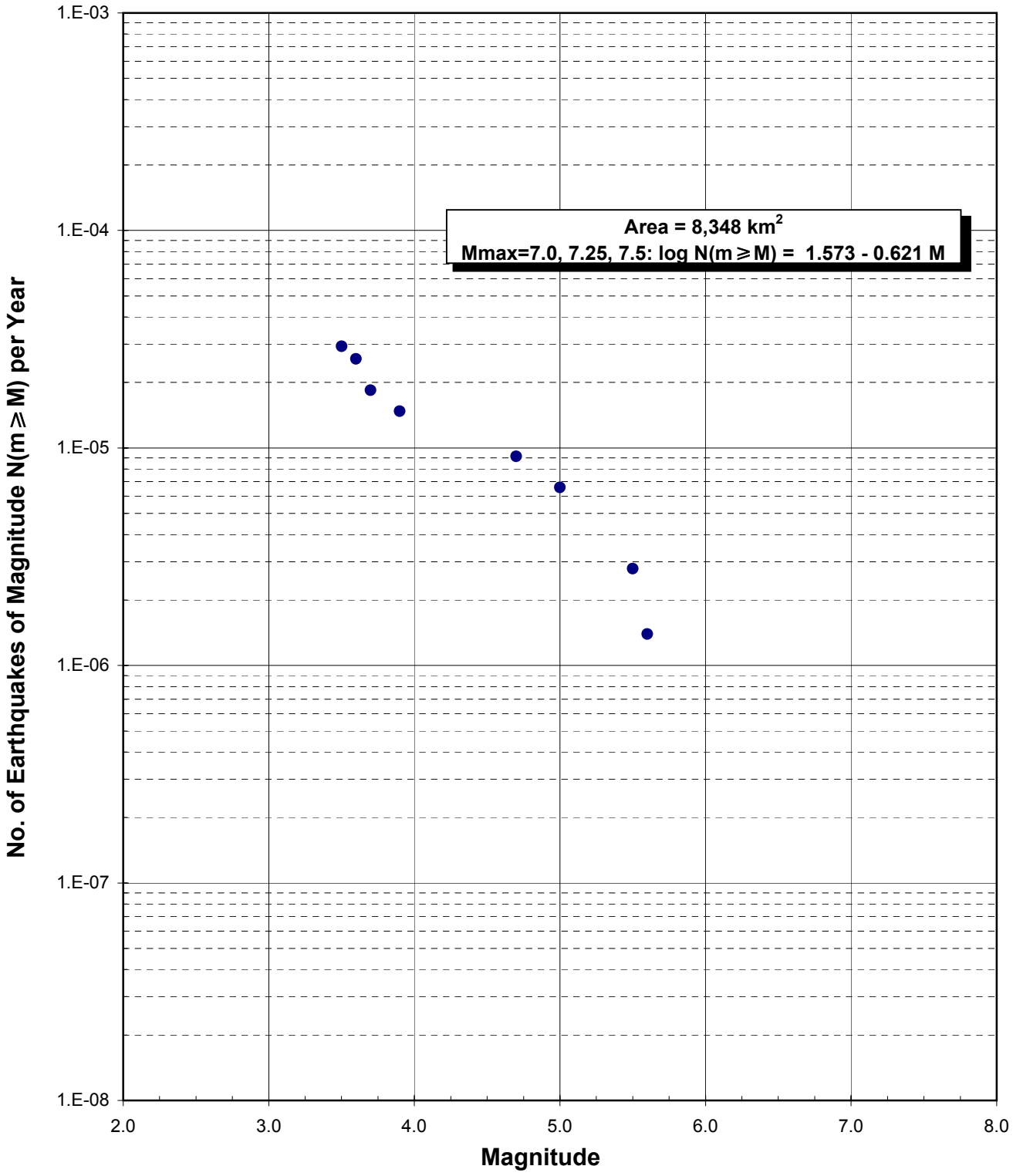

Brightwater Project
Seismic Hazard Analysis
King County Department of Natural Resources

RECURRENCE CURVE FOR WILLAMETTE LOWLAND ZONE

January 2005

FIG. B-5

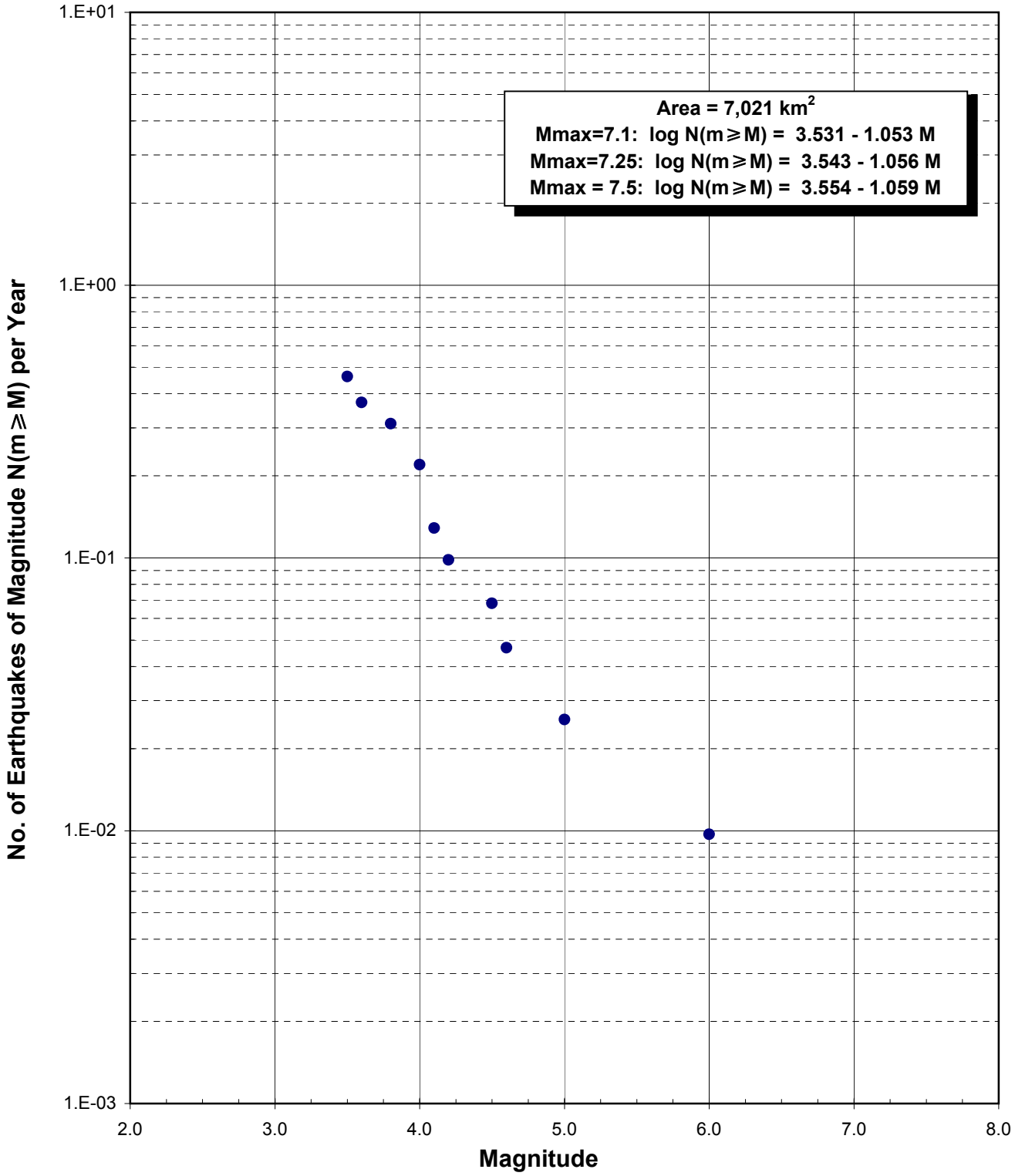

NOTE:
Events smaller than M 4.0 were not used in the regression analysis.

Brightwater Project
Seismic Hazard Analysis
King County Department of Natural Resources

RECURRENCE CURVE FOR NORTH PUGET SOUND ZONE

January 2005

FIG. B-6

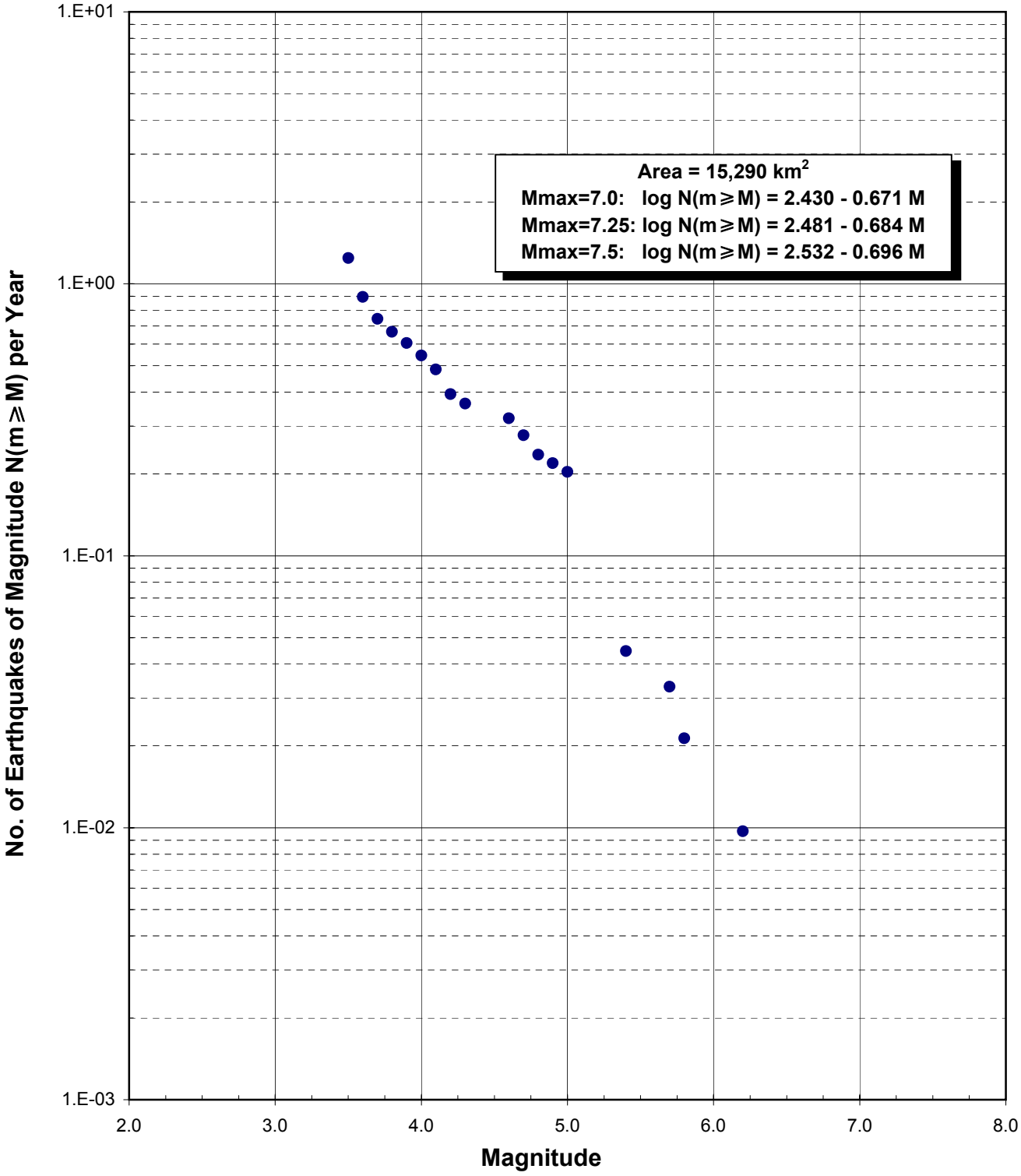

NOTE:
Events smaller than M 4.0 were not used in the regression analysis.

Brightwater Project
Seismic Hazard Analysis
King County Department of Natural Resources

RECURRENCE CURVE FOR CENTRAL PUGET SOUND ZONE

January 2005

FIG. B-7

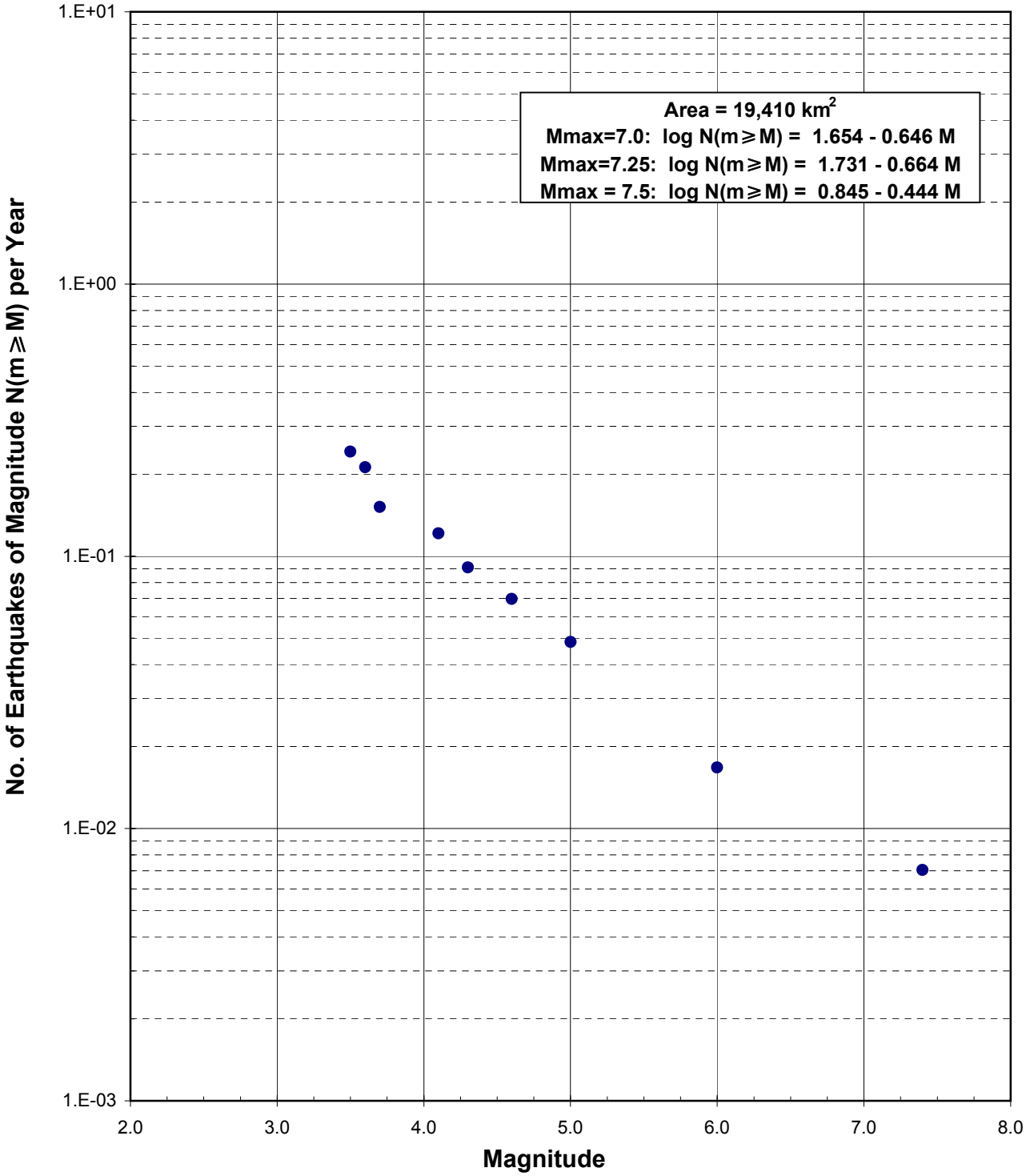

NOTE:
Events smaller than M 4.0 were not used in the regression analysis.

Brightwater Project
Seismic Hazard Analysis
King County Department of Natural Resources

RECURRENCE CURVE FOR NORTH CASCADES ZONE

January 2005

FIG. B-8

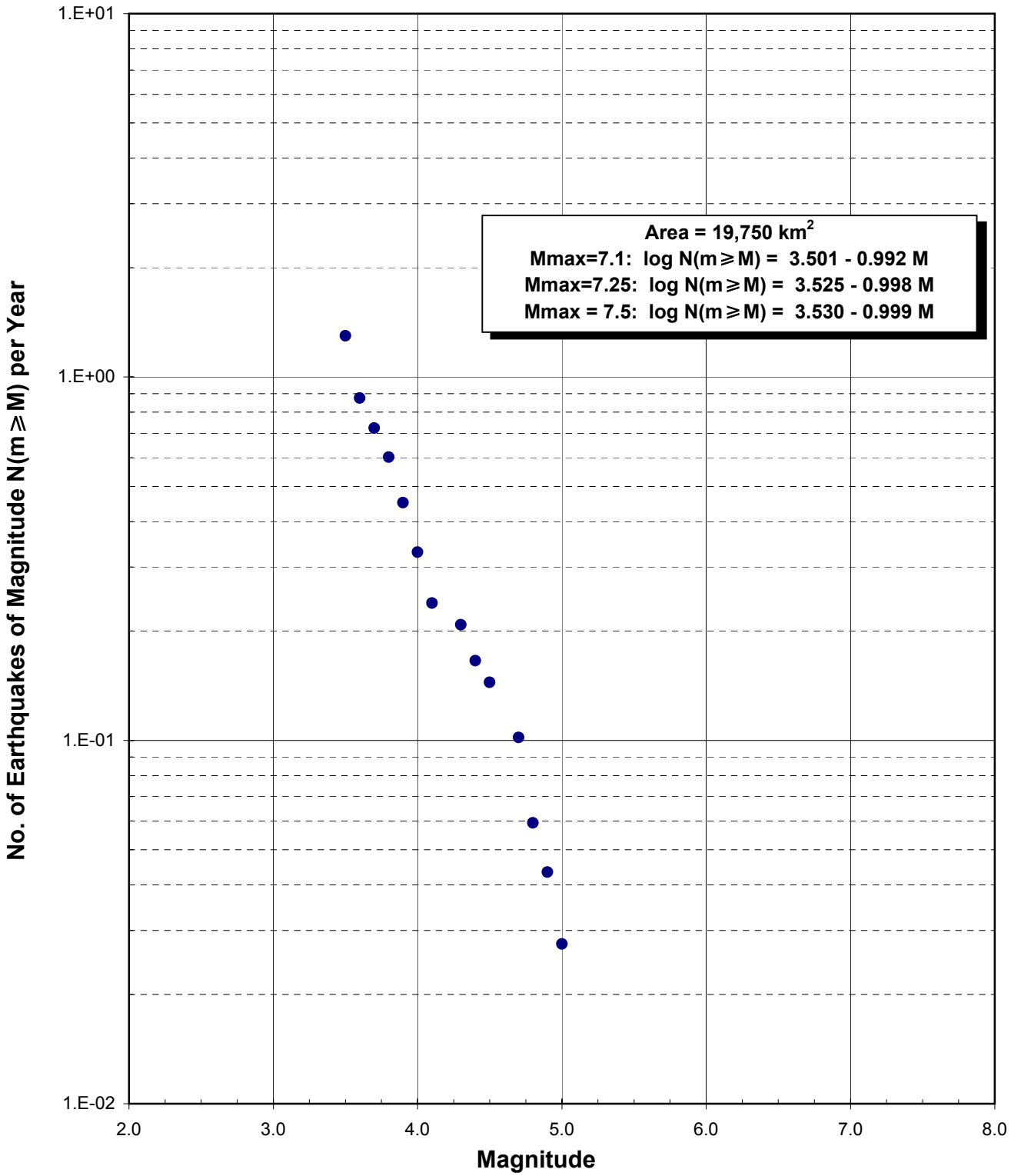

NOTE:
Events smaller than M 4.0 were not used in the regression analysis.

Brightwater Project
Seismic Hazard Analysis
King County Department of Natural Resources

RECURRENCE CURVE FOR SOUTH CASCADES ZONE

January 2005

FIG. B-9

Appendix C

Important Information About Your Geotechnical Report

SHANNON & WILSON, INC.
Geotechnical and Environmental Consultants

Attachment to and part of Report 21-1-20150-002

Date: March 9, 2005
To: Dr. Donald Anderson
CH2M Hill

IMPORTANT INFORMATION ABOUT YOUR GEOTECHNICAL/ENVIRONMENTAL REPORT

CONSULTING SERVICES ARE PERFORMED FOR SPECIFIC PURPOSES AND FOR SPECIFIC CLIENTS.

Consultants prepare reports to meet the specific needs of specific individuals. A report prepared for a civil engineer may not be adequate for a construction contractor or even another civil engineer. Unless indicated otherwise, your consultant prepared your report expressly for you and expressly for the purposes you indicated. No one other than you should apply this report for its intended purpose without first conferring with the consultant. No party should apply this report for any purpose other than that originally contemplated without first conferring with the consultant.

THE CONSULTANT'S REPORT IS BASED ON PROJECT-SPECIFIC FACTORS.

A geotechnical/environmental report is based on a subsurface exploration plan designed to consider a unique set of project-specific factors. Depending on the project, these may include: the general nature of the structure and property involved; its size and configuration; its historical use and practice; the location of the structure on the site and its orientation; other improvements such as access roads, parking lots, and underground utilities; and the additional risk created by scope-of-service limitations imposed by the client. To help avoid costly problems, ask the consultant to evaluate how any factors that change subsequent to the date of the report may affect the recommendations. Unless your consultant indicates otherwise, your report should not be used: (1) when the nature of the proposed project is changed (for example, if an office building will be erected instead of a parking garage, or if a refrigerated warehouse will be built instead of an unrefrigerated one, or chemicals are discovered on or near the site); (2) when the size, elevation, or configuration of the proposed project is altered; (3) when the location or orientation of the proposed project is modified; (4) when there is a change of ownership; or (5) for application to an adjacent site. Consultants cannot accept responsibility for problems that may occur if they are not consulted after factors which were considered in the development of the report have changed.

SUBSURFACE CONDITIONS CAN CHANGE.

Subsurface conditions may be affected as a result of natural processes or human activity. Because a geotechnical/environmental report is based on conditions that existed at the time of subsurface exploration, construction decisions should not be based on a report whose adequacy may have been affected by time. Ask the consultant to advise if additional tests are desirable before construction starts; for example, groundwater conditions commonly vary seasonally.

Construction operations at or adjacent to the site and natural events such as floods, earthquakes, or groundwater fluctuations may also affect subsurface conditions and, thus, the continuing adequacy of a geotechnical/environmental report. The consultant should be kept apprised of any such events, and should be consulted to determine if additional tests are necessary.

MOST RECOMMENDATIONS ARE PROFESSIONAL JUDGMENTS.

Site exploration and testing identifies actual surface and subsurface conditions only at those points where samples are taken. The data were extrapolated by your consultant, who then applied judgment to render an opinion about overall subsurface conditions. The actual interface between materials may be far more gradual or abrupt than your report indicates. Actual conditions in areas not sampled may differ from those predicted in your report. While nothing can be done to prevent such situations, you and your consultant can work together to help reduce their impacts. Retaining your consultant to observe subsurface construction operations can be particularly beneficial in this respect.

A REPORT'S CONCLUSIONS ARE PRELIMINARY.

The conclusions contained in your consultant's report are preliminary because they must be based on the assumption that conditions revealed through selective exploratory sampling are indicative of actual conditions throughout a site. Actual subsurface conditions can be discerned only during earthwork; therefore, you should retain your consultant to observe actual conditions and to provide conclusions. Only the consultant who prepared the report is fully familiar with the background information needed to determine whether or not the report's recommendations based on those conclusions are valid and whether or not the contractor is abiding by applicable recommendations. The consultant who developed your report cannot assume responsibility or liability for the adequacy of the report's recommendations if another party is retained to observe construction.

THE CONSULTANT'S REPORT IS SUBJECT TO MISINTERPRETATION.

Costly problems can occur when other design professionals develop their plans based on misinterpretation of a geotechnical/environmental report. To help avoid these problems, the consultant should be retained to work with other project design professionals to explain relevant geotechnical, geological, hydrogeological, and environmental findings, and to review the adequacy of their plans and specifications relative to these issues.

BORING LOGS AND/OR MONITORING WELL DATA SHOULD NOT BE SEPARATED FROM THE REPORT.

Final boring logs developed by the consultant are based upon interpretation of field logs (assembled by site personnel), field test results, and laboratory and/or office evaluation of field samples and data. Only final boring logs and data are customarily included in geotechnical/environmental reports. These final logs should not, under any circumstances, be redrawn for inclusion in architectural or other design drawings, because drafters may commit errors or omissions in the transfer process.

To reduce the likelihood of boring log or monitoring well misinterpretation, contractors should be given ready access to the complete geotechnical engineering/environmental report prepared or authorized for their use. If access is provided only to the report prepared for you, you should advise contractors of the report's limitations, assuming that a contractor was not one of the specific persons for whom the report was prepared, and that developing construction cost estimates was not one of the specific purposes for which it was prepared. While a contractor may gain important knowledge from a report prepared for another party, the contractor should discuss the report with your consultant and perform the additional or alternative work believed necessary to obtain the data specifically appropriate for construction cost estimating purposes. Some clients hold the mistaken impression that simply disclaiming responsibility for the accuracy of subsurface information always insulates them from attendant liability. Providing the best available information to contractors helps prevent costly construction problems and the adversarial attitudes that aggravate them to a disproportionate scale.

READ RESPONSIBILITY CLAUSES CLOSELY.

Because geotechnical/environmental engineering is based extensively on judgment and opinion, it is far less exact than other design disciplines. This situation has resulted in wholly unwarranted claims being lodged against consultants. To help prevent this problem, consultants have developed a number of clauses for use in their contracts, reports and other documents. These responsibility clauses are not exculpatory clauses designed to transfer the consultant's liabilities to other parties; rather, they are definitive clauses that identify where the consultant's responsibilities begin and end. Their use helps all parties involved recognize their individual responsibilities and take appropriate action. Some of these definitive clauses are likely to appear in your report, and you are encouraged to read them closely. Your consultant will be pleased to give full and frank answers to your questions.

The preceding paragraphs are based on information provided by the
ASFE/Association of Engineering Firms Practicing in the Geosciences, Silver Spring, Maryland